

NUMERICAL SOLUTION OF TWO-DIMENSIONAL

INCOMPRESSIBLE FLOW ABOUT AN AIRFOIL

by

Robert S. Barnes

A Thesis Submitted to the Faculty of the
College of Engineering
in Partial Fulfillment of the Requirements for the Degree of
Master of Science in Engineering

Florida Atlantic University

Boca Raton, Florida

April 1988

NUMERICAL SOLUTION OF TWO-DIMENSIONAL
INCOMPRESSIBLE FLOW ABOUT AN AIRFOIL

by

Robert S. Barnes

This thesis was prepared under the direction of the candidate's thesis advisor, Dr. William Bober, Department of Mechanical Engineering and has been approved by the members of his supervisory committee. It was submitted to the faculty of the College of Engineering and was accepted in partial fulfillment of the requirements for the degree of Master of Science in Engineering.

SUPERVISORY COMMITTEE:

William Bober

Thesis Advisor
Dr. William Bober

Hemayat M. El-Agnaf

Darood Maslamin

Albert Dwyer

Chairperson, Department of
Mechanical Engineering

Alan B. Marcovitz

Dean, College of Engineering

[Signature]

Dean for Graduate Studies

December 30, 1987

Date

ACKNOWLEDGMENTS

I wish to thank my thesis advisor, Dr. William Bober, for his invaluable contribution and advise in writing this paper. It was through his mastery of the subject and constant encouragement which enabled me to complete this work. I would especially like to thank Mrs. Rose Kritzer for her tireless efforts in producing this paper. Finally, without the financial and administrative support of my employer, the US Army, none of this would have been possible.

Robert S. Barnes
Captain(P), US Army

ABSTRACT

Author: Robert S. Barnes
Title: Numerical Solution of Two-Dimensional
Incompressible Flow About An Airfoil
Institution: Florida Atlantic University
Degree: Master of Science in Engineering
Year: 1988

A numerical scheme for determining the two dimensional, incompressible flow field about an airfoil is described. The scheme combines two methods: the Neumann (panel) method to determine the potential flow and a hybrid numerical method to determine the boundary layer flow. In the panel method, the fundamental theorems of potential theory are employed to derive the pressure and velocity fields around and along the airfoil. The velocity field obtained in the panel method is used in the hybrid method to determine the boundary layer thickness along the surface of the airfoil. The hybrid numerical method is an implicit finite difference numerical scheme which combines central and upwind differencing for the convective terms. The boundary layer thickness obtained is introduced back into the panel method to determine new pressure and velocity fields, thus imposing the effects of laminar, viscous flow on the solution. Lift coefficients for various angles of attack are derived and compared with experimental data presented in appropriate NACA technical reports. Reasonable agreement was obtained.

TABLE OF CONTENTS

CHAPTER 1	1
INTRODUCTION	1
Literature Survey	1
Layout	2
CHAPTER 2	4
EXPLANATION OF NUMERICAL METHOD	4
Theoretical Development of Potential Flow Problem	4
Neumann (panel) Method	6
Implicit and Hybrid Methods	23
Geometric Consideration	35
CHAPTER 3	38
DISCUSSION OF RESULTS	38
CHAPTER 4	43
CONCLUSIONS AND RECOMMENDATIONS	43
APPENDIX A	47
APPENDIX B	55
APPENDIX C	67
APPENDIX D	93
REFERENCES	96
BIBLIOGRAPHY	100

LIST OF TABLES

Table No.	Title	Page No.
1	Data Table For CY-14 Airfoil at $\alpha = - 6^\circ$	48
2	Data Table For CY-14 Airfoil at $\alpha = 6^\circ$	49
3	Data Table For CY-14 Airfoil at $\alpha = 12^\circ$	50
4	Table Depicting Comparison of Blasius Closed Form Solution of a Flat Plate to Numerical Solution at $X = 0.0$	51
5	Table Depicting Comparison of Blasius Closed Form Solution of a Flat Plate to Numerical Solution at $X = .033$	52
6	Table Depicting Comparison of Blasius Closed Form Solution of a Flat Plate to Numerical Solution at $X = .133$	53
7	Table Depicting Comparison of Blasius Closed Form Solution of a Flat Plate to Numerical Solution at $X = .233$	54

LIST OF FIGURES

Figure No.	Title	Page No.
1	Boundary Conditions	6
2	Source Distribution Geometry	9
3	Vortex Distribution Geometry	10
4	Element Local Coordinates	11
5	Local to Global Coordinate Transformation	12
6	Application Points for Kutta Condition	19
7	Airfoil to Flat Plate Coordinate Transformation	24
8	Boundary Layer Geometry	31
9	Stagnation Point Flow	32
10	Boundary Condition Adjustment for Boundary Layer Thickness	34
11	Sample NACA Technical Report Data	35
12	Before Axis Rotation of NACA Data	36
13	After Axis Rotation of NACA Data	37
14	Graph Depicting C_L vs α for CY-14 Airfoil	56
15	Graph Depicting C_L vs α for N-68 Airfoil	57
16	Graph Depicting C_L vs α for Gottingen 387 Airfoil	58
17	Graph Depicting C_p vs X/L for $\alpha = -6^\circ$ (CY-14 Airfoil)	59
18	Graph Depicting C_p vs X/L for $\alpha = 6^\circ$ (CY-14 Airfoil)	60
19	Graph Depicting C_p vs X/L for $\alpha = 12^\circ$ (CY-14 Airfoil)	61

20	Graph Depicting C_p vs X/L for $\alpha = 2^\circ$ (NACA 4412 Airfoil)	62
21	Graph Depicting τ_w vs X' for $\alpha = -8^\circ$, Lower Surface, CY-14 Airfoil	63
22	Graph Depicting τ_w vs X' for $\alpha = 2^\circ$, Upper Surface, CY-14 Airfoil	64
23	Graph Depicting τ_w vs X' for $\alpha = 12^\circ$, Upper Surface, CY-14 Airfoil	65
24	Points of Separation for the CY-14 Airfoil	66
25	Diagram of CY-14 Airfoil for Use in Proposed Experiment	95

CHAPTER 1

INTRODUCTION

Literature Survey

The Douglas Aircraft Company has been on the forefront in the use of potential flow theory coupled with boundary layer theory to predict flow characteristics about lifting (e.g., airfoils) and nonlifting (e.g., fuselages) surfaces. The solution of the potential flow (or Neumann) problem was begun in 1954 [1] and a summary report outlining developments from 1954-1965 was published in 1966 [2]. The Douglas method for calculation of boundary layer flow resulted from work begun in 1960 [3-14] through 1968 and resulted in overcoming the weaknesses of earlier attempts [15-17].

Other work in the field of machine calculations of fluid flows grew out of these accomplishments. Callaghan and Beatty used the method to successfully analyze and design multielement airfoils [18]. In an exploratory report, John L. Hess probed the possibility of constructing a computer program for calculating flow about arbitrary three-dimensional configurations including viscous effects [19]. It is from this work by Hess in 1976 and an article he wrote in 1974 [20] that much of the work done in this paper is derived. For the purpose of this paper, only two dimensional flows were considered.

This method is not restricted to airfoils or lifting surfaces. In fact Hess and Smith extended the method to low speed flows in inlets, and ducts and about propeller shrouds [21]. Another application that demonstrates the overall versatility of the method is its use in the design of ships [22]. The Douglas method has been applied to a variety of flows, compressible and incompressible, which seemingly fills the gap left by analytical closed form methods. Before the introduction of the Douglas method, empirical data were absolutely essential for predicting complex flows. Now one can predict complex flows by the Douglas method with reasonable accuracy through machine calculations.

Layout

The paper is organized into three principal parts: explanation of numerical method, results and conclusions. The first part is subdivided into:

- (a) Theoretical development of the potential flow problem.
- (b) Neumann (panel) method.
- (c) Implicit and Hybrid methods for determining the flow field in a boundary layer and the boundary layer thickness.
- (d) Modification of Neumann method to account for boundary layer thickness (i.e., viscous effects).
- (e) Brief discussion of geometric considerations of the problem.

In part two, I will depict graphically the following:

- (a) Coefficient of lift versus angle of attack for the CY-14, N-68, and Göttingen 387 airfoils. Both the ideal flow and boundary layer displaced flow will be graphed as well as compared with NACA (National Advisory Committee on Aeronautics) Technical Report data.
- (b) Coefficient of pressure versus percent chord position for various angles of attack.
- (c) The wall shear stress, τ_w , versus downstream distance and the point of flow separation when it occurs.

In addition to the above, information on the numerical efficiency (e.g., computer time, etc.) of the program is presented.

In part three, an evaluation of results gathered and suggestions for improving the technique are given.

CHAPTER 2

EXPLANATION OF NUMERICAL METHOD

Theoretical Development of Potential Flow Problem

A general, exact, closed form solution for the Navier-Stokes equations does not exist [23]. Furthermore, the use of numerical techniques for solving the Navier-Stokes equations for flows around airfoils would involve excessive computer time and memory. It is for this reason a three tier approach is used to solve the flow field around the airfoil. In the first tier, Potential Flow Theory (Neumann Method) is used to determine the inviscid flow solution around the airfoil. In the second tier, the velocity field derived in the first tier is used to determine the boundary layer thickness. In the last tier, the potential flow solution is modified to account for the boundary layer thickness found in the second tier. That is, the boundary conditions are applied at the edge of the boundary layer instead of on the airfoil surface. This modified solution better simulates the real flow solution.

The focus of this paper is restricted to two dimensional, subsonic flows with Mach numbers less than 0.5. As a result, compressibility effects are negligible [24] and the assumption of constant fluid density is valid.

It is experimentally observed that viscous effects are confined to a very narrow region along the airfoil known as the boundary layer [25]. For subsonic, incompressible flows, there is no significant pressure variation across this boundary layer [26]. Theoretically then, a nonviscous or ideal flow solution can be used to determine lift on an airfoil at low angles of attack. For larger angles of attack, flow separation occurs which nullifies the potential flow solution.

The use of potential flow to determine drag on an airfoil would lead to the erroneous conclusion that the drag is zero. This is known as the d'Alembert's paradox [27]. However, by solving the boundary layer equations one can calculate the drag force on an airfoil from the wall shear stress provided that there is no flow separation [28]. When flow separation occurs, the boundary layer solution is no longer valid and in addition, a pressure drag occurs as a result of the development of a low pressure area downstream of the point of separation [29].

In treating an ideal flow around an airfoil, it is usually assumed that the flow is irrotational; i.e.

$$\nabla \times \underline{v} = 0 \quad (2.1)$$

where \underline{v} is the fluid velocity vector. Justification for this assumption is based on Kelvin's Theorem and the fact that the flow field is uniform far upstream from the airfoil [30].

Neumann (Panel) Method

When the flow field is irrotational, the fluid velocity vector can be expressed as the gradient of a scalar [31]; i.e.,

$$\underline{v} = \nabla \phi \quad (2.2)$$

where ϕ is the potential function. The governing field Equation for potential flow is obtained by substituting Equation (2.2) into the continuity equation shown below:

$$\nabla \cdot \underline{v} = \frac{\partial u}{\partial X} + \frac{\partial v}{\partial Y} = 0 \quad (2.3)$$

This gives:

$$\nabla^2 \phi = \frac{\partial^2 \phi}{\partial X^2} + \frac{\partial^2 \phi}{\partial Y^2} = 0 \quad (2.4)$$

The boundary conditions for the problem are (see Figure 1):

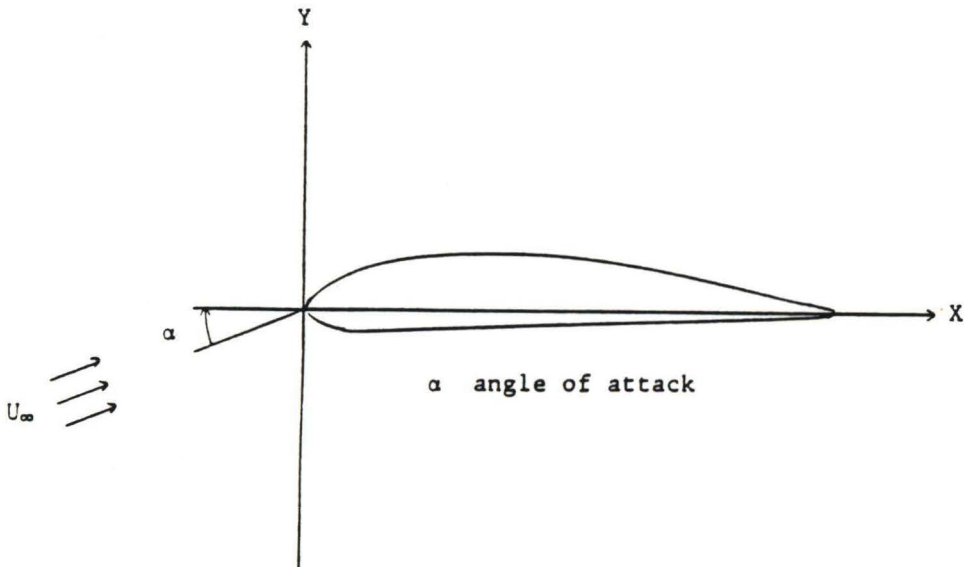


Figure 1 Boundary Conditions

Therefore,

$$\underline{v}(-\infty, Y) = U_{\infty}[\cos\alpha\underline{i} + \sin\alpha\underline{j}] \quad (2.5)$$

and on the boundary:

$$\underline{v}(B) \cdot \underline{n}(B) = 0 \quad (2.6)$$

where

$\underline{v}(B)$ is the velocity on the airfoil boundary

and

$\underline{n}(B)$ is the unit normal vector on the airfoil surface.

The potential flow solution allows a non-zero tangential velocity component on the surface of the airfoil, which is not consistent with the no slip boundary condition observed experimentally. However, the boundary layer is very thin and the allowance of a non-zero tangential velocity component on the surface of the airfoil instead of the edge of the boundary layer introduces only a small error. This small error is compensated for by the third tier.

Superpositioning of some simple flow configurations such as sources, sinks, and vortices can lead to streamline patterns that simulate some particular flow of interest [32]. Each simple flow configuration by itself satisfies Laplace's equation. The addition of several simple flow solutions also satisfies Laplace's equation. This is so because Laplace's equation is linear.

In the panel method the velocity potential, Φ , is assumed to be

the superposition of the velocity potential of a uniform stream, and source and vortex distributions on the airfoil, i.e.,

$$\Phi = U_{\infty} \cos\alpha X + U_{\infty} \sin\alpha Y + \phi_s + \phi_v \quad (2.7)$$

where:

U_{∞} is the free stream velocity.

α is the angle of attack of the airfoil.

ϕ_s is the potential from the source distribution.

ϕ_v is the potential from the vortex distribution.

Substituting equation (2.7) into the above equations yields:

$$[U_{\infty} \cos\alpha \underline{i} + U_{\infty} \sin\alpha \underline{j} + \nabla\phi_s(B) + \nabla\phi_v(B)] \cdot \underline{n}(B) = 0 \quad (2.8)$$

The above source distribution in equation (2.8) is assumed to have a variable strength (σ) while the vortex distribution is assumed to have a uniform strength (σ_v). Thus,

$$\phi_s = \oint_c \sigma(c) \log r \, d\lambda \quad (2.9)$$

where

$$r = \sqrt{(X - \bar{X})^2 + (Y - \bar{Y})^2}$$

and (X, Y) are the coordinates of a point in the flow field, (\bar{X}, \bar{Y}) are the coordinates of a point on the airfoil (see Figure 2), and $d\ell$ is an arc length on the airfoil (see Figure 2).

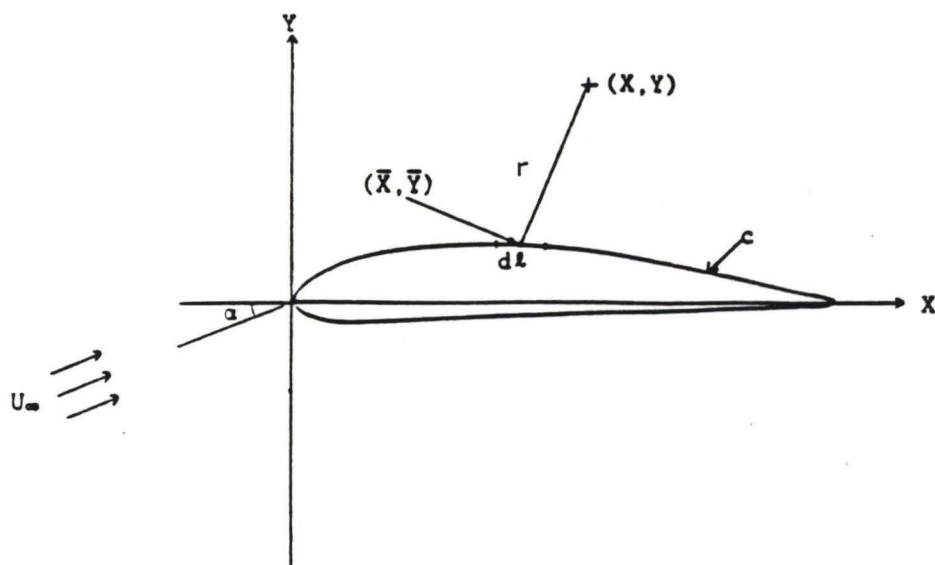


Figure 2 Source Distribution Geometry

Subdividing the airfoil into M segments yields:

$$\oint_c \sigma(c) \log r \, d\ell \approx \sum_{m=1}^M \sigma_m \int_{c_m} \log r \, d\ell = \sum_{m=1}^M \sigma_m U_m \quad (2.10)$$

In this method, $\sigma(c)$ is taken to be a constant on each line segment but has varying values for different line segments. The potential function, ϕ_v , due to the vortex distribution is given by:

$$\phi_v = \sigma_v \oint_c \theta \, d\ell \approx \sigma_v \sum_{m=1}^M V_m \quad (2.11)$$

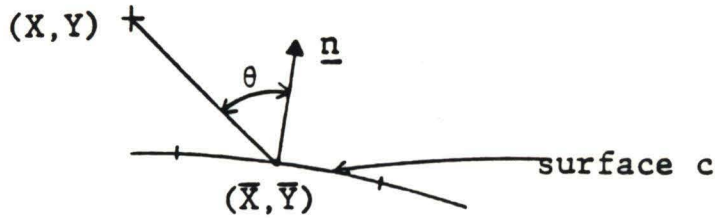


Figure 3 Vortex Distribution Geometry

where θ is the angle (in radians) between the line connecting the points (X, Y) and (\bar{X}, \bar{Y}) and the normal line to the airfoil as shown in Figure 3.

One can see that there are $(M + 1)$ unknowns: $\sigma_1, \sigma_2, \dots, \sigma_M$ and σ_v . Application of the boundary condition at the control points on each element provides M linear algebraic equations. The Kutta condition provides one additional equation, making the system solvable. The control points, (\bar{X}_m, \bar{Y}_m) , are taken to be the center point on each element.

U_m and V_m are best written in terms of the local coordinates associated with each line segment. If (x, y) are the local coordinates of a point in the flow field and $(0, \bar{y})$ are the coordinates of a point on the airfoil line segment (see Figure 4 below), then [33]:

$$U_m = \frac{1}{2} \int_{-\lambda/2}^{\lambda/2} \log [x^2 + (y - \bar{y})^2] d\bar{y} \quad (2.12)$$

and

$$V_m = \int_{-\lambda/2}^{\lambda/2} \arctan \left(\frac{y - \bar{y}}{x} \right) d\bar{y} \quad (2.13)$$

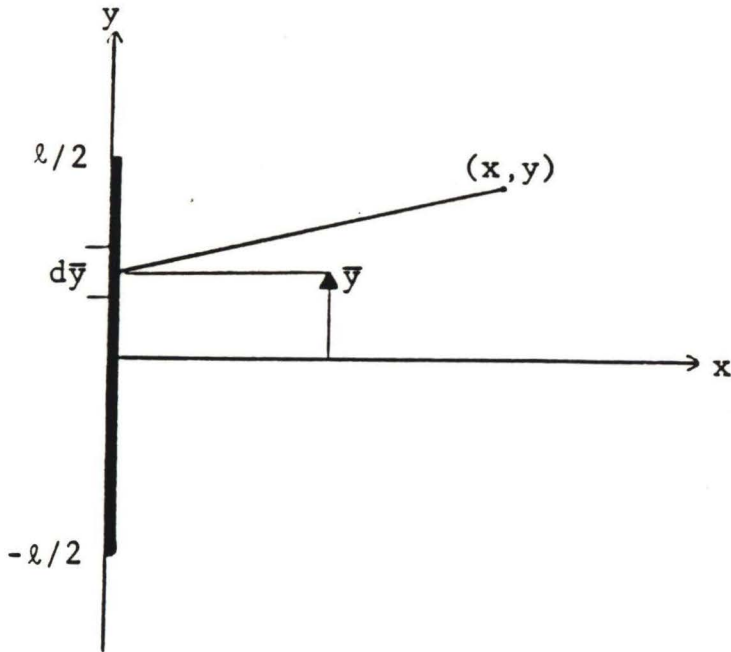


Figure 4 Element Local Coordinates

The local coordinates of a point in space can be related to a global coordinate system (X, Y) by the following equations (see Figure 5):

$$x = (X - \bar{X}_m) \cos \gamma_m + (Y - \bar{Y}_m) \sin \gamma_m \quad (2.14)$$

$$y = -(X - \bar{X}_m) \sin \gamma_m + (Y - \bar{Y}_m) \cos \gamma_m \quad (2.15)$$

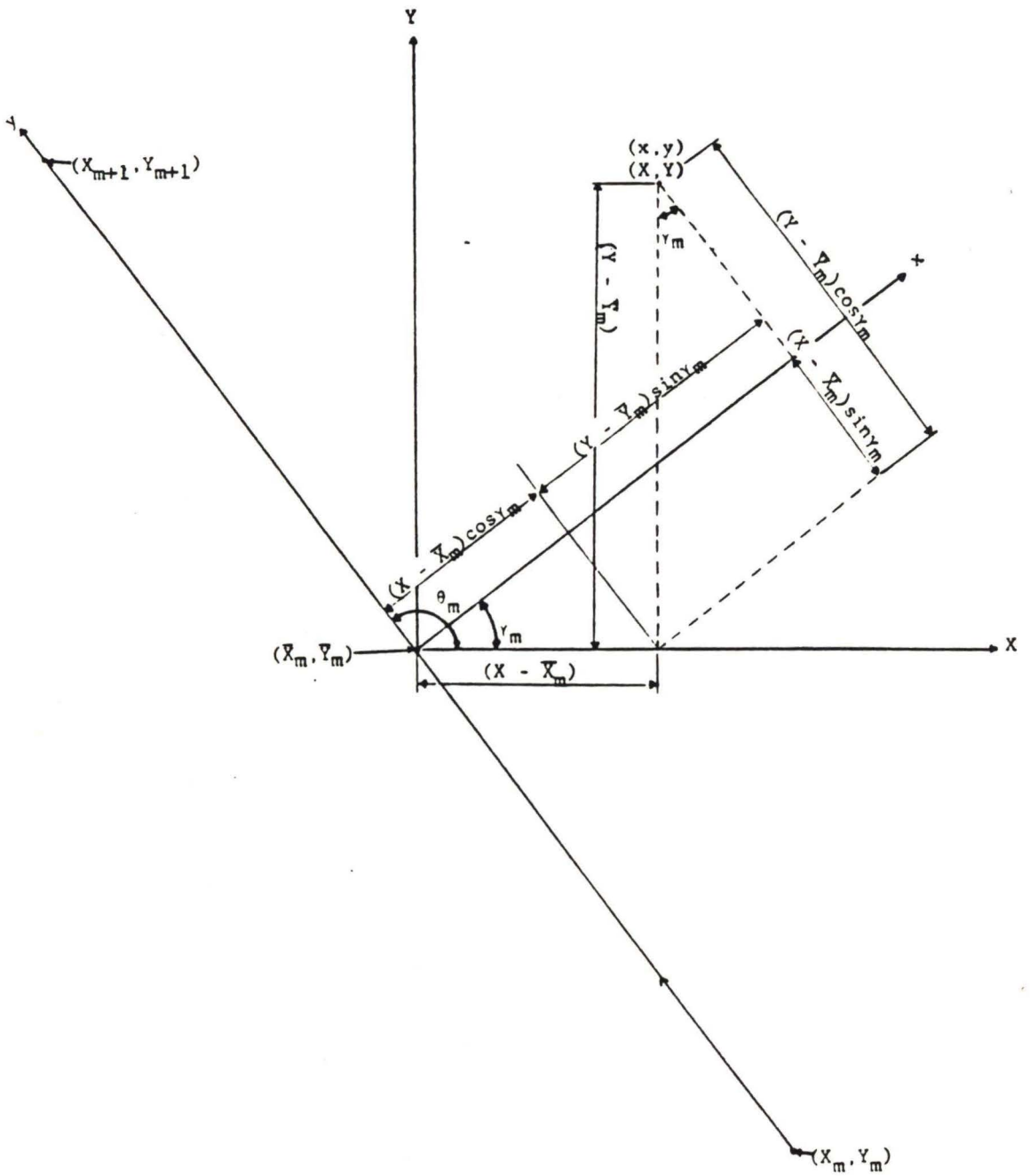


Figure 5 Local to Global Coordinate Transformation

The unit vector in the direction of the line segment, $(\underline{e}_y)_m$, is given by:

$$(\underline{e}_y)_m = \cos \theta_m \underline{i} + \sin \theta_m \underline{j} = (e_1)_m \underline{i} + (e_2)_m \underline{j} \quad (2.16)$$

The unit normal vector to the line segment, \underline{n}_m , is then:

$$\begin{aligned} \underline{n}_m &= \cos(\theta_m - \pi/2) \underline{i} + \sin(\theta_m - \pi/2) \underline{j} \\ &= \sin \theta_m \underline{i} - \cos \theta_m \underline{j} = (e_2)_m \underline{i} - (e_1)_m \underline{j} \end{aligned} \quad (2.17)$$

Recall that:

$$\phi_s = \sum \sigma_m U_m \quad (\text{from Equation (2.10)})$$

and

$$\phi_v = \sigma_v \sum V_m \quad (\text{from Equation (2.11)})$$

Therefore:

$$\nabla \phi_s = \sum_{m=1}^M \sigma_m \left[\frac{\partial U_m}{\partial X} \underline{i} + \frac{\partial U_m}{\partial Y} \underline{j} \right] \quad (2.18)$$

and

$$\nabla \phi_v = \sigma_v \sum_{m=1}^M \left[\frac{\partial V_m}{\partial X} \underline{i} + \frac{\partial V_m}{\partial Y} \underline{j} \right] \quad (2.19)$$

We can express Equations (2.18) and (2.19) in terms of local coordinates by use of the chain rule:

$$\frac{\partial U_m}{\partial X} = \frac{\partial U_m}{\partial x} \cdot \frac{\partial x}{\partial X} + \frac{\partial U_m}{\partial y} \cdot \frac{\partial y}{\partial X} \quad (2.20)$$

and

$$\frac{\partial U_m}{\partial Y} = \frac{\partial U_m}{\partial x} \cdot \frac{\partial x}{\partial Y} + \frac{\partial U_m}{\partial y} \cdot \frac{\partial y}{\partial Y} \quad (2.21)$$

The derivatives of (x,y) with respect to (X,Y) can be obtained from Equations, (2.14) and (2.15). Similar relations can be obtained for $\partial V_m/\partial X$ and $\partial V_m/\partial Y$.

To obtain a set of equations for the set $\{\sigma_n\}$, one needs to apply Equation (2.8) to the control points on each element, i.e., points (\bar{X}_n, \bar{Y}_n) . To do this, expressions for $\nabla\phi_s$ and $\nabla\phi_v$ must first be obtained. Then, evaluating $\nabla\phi_s$ and $\nabla\phi_v$ at the boundary points (\bar{X}_n, \bar{Y}_n) and combining the results with Equation (2.8) yields:

$$U_\infty \cos\alpha \cdot (e_2)_n - U_\infty \sin\alpha \cdot (e_1)_n + \pi \sigma_n + \sum_{m \neq n} \sigma_m \left\{ (e_2)_n \left[(e_2)_m \cdot \frac{\partial U_m}{\partial x} (\bar{X}_n, \bar{Y}_n) + (e_1)_m \frac{\partial U_m}{\partial y} (\bar{X}_n, \bar{Y}_n) \right] - (e_1)_n \left[- (e_1)_m \cdot \frac{\partial U_m}{\partial x} (\bar{X}_n, \bar{Y}_n) + (e_2)_m \frac{\partial U_m}{\partial y} (\bar{X}_n, \bar{Y}_n) \right] \right\} + \sigma_v \sum_{m \neq n} \left\{ (e_2)_n \left[(e_2)_m \frac{\partial V_m}{\partial x} (\bar{X}_n, \bar{Y}_n) + (e_1)_m \frac{\partial V_m}{\partial y} (\bar{X}_n, \bar{Y}_n) \right] \right\}$$

$$- (e_1)_n \left[- (e_1)_m \frac{\partial V_m}{\partial x} (\bar{X}_n, \bar{Y}_n) + (e_2)_m \frac{\partial V_m}{\partial y} (\bar{X}_n, \bar{Y}_n) \right] \Bigg\} = 0 \quad (2.22)$$

Subscript n refers to a control point on the element where the boundary condition is being applied and m refers to the source and vortex contributions from the m th element. Equation (2.22) can be written in index notation, i.e.,

$$A_{nm} \sigma_m = B_n \quad (2.23)$$

where:

$$A_{nm} = \left[(e_2)_n (e_2)_m + (e_1)_n (e_1)_m \right] \cdot \frac{\partial U_m}{\partial x} (\bar{X}_n, \bar{Y}_n) + \left[(e_2)_n (e_1)_m - (e_1)_n (e_2)_m \right] \cdot \frac{\partial U_m}{\partial y} (\bar{X}_n, \bar{Y}_n) \quad (2.24)$$

$$A_{nn} = \pi$$

and

$$B_n = - U_\infty \left[\cos \alpha (e_2)_n - \sin \alpha (e_1)_n \right] - \sigma_v \sum_{m \neq n} \left\{ \left[(e_2)_n (e_2)_m + (e_1)_n (e_1)_m \right] \cdot \frac{\partial V_m}{\partial y} (\bar{X}_n, \bar{Y}_n) + \left[(e_2)_n (e_1)_m - (e_1)_n (e_2)_m \right] \cdot \frac{\partial V_m}{\partial x} (\bar{X}_n, \bar{Y}_n) \right\} \quad (2.25)$$

The derivatives $\frac{\partial U_m}{\partial x}$, $\frac{\partial U_m}{\partial y}$, $\frac{\partial V_m}{\partial x}$ and $\frac{\partial V_m}{\partial y}$ can be determined analytically. It should be noted that these partial derivatives are in terms of the local coordinates; but, through the chain rule they can be expressed in terms of the global coordinates. Recall that from Equations (2.12) and (2.13):

$$U_m = \frac{1}{2} \int_{-\ell/2}^{\ell/2} \log [x^2 + (y - \bar{y})^2] d\bar{y} \quad (2.26)$$

and

$$V_m = \int_{-\ell/2}^{\ell/2} \tan^{-1} \frac{y - \bar{y}}{x} d\bar{y} \quad (2.27)$$

To evaluate these integrals, let $z = y - \bar{y}$; then

$$\begin{aligned} U_m &= -\frac{1}{2} \int_{y+\ell/2}^{y-\ell/2} \log [x^2 + z^2] dz \\ &= \frac{1}{2} \int_{y-\ell/2}^{y+\ell/2} \log [x^2 + z^2] dz \end{aligned} \quad (2.28)$$

From the use of integral tables, we obtain

$$\begin{aligned} U_m &= \frac{1}{2} \left\{ (y + \ell/2) \log [x^2 + (y + \ell/2)^2] - \ell \right. \\ &\quad \left. + 2x \tan^{-1} \left(\frac{y + \ell/2}{x} \right) - (y - \ell/2) \log [x^2 + (y - \ell/2)^2] \right. \\ &\quad \left. - 2x \tan^{-1} \left(\frac{y - \ell/2}{x} \right) \right\} \end{aligned} \quad (2.29)$$

Taking the derivative of Equation (2.29) with respect to x and y yields:

$$\frac{\partial U_m}{\partial x} = \tan^{-1} \left(\frac{y + \lambda/2}{x} \right) - \tan^{-1} \left(\frac{y - \lambda/2}{x} \right) \quad (2.30)$$

$$\frac{\partial U_m}{\partial y} = \frac{1}{2} \log \left[\frac{x^2 + (y + \lambda/2)^2}{x^2 + (y - \lambda/2)^2} \right] \quad (2.31)$$

For the special case where $(x,y) = (0,0)$,

$$\begin{aligned} \frac{\partial U_m}{\partial x} (0,0) &= \tan^{-1}(+\infty) - \tan^{-1}(-\infty) \\ &= \pi/2 - (-\pi/2) = \pi \end{aligned} \quad (2.32)$$

and

$$\frac{\partial U_m}{\partial y} (0,0) = \frac{1}{2} \log \left[\frac{(\lambda/2)^2}{(-\lambda/2)^2} \right] = \frac{1}{2} \log 1 = 0 \quad (2.33)$$

Similarly,

$$V_m = \int_{y-\lambda/2}^{y+\lambda/2} \tan \frac{z}{x} dz \quad (2.34)$$

From integral tables:

$$\int \tan^{-1} ax dx = x \tan^{-1} ax - \frac{1}{2a} \log (1 + a^2 x^2) \quad (2.35)$$

Therefore,

$$V_m = (y + \ell/2) \tan^{-1} \left(\frac{y + \ell/2}{x} \right) - (y - \ell/2) \tan^{-1} \left(\frac{y - \ell/2}{x} \right) \\ - \frac{x}{2} \log \left[1 + \left(\frac{y + \ell/2}{x} \right)^2 \right] + \frac{x}{2} \log \left[1 + \left(\frac{y - \ell/2}{x} \right)^2 \right] \quad (2.36)$$

Taking the derivative with respect to x and y yields:

$$\frac{\partial V_m}{\partial x} = \frac{1}{2} \log \left[\frac{x^2 + (y - \ell/2)^2}{x^2 + (y + \ell/2)^2} \right] \quad (2.37)$$

and

$$\frac{\partial V_m}{\partial y} = \tan^{-1} \left(\frac{y + \ell/2}{x} \right) - \tan^{-1} \left(\frac{y - \ell/2}{x} \right) \quad (2.38)$$

For the special case $(x,y) = (0,0)$

$$\frac{\partial V_m}{\partial x} (0,0) = \frac{1}{2} \log 1 = 0 \quad (2.39)$$

and

$$\frac{\partial V_m}{\partial y} (0,0) = \tan^{-1}(+\infty) - \tan^{-1}(-\infty) = \pi \quad (2.40)$$

The superposition of a vortex distribution of uniform strength induces a lift on the airfoil, but makes the solution multivalued. However, the use of the Kutta condition makes the solution unique. In the panel method the Kutta condition is achieved by making the velocities at the trailing edge control points (points A and B, Figure 6) the same.

To apply the Kutta condition, we need to obtain an expression for the tangential velocity, V_t . This is accomplished as follows:

$$V_t(\bar{X}_n, \bar{Y}_n) = \underline{v}(\bar{X}_n, \bar{Y}_n) \cdot (\underline{e}_y)_n \quad (2.41)$$

where:

$$(\underline{e}_y)_n = (e_1)_n \underline{i} + (e_2)_n \underline{j} \quad (2.42)$$

Thus:

$$\begin{aligned} V_t(\bar{X}_n, \bar{Y}_n) &= U_\infty [\cos \alpha (e_1)_n + \sin \alpha (e_2)_n] \\ &+ \sum_{m \neq n} \sigma_m \left\{ \left[(e_1)_n (e_2)_m - (e_2)_n (e_1)_m \right] \frac{\partial U_m}{\partial x} (\bar{X}_n, \bar{Y}_n) + \right. \\ &\left. \left[(e_1)_n (e_1)_m + (e_2)_n (e_2)_m \right] \frac{\partial U_m}{\partial y} (\bar{X}_n, \bar{Y}_n) \right\} \\ &+ \sigma_v \pi + \sigma_v \sum_{m \neq n} \left\{ \left[(e_1)_n (e_2)_m - (e_2)_n (e_1)_m \right] \frac{\partial v_m}{\partial x} (\bar{X}_n, \bar{Y}_n) \right. \\ &\left. + \left[(e_1)_n (e_1)_m + (e_2)_n (e_2)_m \right] \frac{\partial v_m}{\partial y} (\bar{X}_n, \bar{Y}_n) \right\} \quad (2.43) \end{aligned}$$

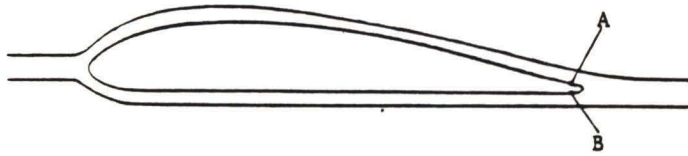


Figure 6 Application Points for Kutta Condition

An iterative scheme is employed to determine the value of σ_v that will satisfy the Kutta condition, i.e.,

1. A value for σ_v was assumed ($\sigma_v = 0.0$ was used for the first iteration).
2. Tangential velocities, V_t , were determined at points A and B by the use of Equation (2.43).
3. A correction term, $\Delta\sigma_v$ was determined which was proportional to the difference of tangential velocities at points A and B, i.e. [34]:

$$\Delta\sigma_v = \frac{\left| |V_t(A)| - |V_t(B)| \right| \cdot W}{V_{t,v}(A) + V_{t,v}(B)} \quad (2.44)$$

where

$V_{t,v}$ is the tangential velocity due to a vortex distribution of unit strength and W is some weighting factor less than one.

W is initially taken as 0.5 which from experience provides faster convergence than a value of 1.0 throughout the iteration process.

4. A new σ_v is obtained utilizing the $\Delta\sigma_v$ obtained in (3), i.e.,

$$\sigma_v^{n+1} = \sigma_v^n + \Delta\sigma_v \quad (2.45)$$

Iteration continues until the the values of $V_t(A)$ and $V_t(B)$ are the same within 1.0×10^{-6} ft/s.

At this point, the nonviscous solution for flow around an airfoil is solved. To determine the accuracy of the obtained solution, it is necessary to compare the obtained results with some experimental data or documented data by others, such as those presented in Technical Reports published by the National Advisory Committee on Aeronautics (NACA). Originally, we had planned to conduct tests which would have provided the local pressure distribution along the airfoil. However, due to complications with using the wind tunnel in the Department of Ocean Engineering, the experiment was cancelled. For details on the experimental procedure see Appendix D. Therefore, attention was focused on NACA Technical Reports on airfoil performance [35]. To compare results with these data, it was necessary to calculate the lift coefficient, C_L , versus the angle of attack. The lift coefficient is related to the circulation, Γ , around the airfoil and is given by [36]

$$C_L = \frac{-2 \Gamma}{c U_\infty} \quad (2.46)$$

where c is the chord length, U_∞ is the free stream velocity and Γ is the circulation defined by:

$$\Gamma = \oint \underline{v} \cdot \underline{e}_t \, d\lambda \approx \sum_n \int c_n V_t \, d\lambda \quad (2.47)$$

It should be noted that for positive angles of attack, Γ is negative when the line integral is taken in the counter clockwise direction. Since in the program, the line integral was taken in the counter-clockwise direction, the negative sign in Equation (2.46) gives a positive C_L when the angle of attack is positive. In evaluating Γ , as given by Equation (2.47), it should be observed that V_t varies along c_n . It is convenient to express V_t in terms of the local coordinates. It should also be noted that only the vortex contribution to V_t results in a non-zero circulation [37].

Thus:

$$\Gamma = \sum_n \sigma_v \sum_m [(e_1)_n (e_2)_m - (e_2)_n (e_1)_m] \int_{-\lambda_{n/2}}^{\lambda_{n/2}} \frac{\partial v_m}{\partial x_m} (c_n) d\bar{y} + [(e_1)_n (e_1)_m + (e_2)_n (e_2)_m] \int_{-\lambda_{n/2}}^{\lambda_{n/2}} \frac{\partial v_m}{\partial y_m} (c_n) d\bar{y} \quad (2.48)$$

where

$$x_m(c_n) = [\bar{X}_n - \bar{X}_m + (e_1)_n \bar{y}] (e_2)_m - [\bar{Y}_n - \bar{Y}_m + (e_2)_n \bar{y}] (e_1)_m \quad (2.49)$$

and

$$y_m(c_n) = [\bar{X}_n - \bar{X}_m + (e_1)_n \bar{y}] (e_1)_m + [\bar{Y}_n - \bar{Y}_m + (e_2)_n \bar{y}] (e_2)_m \quad (2.50)$$

The integrals in Equation (2.48) were calculated numerically by the use of the trapezoidal rule with 100 sub-divisions on each element.

Implicit and Hybrid Methods

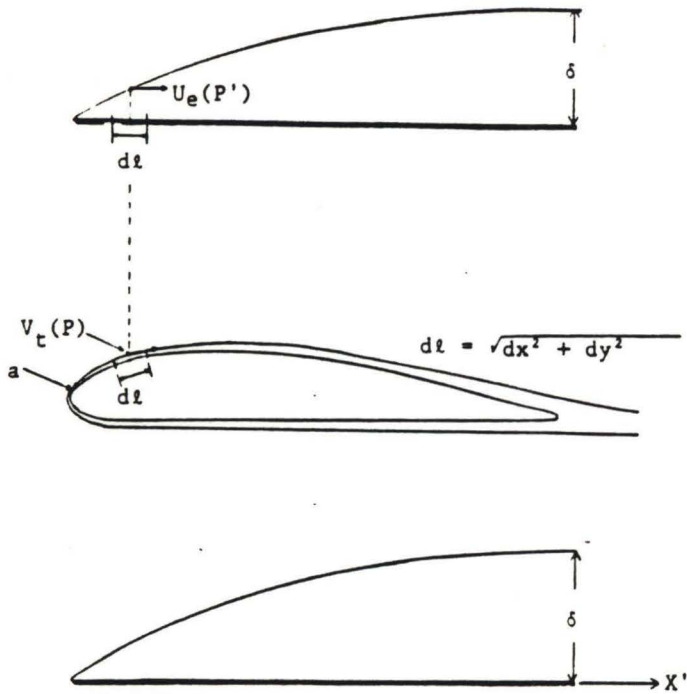
Up to this point, fluid viscous effects have not been considered. As stated before, the potential flow solution allows for a non-zero tangential velocity component on the surface of the airfoil. In reality, this premise does not agree with experimental observation. In 1904, Ludwig Prandtl demonstrated the existence of a thin boundary layer adjacent to a solid surface in a fluid flow [38]. The characteristics of boundary layer flow are:

- 1) Fluid viscous effects are important.
- 2) At normal fluid densities a "no-slip" condition exists at the wall (experimental observation).
- 3) Boundary layer thickness increases with distance downstream.
- 4) Skin friction drag is determined by wall shear stress.
- 5) Flow outside the boundary layer is inviscid.

There are several objectives in determining the boundary layer flow for the airfoils of interest. First, it is used to modify the potential flow solution, thus imposing fluid viscous effects onto the solution. This is accomplished by displacing the boundary condition from the surface of the airfoil to the edge of the boundary layer.

Second, it is used to determine the point of separation along the airfoil. Finally, it can be used to determine drag when there is no separation.

When the airfoil is thin, the geometry of the boundary layer problem may be simplified by projecting it onto two flat plates as shown:



δ boundary layer thickness

Point P' is on the flat plate and U_e is at the edge of the boundary layer. Point P is on the airfoil.

Figure 7 Airfoil to Flat Plate Coordinate Transformation

The stagnation point (point a, Figure 7) was determined through linear interpolation between the two points near the nose where the tangential velocity changes direction. Once the stagnation point is located, $U_e(P')$ is set equal to the tangential velocity ($V_t(P)$), where P is a point on the airfoil and P' is its corresponding point on the flat plate (see Figure 7). Thus, the tangential velocities at the control points on the airfoil become the $U_e(X)$ in the boundary layer equations.

The boundary layer equations are [39]:

continuity

$$\frac{\partial u}{\partial x} + \frac{\partial v}{\partial y} = 0 \quad (2.51)$$

momentum

$$u \frac{\partial u}{\partial x} + v \frac{\partial u}{\partial y} = U_e \frac{dU_e}{dx} + \nu \frac{\partial^2 u}{\partial y^2} \quad (2.52)$$

where

$$u(x,0) = v(x,0) = 0$$

$$u(x,\delta) = U_e(x)$$

To obtain the finite difference equations, one uses the first few terms of a Taylor series expansion. Using central differencing, the continuity equation becomes:

$$\frac{u_{n+1,m} - u_{n-1,m}}{2\Delta x} + \frac{v_{n,m+1} - v_{n,m-1}}{2\Delta y} = 0 \quad (2.53)$$

where $u(x_n, y_m) = u_{n,m}$. On the other hand, using forward differencing, one obtains:

$$\frac{u_{n+1,m} - u_{n,m}}{\Delta x} + \frac{v_{n,m+1} - v_{n,m}}{\Delta y} = 0 \quad (2.54)$$

In Equation (2.54), the order of error is Δx whereas in Equation (2.53), the order of error is $(\Delta x)^2$. Thus, the more accurate of the two is central differencing.

There are various schemes or approaches to solving the boundary layer equations. A discussion of two of these, explicit and implicit, follows: In the explicit method, forward differencing is used for the $\frac{\partial u}{\partial x}$ term on the left hand side of Equation (2.52), while central differencing is used for the $\frac{\partial^2 u}{\partial y^2}$ term. In addition, the latter term is evaluated at position x_n . This gives:

$$u_{n,m} \left(\frac{u_{n+1,m} - u_{n,m}}{\Delta x} \right) + v_{n,m} \left(\frac{u_{n,m+1} - u_{n,m}}{\Delta y} \right) =$$

$$(U_e)_n \frac{[U_e^{n+1} - U_e^n]}{\Delta x} + v \left(\frac{u_{n,m+1} + u_{n,m-1} - 2u_{n,m}}{(\Delta y)^2} \right) \quad (2.55)$$

Solving Equation (2.56) for $u_{n+1,m}$ yields:

$$u_{n+1,m} = u_{n,m} - \frac{\Delta x}{u_{n,m}} \left\{ v_{n,m} \left(\frac{u_{n,m+1} - u_{n,m}}{\Delta y} \right) - \frac{U_e^n [U_e^{n+1} - U_e^n]}{\Delta x} - v \left(\frac{u_{n,m+1} + u_{n,m-1} - 2u_{n,m}}{(\Delta y)^2} \right) \right\} \quad (2.56)$$

Equation (2.56) is an explicit expression for $u_{n+1,m}$, since all of the other terms are considered to be known [40].

It should be noted that explicit methods are inherently unstable [41]. In the implicit method, the differential equation is

approximated by using central differencing for the $\frac{\partial^2 u}{\partial y^2}$ term but it is evaluated at x_{n+1} [42], which gives:

$$u_{n,m} \left(\frac{u_{n+1,m} - u_{n,m}}{\Delta x} \right) + v_{n,m} \left(\frac{u_{n,m+1} - u_{n,m-1}}{2\Delta y} \right) = \frac{U_e^n [U_e^{n+1} - U_e^n]}{\Delta x} + v \left(\frac{u_{n+1,m+1} - 2u_{n+1,m} + u_{n+1,m-1}}{\Delta y^2} \right) \quad (2.57)$$

This formulation does not permit the explicit calculation of $u_{n+1,m}$ in terms of known variables and must be solved through a system of algebraic equations. However, the coefficient matrix is tri-diagonal and thus this system of equations can be solved more readily than one

that requires the use of a Gaussian elimination procedure. Implicit methods are touted to be unconditionally stable [43]. Solving Equation (2.57) for the $u_{n+1,m}$ term yields:

$$D_m U_{n+1,m} = A_m U_{n+1,m+1} + B_m U_{n+1,n-1} + C_m \quad (2.58)$$

where:

$$A_m = \frac{v}{(\Delta y)^2} + \frac{v_{n,m}}{2\Delta y}$$

$$B_m = \frac{v}{(\Delta y)^2} + \frac{v_{n,m}}{2\Delta y}$$

$$C_m = \frac{U_e^n [U_e^{n+1} - U_e^n]}{\Delta x} + \frac{(U_{n,m})^2}{\Delta x}$$

$$D_m = \left(\frac{u_{n,m}}{\Delta x} + \frac{2v}{\Delta y^2} \right)$$

This scheme is purely implicit with central differencing for the advection term. Numerical stability requires that A_m and B_m be greater than zero when $v_{n,m}$ is greater than zero. This requires:

$$\frac{v_{n,m}}{v} \Delta y > 2 \quad (2.59)$$

If one uses upwind differencing for the advection term, the numerical scheme becomes more stable. However, the truncation error of this scheme introduces an artificial viscosity which may result in an inaccurate solution [44].

A method that contains the best features of central and upwind differencing is the hybrid method. In the hybrid method, the convective term is taken as:

$$v \frac{\partial u}{\partial y} \approx \left(\frac{R_c}{R} \right) v_{n,m} \frac{(u_{n+1,m+1} - u_{n+1,m-1})}{2\Delta y} + \left(1 - \frac{R_c}{R} \right) v_{n,m} \frac{(u_{n+1,m} - u_{n+1,m-1})}{\Delta y} \quad (2.60)$$

when $v_{n,m} > 0$, and

$$v \frac{\partial u}{\partial y} \approx \left(\frac{R_c}{R} \right) v_{n,m} \frac{(u_{n+1,m+1} - u_{n+1,m-1})}{2\Delta y} + \left(1 - \frac{R_c}{R} \right) v_{n,m} \frac{(u_{n+1,m+1} - u_{n+1,m})}{\Delta y} \quad (2.61)$$

when $v_{n,m} < 0$. In the above formula, R_c is a constant ≤ 2

and R is a local Reynolds number defined by:

$$R = \frac{|v_{n,m}| \Delta y}{\nu} \quad (2.62)$$

We can see that when $R \gg 2$, upward differencing will dominate, while for R approximately equal to R_c , central differencing dominates. Incorporating the hybrid method into Equation (2.58) yields:

$$u_{n+1,m} = A_m^* u_{n+1,m+1} + B_m^* u_{n+1,m-1} + C_m^* \quad (2.63)$$

where:

$$A_m^* = \left\{ \frac{v}{\Delta y^2} - \frac{R_c}{R} \frac{v_{n,m}}{2\Delta y} - \left(1 - R_c/R \frac{v_{n,m}}{\Delta y} \right) \right\} / D_m^*$$

$$B_m^* = \left\{ \frac{v}{\Delta y^2} + \frac{R_c}{R} \frac{v_{n,m}}{2\Delta y} + \left(1 - R_c/R \frac{v_{n,m}}{\Delta y} \right) \right\} / D_m^*$$

$$C_m^* = \left\{ \frac{u_e^n}{\Delta x} \left[U_e^{n+1} - U_e^n \right] + \frac{(u_{n,m})^2}{\Delta x} \right\} / D_m^*$$

and:

$$D_m^* = \frac{u_{n,m}}{\Delta y} + \frac{2v}{\Delta y^2} \pm \left(1 - \frac{R_c}{R} \right) \frac{v_{n,m}}{\Delta y}$$

Note: Upper option is applicable for $v_{n,m} > 0$ and lower option is applicable for $v_{n,m} < 0$.

A no slip boundary condition is imposed at the wall and u is set equal to the potential velocity (U_e^n) at a y position outside of the boundary layer (see Figure 8):

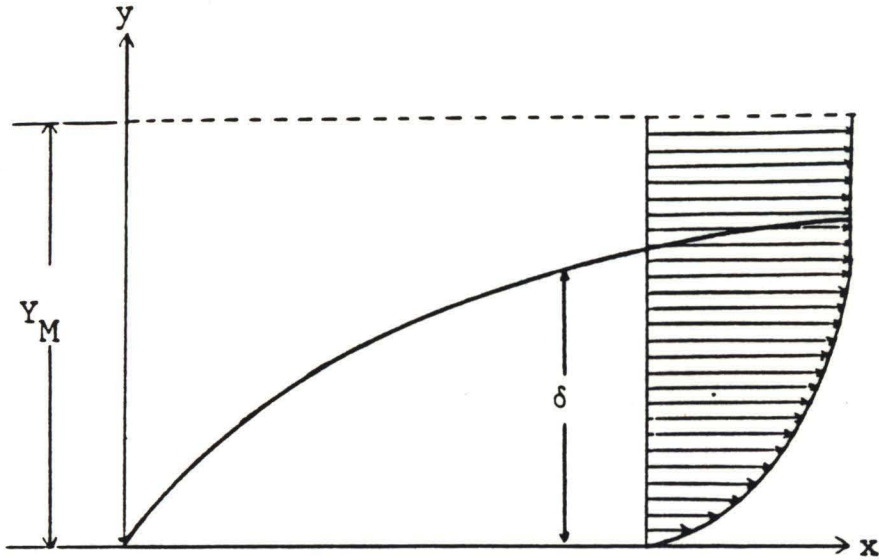


Figure 8 Boundary Layer Geometry

Therefore:

$$\text{at } y = 0: A_1 = B_1 = C_1 = 0$$

$$\text{at } y = Y_M: A_M = B_M = 0 \text{ and } C_M = U_e^n$$

where Y_M is the largest y position carried in the program and was determined by estimating the boundary layer thicknesses through experience and successive trials. The v velocity component was solved explicitly through the use of the continuity equation; i.e.

$$v_{n+1,m} = v_{n+1,m-1} - \frac{\Delta y}{2\Delta x} (u_{n+1,m} - u_{n,m} + u_{n+1,m-1} - u_{n,m-1}) \quad (2.64)$$

The use of $u_{1,m} = U_e(0)$ for all m as a starting condition results in a numerical instability. A remedy was obtained by using the Hiemenz (stagnation flow) solution near the stagnation point [45]. Hiemenz obtained a solution to the stagnation flow problem (see Figure 9) by searching for a similarity solution in the form:

$$u = Bxf'(\eta) \text{ and } v = -\sqrt{B\nu} f(\eta) \quad (2.65)$$

where:

$$\eta = y \sqrt{\frac{B}{\nu}} \quad (2.66)$$

Substituting the above into the Navier-Stokes equations gives the governing equation for f , i.e.,

$$f''' + ff'' + (1 - f^2) = 0 \quad (2.67)$$

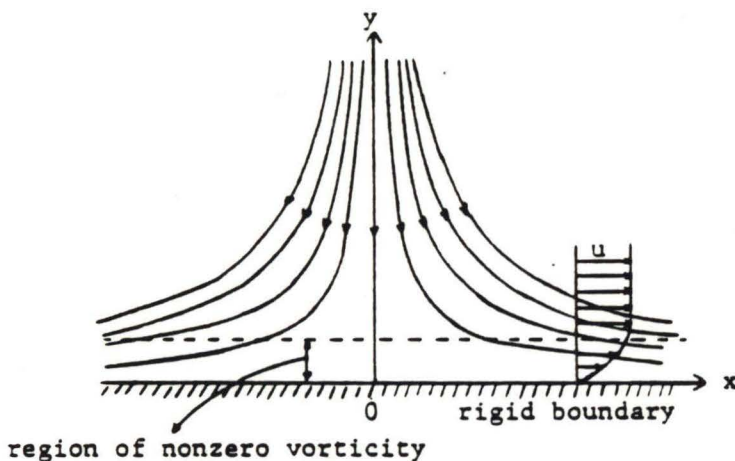


Figure 9 Stagnation Point Flow

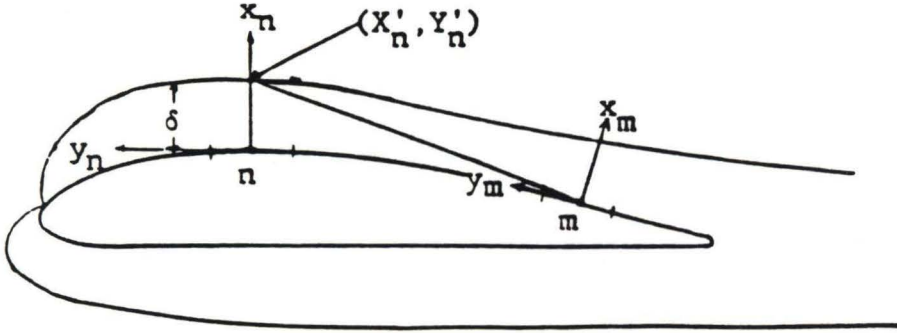
Imposing the following boundary conditions:

$$f(0) = f'(0) = 0 \text{ and } f'(\infty) \rightarrow 1.$$

values for f' and f can then be determined for a given y . This solution is used at a station just downstream of the stagnation point (at $x = 1.0 \times 10^{-6}$ ft) to provide starting values for the numerical scheme.

Values for $u_{n,m}$ and $v_{n,m}$ can now be determined. From these quantities, the boundary layer thickness, δ_n , can be obtained. δ_n was found numerically by satisfying the condition that at the edge of the boundary layer, $u(x, \delta) = .95 U_e(x)$. Linear interpolation was used to determine the position of δ_n along the y axis. A discussion on how the use of δ_n was used to improve the potential flow solution follows.

Once δ_n is determined for all n , we are in a position to modify the Neumann method to account for boundary layer thickness. This is accomplished by applying the boundary condition at the edge of the boundary layer instead of on the surface of the airfoil. This in effect lifts the potential flow solution away from the airfoil surface. The geometry of this modification is shown in Figure 10.



Note: δ is exaggerated for purposes of clarity.

Figure 10 Boundary Condition Adjustment for Boundary Layer Thickness

The (X'_n, Y'_n) coordinates are determined by:

$$X'_n = \bar{X}_n + \delta_n (\underline{e}_x)_n \cdot \underline{i} \quad (2.68)$$

and

$$Y'_n = \bar{Y}_n + \delta_n (\underline{e}_x)_n \cdot \underline{j} \quad (2.69)$$

Note: $(\underline{e}_x)_n \cdot \underline{i} = e_2$ and $(\underline{e}_x)_n \cdot \underline{j} = -e_1$ (2.70)

Thus, the local coordinates adjusted for the boundary layer thickness become:

$$\begin{aligned} x_m = & [\bar{X}_n + \delta_n (e_2)_n - \bar{X}_m] (e_2)_m - \\ & [\bar{Y}_n - \delta_n (e_1)_n - \bar{Y}_m] (e_1)_m \end{aligned} \quad (2.71)$$

and

$$y_m = [\bar{X}_n + \delta_n(e_2)_n - \bar{X}_m](e_1)_m + [\bar{Y}_n - \delta_n(e_1)_n - \bar{Y}_m](e_2)_m \quad (2.72)$$

These local coordinates are used once again to evaluate $\partial U_m/\partial x$, $\partial U_m/\partial y$, $\partial V_m/\partial x$, and $\partial V_m/\partial y$ (Equations (2.30), (2.31), (2.37) and (2.38)).

Geometric Considerations

The final item to be discussed is the airfoil geometry. Standard NACA data provides x and y coordinates along the surface of the airfoil as a percentage of the chord length (see Figure 11).

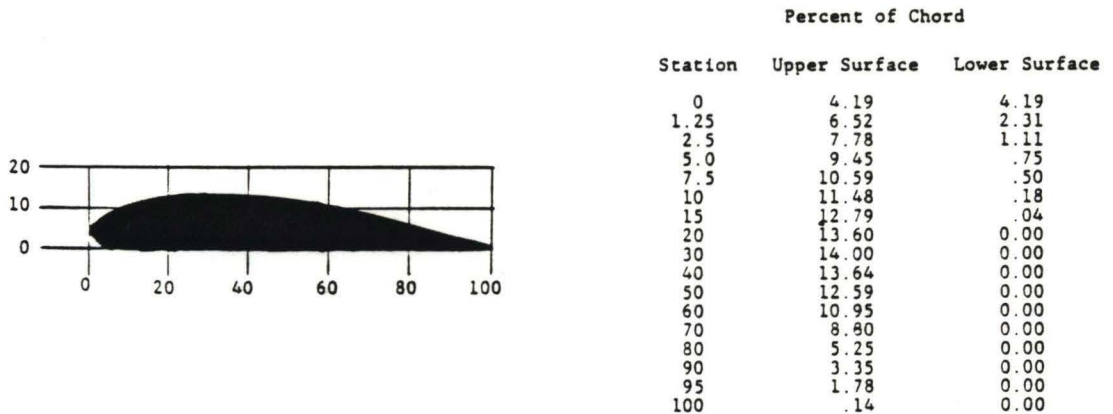


Figure 11 Sample NACA Technical Report Data

For the CY 14 and Göttingen 387 airfoils, the data plots as follows:

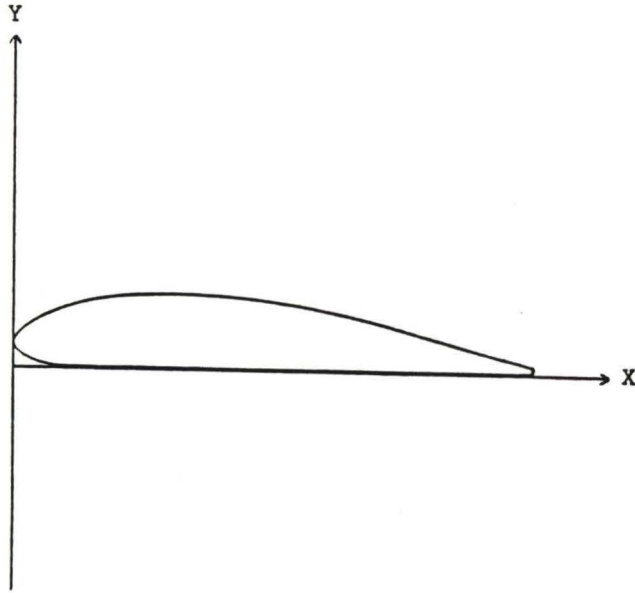


Figure 12 Before Axis Rotation of NACA Data

Since angles of attack are normally given with respect to the line connecting the nose and the trailing edge, the NACA coordinates were transformed such that the x axis runs along the chord length as shown in Figure 13.

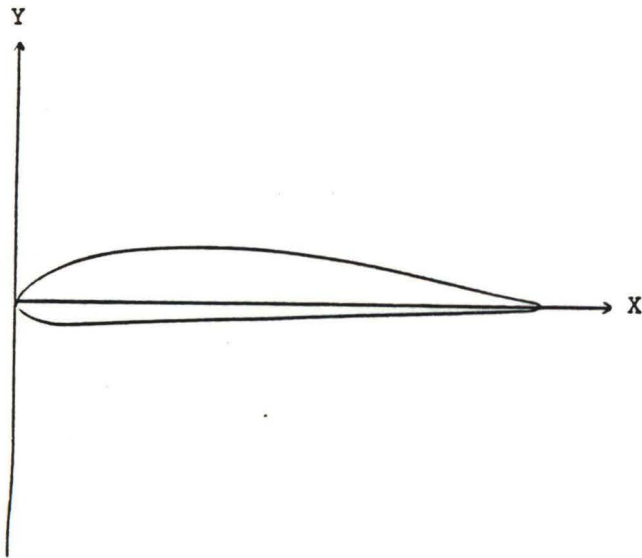


Figure 13 After Axis Rotation of NACA Data

Points were added by a cubic spline curve fitting subroutine at each five percent chord length position to refine the solution and smooth the geometry.

CHAPTER 3

DISCUSSION OF RESULTS

The results from both the Neumann (nonviscous flow) Method and Neumann/Boundary Layer Combination (viscous flow) Method were compared with the test data presented in NACA Technical Report Number 628 [46]. The technical report provides C_L versus angle of attack and C_L versus C_D for two-dimensional airfoils. The coefficient of lift was determined for angles of attack from 2° to 18° by both methods. Plots of these along with NACA test data are shown in Figures 14 - 16, Appendix B. In order to adequately compare results with the NACA test data, the slopes of the straight line portions of the graphs were determined. In the case of the NACA test data and the nonviscous flow solution, the slopes were calculated by dividing the difference of the extremes of C_L with the difference of the extremes of α . However, for the viscous flow solution, it was necessary to use a least squares fit approximation of the slope since the points did not clearly fall on a straight line. The following equation for slope was used [47]:

$$a = \frac{n \sum(x_i y_i) - (\sum x_i)(\sum y_i)}{n \sum x_i^2 - (\sum x_i)^2} \quad (3.1)$$

where:

a is the slope of the C_L vs α curve.

n is the number of data points.

x corresponds to α .

and

y corresponds to C_L .

The results of this comparison were as follows:

1. CY-14 airfoil.
 - a. NACA Test Data
a = .095 -- for angles of attack from -6° to 4° .
 - b. Nonviscous Flow Solution
a = .1219 (28.3% error)
 - c. Viscous Flow Solution
a = .099953 (5.214% error)
2. N68 airfoil.
 - a. NACA Test Data
a = .0975 -- for angles of attack from -2° to 6° .
 - b. Nonviscous Flow Solution
a = .11675 (19.74% error)
 - c. Viscous Flow Solution
a = .089614 (8.09% error)
3. Göttingen 387 airfoil.
 - a. NACA Test Data
a = .099 -- for angles of attack from -6° to 4° .

b. Nonviscous Flow Solution

$$a = .1225 \quad (23.74\% \text{ error})$$

c. Viscous Flow Solution

$$a = .10624 \quad (7.32\% \text{ error})$$

The nonviscous flow solution deviates significantly from NACA data at the higher values for angle of attack. Adding viscous flow effects improves results, particularly for these higher angles of attack. These results are reasonable in that according to Hess, applying the Kutta condition alone for smooth bodies with sharp trailing edges can result in errors as high as 20 percent [48]. Further, it should be noted that the accuracy of the solution is enhanced by as much as 15 percent when boundary layer effects are included in the solution.

Plots of coefficient of pressures versus the percent chord position for the CY-14 airfoil at angles of attack of -6° , 6° , and 12° are shown in Figures 17 thru 19, Appendix B and tables 1 thru 3, Appendix A. At -6° angles of attack, the upper surfaces values for C_p are positive near the leading edge and turn negative at X/L equal to .1; the lower surface C_p values begin negative and turn positive at X/L equal to .77. However, the area between the lower and upper surface C_p curves is less in front than in rear, thus, the overall lift is negative.

For a positive angle of attack, such as 6° , the C_p values for the lower surface remain positive while for the upper surface they remain negative. This leads to a positive value for lift. Although, the anticipated "flattening" out of the upper surface curve failed to

materialize after flow separation (see Figure 19, Appendix B), the overall characteristics of these curves plot as expected. To further illustrate this, C_p values derived by Hemke for the NACA 4412 airfoil at -2° angle of attack [49] are compared with C_p values derived by the viscous flow solution (see Figure 20, Appendix B).). As can be seen, good agreement exists between the two.

Plots of the wall shear stress, τ_w , versus X' position along the flat plate are shown in Figures 21 thru 23, Appendix B. The salient feature of this family of curves is to show whether or not the flow separates as a result of the value for τ_w becoming negative. One can note that for the laminar region of flow (low angles of attack), the value for τ_w gradually reduces to zero whereas the degradation of this value becomes acute for the higher angles of attack where the flow separates. These results correlate well with observed phenomenon.

The locations of the points of separation on both the upper and lower surfaces at several different angles of attack are shown in Figure 24, Appendix B. It can be seen that at -8° angle of attack, the separation point is on the lower surface. For angles of attack greater than 10° , separation occurs on the upper surface and moves closer to the nose of the airfoil as the angle of attack increases. These results appear to correlate well with physical reality.

Typical computer time to complete the nonviscous solution for an angle of attack was 2 minutes and 47.01 seconds. The number of iterations necessary to satisfy the Kutta condition was typically 39.

For the viscous solution, computer time expended was 5 minutes and 28.53 seconds with convergence occurring within 41 iterations. For the boundary layer subroutine, a mesh size of approximately .01055 ft in the x direction (24 steps) and 1.25×10^{-5} ft in the y direction (80 steps) was used.

CHAPTER 4

CONCLUSIONS AND RECOMMENDATIONS

After many months of work on this method, we have come to the following realizations:

1. The Neumann Method is a very powerful method for determining all types of flows about complex geometric figures.
2. The accuracy of this method can be greatly enhanced by combining the Neumann Method with a boundary layer algorithm. It is the boundary layer algorithm that appears to be the weakest part of the program and is therefore the area that can be improved the most. A copy of the algorithm developed for this thesis is given in Appendix C.

Before I discuss possible improvements in the boundary layer algorithm, I would like to touch lightly on a possible improvement to the potential flow solution. According to Douglas Aircraft Company, for two-dimensional or axisymmetric bodies, a minimum of 60 elements must be used to acquire needed accuracy [50]. Since the NACA data did not provide that many data points for the airfoil profile, a cubic spline routine had to be used to create additional profile points. Points were obtained at every 2.5 percent chord (which exceeded this 60 element minimum) as well as at every 5 percent chord (which did not satisfy this 60 element minimum). The use of points at every 2.5

percent chord resulted in only a minimal improvement in the results (i.e., to the third place in the lift coefficient). Therefore, this was discounted as a possible method for meaningful improvement.

We also tried sub-dividing the elements adjacent to the trailing edge into several elements, thus, moving the points of application of the Kutta condition closer together. We found that if the points where the Kutta condition is applied are too close, the iteration scheme for determining σ_v did not converge. Further investigation on selecting an optimum size for the elements adjacent to the trailing edge is warranted.

As can be seen by the references (i.e., [3 -14] in particular), much work has already been done in the area of boundary layer theory, including the method used in this thesis. An alternate method for treating the boundary layer problem was given by Smith/Clutter. They used non-dimensional variables obtained in the similarity solution method for a flat plate and combined it with an implicit finite difference method [51]. This effort resulted in circumventing the singularity problem at the stagnation point. Even though this method holds much promise, there is a hint of stability problems with the velocity profile [52]. It should be noted that the method employed in this thesis is not without these same problems. In fact, the velocity profiles at several stations just downstream from the stagnation point showed a bulge instead of the asymptotic behavior as expected in boundary layer theory. However, when the algorithm used in this thesis was employed in the flat plate problem and compared with the

Blasius closed form solution, reasonable agreement in the velocity profiles was obtained (see Tables 4 thru 7, Appendix A). We suspect that the overall results can be improved by the use of the Smith/Clutter approach.

Another possible area for improvement, is to modify the boundary condition at the edge of the boundary layer [53]. In our algorithm, we displaced the zero normal velocity component at the surfaces of the airfoil to the edge of the boundary layer. However, due to the viscous effects along the body of the airfoil, fluid is entrained into the boundary layer, resulting in a non-zero (but small) normal velocity component. When we applied the normal velocity component obtained in the boundary layer algorithm to correct the Neumann Method (tier 3), we obtained a coefficient of lift that significantly deviated from the NACA data. This led us to conclude that the v values obtained in the boundary layer algorithm were not sufficiently accurate to yield good results.

Finally, more sophisticated flow models could be used to account for the existence of a wake (when flow separation occurs) or the onset of turbulence [54]. Since the flow speeds analyzed in this paper required only a laminar approximation (i.e., Reynolds number never met nor exceeded the critical Reynolds number necessary for turbulence), there was no need to include a turbulent model. The inclusion of a wake model was beyond the scope of this thesis.

Based on the obtained results, the following conclusions can be made:

1. The results obtained by the Neumann Method agreed reasonably well with documented test data.
2. Results can be further enhanced by imposing the effects of laminar, viscous flow on the potential flow solution via a viscous boundary layer theory.
3. There is potential for improvement.
4. The use of numerical methods can close the void left by analytical closed form methods, particularly when the flow is about irregular shaped bodies.

APPENDIX A

Table 1 Data Table for CY-J4 Airfoil at $\alpha = -6^\circ$

LIFT COEFFICIENT - -0.160						
ANGLE OF ATTACK (DEGREES)	FREE STREAM VELOCITY (FT/SEC)	CHORD LENGTH (INCHES)	AMBIENT PRESSURE (LBF/SQFT)	DENSITY (LBM/CUFT)	VORTEX ST	QTH
-6.00	70.40	5.0	2116.2	0.0735	0.4376	00
STATION	X/L	TANGENTIAL VELOCITY	COMPUTED VALUE OF CP	LOCAL PRES. D		
1	.00625	0.12905E+03	-0.23602E+01	-0.13361E+0		
2	.01875	0.13871E+03	-0.28823E+01	-0.16317E+0		
3	.03750	0.11972E+03	-0.18919E+01	-0.10710E+0		
4	.06250	0.10843E+03	-0.13722E+01	-0.77680E+0		
5	.08750	0.10170E+03	-0.10868E+01	-0.61522E+0		
6	.12500	0.95817E+02	-0.85244E+00	-0.48257E+0		
7	.17500	0.90229E+02	-0.64266E+00	-0.36381E+0		
8	.22500	0.85781E+02	-0.48471E+00	-0.27440E+0		
9	.27500	0.82725E+02	-0.38078E+00	-0.21556E+0		
10	.32500	0.80604E+02	-0.31090E+00	-0.17600E+0		
11	.37500	0.78739E+02	-0.25093E+00	-0.14205E+0		
12	.42500	0.77238E+02	-0.20369E+00	-0.11531E+0		
13	.47500	0.76024E+02	-0.16614E+00	-0.94053E+0		
14	.52500	0.74924E+02	-0.13264E+00	-0.75088E+0		
15	.57500	0.73877E+02	-0.10122E+00	-0.57303E+0		
16	.62500	0.72882E+02	-0.71746E-01	-0.40616E+0		
17	.67500	0.71904E+02	-0.43182E-01	-0.24446E+0		
18	.72500	0.70924E+02	-0.14947E-01	-0.84613E-0		
19	.77500	0.69886E+02	0.14535E-01	0.82286E-0		
20	.82500	0.68761E+02	0.46029E-01	0.26057E+0		
21	.87500	0.67497E+02	0.81858E-01	0.46340E+0		
22	.92500	0.65769E+02	0.12725E+00	0.72034E+0		
23	.97500	0.62808E+02	0.20406E+00	0.11552E+0		
24	.97500	-0.62808E+02	0.20406E+00	0.11552E+0		
25	.92500	-0.68963E+02	0.40398E-01	0.22869E+0		
26	.87500	-0.72086E+02	-0.48480E-01	-0.27445E+0		
27	.82500	-0.74122E+02	-0.10852E+00	-0.61434E+0		
28	.77500	-0.76302E+02	-0.17471E+00	-0.98906E+0		
29	.72500	-0.77597E+02	-0.21490E+00	-0.12166E+0		
30	.67500	-0.79476E+02	-0.27445E+00	-0.15537E+0		
31	.62500	-0.80336E+02	-0.30220E+00	-0.17108E+0		
32	.57500	-0.82002E+02	-0.35675E+00	-0.20196E+0		
33	.52500	-0.82147E+02	-0.36155E+00	-0.20468E+0		
34	.47500	-0.83389E+02	-0.40305E+00	-0.22817E+0		
35	.42500	-0.82706E+02	-0.38015E+00	-0.21520E+0		
36	.37500	-0.84191E+02	-0.43017E+00	-0.24352E+0		
37	.32500	-0.82313E+02	-0.37372E+00	-0.21156E+0		
38	.27500	-0.81175E+02	-0.32952E+00	-0.18654E+0		
39	.22500	-0.81414E+02	-0.33736E+00	-0.19098E+0		
40	.17500	-0.77751E+02	-0.21975E+00	-0.12440E+0		
41	.12500	-0.70493E+02	-0.26461E-02	-0.14980E-0		
42	.08750	-0.64096E+02	0.17106E+00	0.96839E+0		
43	.06250	-0.56730E+02	0.35065E+00	0.19851E+0		
44	.03750	-0.40016E+02	0.67691E+00	0.38200E+0		
45	.01875	-0.17473E+02	0.93840E+00	0.53123E+0		
46	.00625	0.29507E+02	0.82432E+00	0.46665E+0		

Table 2 Data Table for CY-14 Airfoil at $\alpha = 6^\circ$

LIFT COEFFICIENT - 1.122

ANGLE OF ATTACK (DEGREES)	FREE STREAM VELOCITY (FT/SEC)	CHORD LENGTH (INCHES)	AMBIENT PRESSURE (LBF/SQFT)	DENSITY (LBM/CUFT)	VORTEX ST	QTH
6.00	70.40	5.0	2116.2	0.0735	-0.3069	01
STATION	X/L	TANGENTIAL VELOCITY	COMPUTED VALUE OF CP	LOCAL PRES. D		
1	.00625	-0.18254E+02	0.93277E+00	0.52805E+0		
2	.01875	0.34820E+02	0.75536E+00	0.42762E+0		
3	.03750	0.45837E+02	0.57607E+00	0.32612E+0		
4	.06250	0.53519E+02	0.42207E+00	0.23894E+0		
5	.08750	0.56166E+02	0.36350E+00	0.20578E+0		
6	.12500	0.58785E+02	0.30276E+00	0.17139E+0		
7	.17500	0.61001E+02	0.24919E+00	0.14107E+0		
8	.22500	0.61836E+02	0.22850E+00	0.12936E+0		
9	.27500	0.61988E+02	0.22471E+00	0.12721E+0		
10	.32500	0.62403E+02	0.21428E+00	0.12131E+0		
11	.37500	0.62833E+02	0.20341E+00	0.11515E+0		
12	.42500	0.63061E+02	0.19763E+00	0.11188E+0		
13	.47500	0.63385E+02	0.18935E+00	0.10719E+0		
14	.52500	0.63720E+02	0.18076E+00	0.10233E+0		
15	.57500	0.63975E+02	0.17421E+00	0.98621E+0		
16	.62500	0.64134E+02	0.17010E+00	0.96293E+0		
17	.67500	0.64057E+02	0.17207E+00	0.97412E+0		
18	.72500	0.63695E+02	0.18141E+00	0.10270E+0		
19	.77500	0.63329E+02	0.19080E+00	0.10801E+0		
20	.82500	0.62931E+02	0.20093E+00	0.11375E+0		
21	.87500	0.62479E+02	0.21237E+00	0.12022E+0		
22	.92500	0.61618E+02	0.23392E+00	0.13243E+0		
23	.97500	0.60598E+02	0.25908E+00	0.14667E+0		
24	.97500	-0.60598E+02	0.25908E+00	0.14667E+0		
25	.92500	-0.70245E+02	0.44043E-02	0.24933E-0		
26	.87500	-0.74315E+02	-0.11431E+00	-0.64713E+0		
27	.82500	-0.78447E+02	-0.24168E+00	-0.13681E+0		
28	.77500	-0.81024E+02	-0.32458E+00	-0.18375E+0		
29	.72500	-0.84885E+02	-0.45386E+00	-0.25693E+0		
30	.67500	-0.86804E+02	-0.52830E+00	-0.29455E+0		
31	.62500	-0.90672E+02	-0.65883E+00	-0.37297E+0		
32	.57500	-0.92330E+02	-0.72006E+00	-0.40763E+0		
33	.52500	-0.96038E+02	-0.86098E+00	-0.48741E+0		
34	.47500	-0.97280E+02	-0.90941E+00	-0.51482E+0		
35	.42500	-0.10072E+03	-0.10468E+01	-0.59259E+0		
36	.37500	-0.10211E+03	-0.11038E+01	-0.62485E+0		
37	.32500	-0.10604E+03	-0.12686E+01	-0.71815E+0		
38	.27500	-0.10617E+03	-0.12745E+01	-0.72152E+0		
39	.22500	-0.10998E+03	-0.14405E+01	-0.81548E+0		
40	.17500	-0.11391E+03	-0.16182E+01	-0.91609E+0		
41	.12500	-0.11442E+03	-0.16418E+01	-0.92941E+0		
42	.08750	-0.11640E+03	-0.17338E+01	-0.98150E+0		
43	.06250	-0.11700E+03	-0.17620E+01	-0.99746E+0		
44	.03750	-0.11514E+03	-0.16747E+01	-0.94808E+0		
45	.01875	-0.11171E+03	-0.15180E+01	-0.85935E+0		
46	.00625	-0.96713E+02	-0.88721E+00	-0.50225E+0		

Table 3 Data Table for CY-J4 Airfoil at $\alpha = 12^\circ$

LIFT COEFFICIENT - 1.580

ANGLE OF ATTACK (DEGREES)	FREE STREAM VELOCITY (FT/SEC)	CHORD LENGTH (INCHES)	AMBIENT PRESSURE (LBF/SQFT)	DENSITY (LBM/CUFT)	VORTEX ST	QTH
12.00	70.40	5.0	2116.2	0.0735	-0.4321	01
STATION	X/L	TANGENTIAL VELOCITY	COMPUTED VALUE OF CP	LOCAL PRES. D		
1	.00625	-0.77534E+02	-0.21294E+00	-0.12055E+0		
2	.01875	-0.76326E+01	0.98825E+00	0.55945E+0		
3	.03750	0.15816E+02	0.94953E+00	0.53753E+0		
4	.06250	0.31616E+02	0.79832E+00	0.45193E+0		
5	.08750	0.37981E+02	0.70893E+00	0.40133E+0		
6	.12500	0.44024E+02	0.60896E+00	0.34473E+0		
7	.17500	0.49661E+02	0.50238E+00	0.28440E+0		
8	.22500	0.52837E+02	0.43672E+00	0.24723E+0		
9	.27500	0.54441E+02	0.40198E+00	0.22757E+0		
10	.32500	0.55951E+02	0.36836E+00	0.20853E+0		
11	.37500	0.57285E+02	0.33788E+00	0.19128E+0		
12	.42500	0.58114E+02	0.31859E+00	0.18036E+0		
13	.47500	0.58834E+02	0.30160E+00	0.17074E+0		
14	.52500	0.59202E+02	0.29283E+00	0.16577E+0		
15	.57500	0.59094E+02	0.29540E+00	0.16723E+0		
16	.62500	0.58990E+02	0.29789E+00	0.16864E+0		
17	.67500	0.59056E+02	0.29630E+00	0.16774E+0		
18	.72500	0.59146E+02	0.29416E+00	0.16652E+0		
19	.77500	0.59208E+02	0.29268E+00	0.16569E+0		
20	.82500	0.59131E+02	0.29452E+00	0.16673E+0		
21	.87500	0.59000E+02	0.29763E+00	0.16849E+0		
22	.92500	0.58472E+02	0.31016E+00	0.17558E+0		
23	.97500	0.58172E+02	0.31722E+00	0.17938E+0		
24	.97500	-0.58171E+02	0.31723E+00	0.17939E+0		
25	.92500	-0.68798E+02	0.44980E-01	0.25464E+0		
26	.87500	-0.73035E+02	-0.76246E-01	-0.43163E+0		
27	.82500	-0.77894E+02	-0.22424E+00	-0.12695E+0		
28	.77500	-0.80608E+02	-0.31103E+00	-0.17608E+0		
29	.72500	-0.85532E+02	-0.47607E+00	-0.26951E+0		
30	.67500	-0.87619E+02	-0.54901E+00	-0.31080E+0		
31	.62500	-0.92917E+02	-0.74198E+00	-0.42004E+0		
32	.57500	-0.94960E+02	-0.81942E+00	-0.46388E+0		
33	.52500	-0.10058E+03	-0.10411E+01	-0.58935E+0		
34	.47500	-0.10264E+03	-0.11255E+01	-0.63718E+0		
35	.42500	-0.10924E+03	-0.14078E+01	-0.79695E+0		
36	.37500	-0.11137E+03	-0.15025E+01	-0.85059E+0		
37	.32500	-0.11554E+03	-0.16935E+01	-0.95869E+0		
38	.27500	-0.11510E+03	-0.16729E+01	-0.94705E+0		
39	.22500	-0.11926E+03	-0.18699E+01	-0.10586E+0		
40	.17500	-0.12513E+03	-0.21594E+01	-0.12225E+0		
41	.12500	-0.12850E+03	-0.23317E+01	-0.13200E+0		
42	.08750	-0.13431E+03	-0.26397E+01	-0.14943E+0		
43	.06250	-0.13812E+03	-0.28492E+01	-0.16129E+0		
44	.03750	-0.14270E+03	-0.31085E+01	-0.17598E+0		
45	.01875	-0.14745E+03	-0.33868E+01	-0.19173E+0		
46	.00625	-0.14577E+03	-0.32876E+01	-0.18611E+0		

Table 4 Table Depicting Comparison of Blasius Closed Form Solution of a Flat Plate to Numerical Solution at X = 0.0

COORDINATE	U VELOCITY	V VELOCITY	BLAS U VEL	BLAS V VEL
0.0000	0.7000	0.0000	0.7000	0.0000
0.0002	0.7000	0.0000	0.7000	0.0000
0.0003	0.7000	0.0000	0.7000	0.0000
0.0005	0.7000	0.0000	0.7000	0.0000
0.0006	0.7000	0.0000	0.7000	0.0000
0.0008	0.7000	0.0000	0.7000	0.0000
0.0011	0.7000	0.0000	0.7000	0.0000
0.0012	0.7000	0.0000	0.7000	0.0000
0.0014	0.7000	0.0000	0.7000	0.0000
0.0015	0.7000	0.0000	0.7000	0.0000
0.0016	0.7000	0.0000	0.7000	0.0000
0.0018	0.7000	0.0000	0.7000	0.0000
0.0019	0.7000	0.0000	0.7000	0.0000
0.0021	0.7000	0.0000	0.7000	0.0000
0.0022	0.7000	0.0000	0.7000	0.0000
0.0024	0.7000	0.0000	0.7000	0.0000
0.0025	0.7000	0.0000	0.7000	0.0000
0.0027	0.7000	0.0000	0.7000	0.0000
0.0028	0.7000	0.0000	0.7000	0.0000
0.0030	0.7000	0.0000	0.7000	0.0000
0.0031	0.7000	0.0000	0.7000	0.0000
0.0033	0.7000	0.0000	0.7000	0.0000
0.0034	0.7000	0.0000	0.7000	0.0000
0.0036	0.7000	0.0000	0.7000	0.0000
0.0037	0.7000	0.0000	0.7000	0.0000
0.0039	0.7000	0.0000	0.7000	0.0000
0.0040	0.7000	0.0000	0.7000	0.0000
0.0042	0.7000	0.0000	0.7000	0.0000
0.0044	0.7000	0.0000	0.7000	0.0000
0.0045	0.7000	0.0000	0.7000	0.0000
0.0047	0.7000	0.0000	0.7000	0.0000
0.0048	0.7000	0.0000	0.7000	0.0000
0.0050	0.7000	0.0000	0.7000	0.0000
0.0051	0.7000	0.0000	0.7000	0.0000
0.0053	0.7000	0.0000	0.7000	0.0000
0.0054	0.7000	0.0000	0.7000	0.0000
0.0056	0.7000	0.0000	0.7000	0.0000
0.0057	0.7000	0.0000	0.7000	0.0000
0.0059	0.7000	0.0000	0.7000	0.0000
0.0060	0.7000	0.0000	0.7000	0.0000
0.0063	0.7000	0.0000	0.7000	0.0000
0.0065	0.7000	0.0000	0.7000	0.0000
0.0066	0.7000	0.0000	0.7000	0.0000
0.0069	0.7000	0.0000	0.7000	0.0000
0.0071	0.7000	0.0000	0.7000	0.0000
0.0072	0.7000	0.0000	0.7000	0.0000
0.0074	0.7000	0.0000	0.7000	0.0000
0.0075	0.7000	0.0000	0.7000	0.0000
0.0077	0.7000	0.0000	0.7000	0.0000
0.0078	0.7000	0.0000	0.7000	0.0000
0.0080	0.7000	0.0000	0.7000	0.0000
0.0081	0.7000	0.0000	0.7000	0.0000
0.0083	0.7000	0.0000	0.7000	0.0000
0.0084	0.7000	0.0000	0.7000	0.0000
0.0086	0.7000	0.0000	0.7000	0.0000
0.0087	0.7000	0.0000	0.7000	0.0000
0.0089	0.7000	0.0000	0.7000	0.0000
0.0090	0.7000	0.0000	0.7000	0.0000
0.0092	0.7000	0.0000	0.7000	0.0000
0.0093	0.7000	0.0000	0.7000	0.0000
0.0095	0.7000	0.0000	0.7000	0.0000
0.0096	0.7000	0.0000	0.7000	0.0000
0.0098	0.7000	0.0000	0.7000	0.0000
0.0099	0.7000	0.0000	0.7000	0.0000
0.0101	0.7000	0.0000	0.7000	0.0000
0.0102	0.7000	0.0000	0.7000	0.0000
0.0104	0.7000	0.0000	0.7000	0.0000
0.0105	0.7000	0.0000	0.7000	0.0000
0.0107	0.7000	0.0000	0.7000	0.0000
0.0108	0.7000	0.0000	0.7000	0.0000
0.0110	0.7000	0.0000	0.7000	0.0000
0.0111	0.7000	0.0000	0.7000	0.0000
0.0112	0.7000	0.0000	0.7000	0.0000
0.0114	0.7000	0.0000	0.7000	0.0000
0.0115	0.7000	0.0000	0.7000	0.0000
0.0117	0.7000	0.0000	0.7000	0.0000
0.0118	0.7000	0.0000	0.7000	0.0000
0.0120	0.7000	0.0000	0.7000	0.0000

APPENDIX B

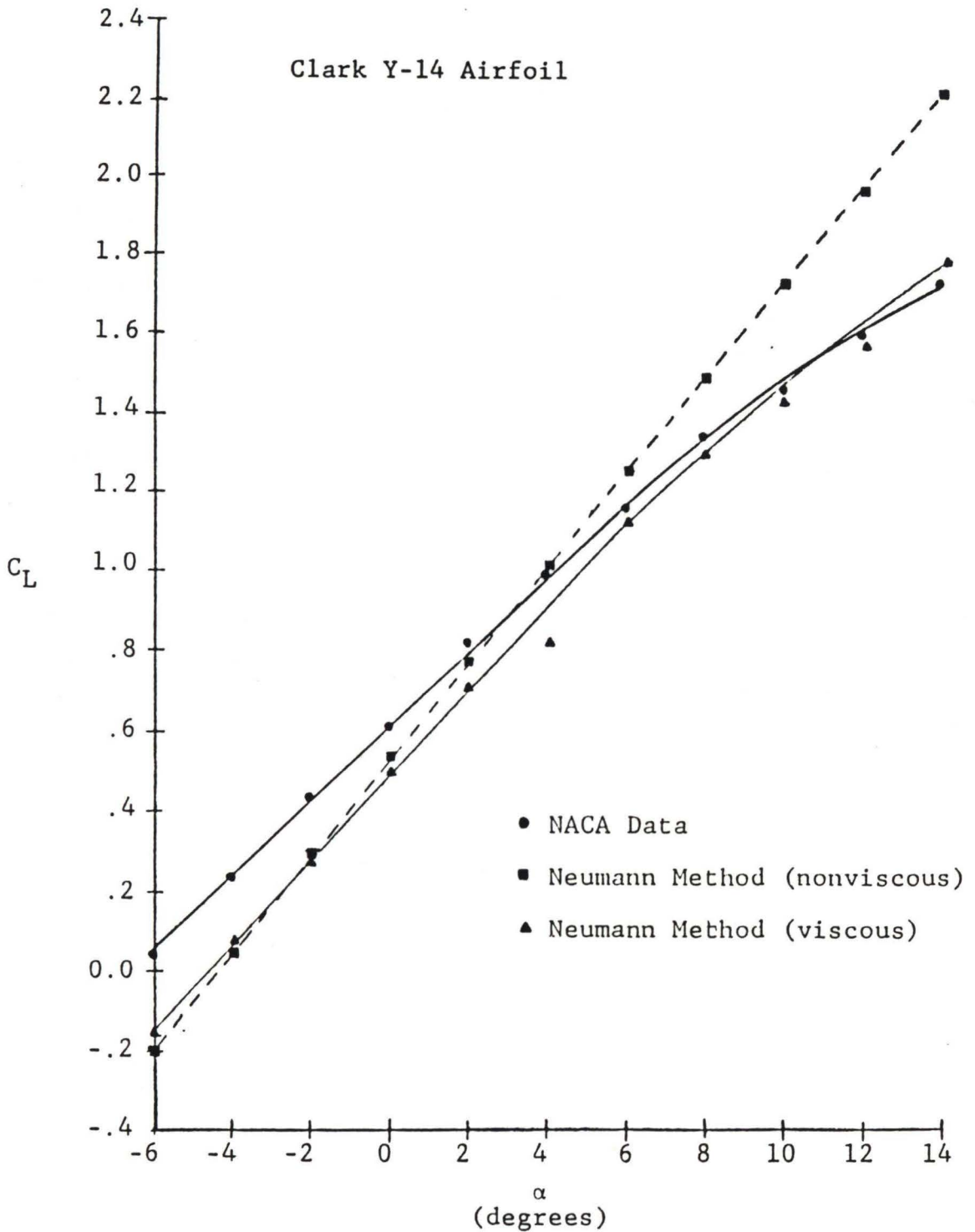


Figure 14 Graph Depicting C_L vs α for CY-14 Airfoil

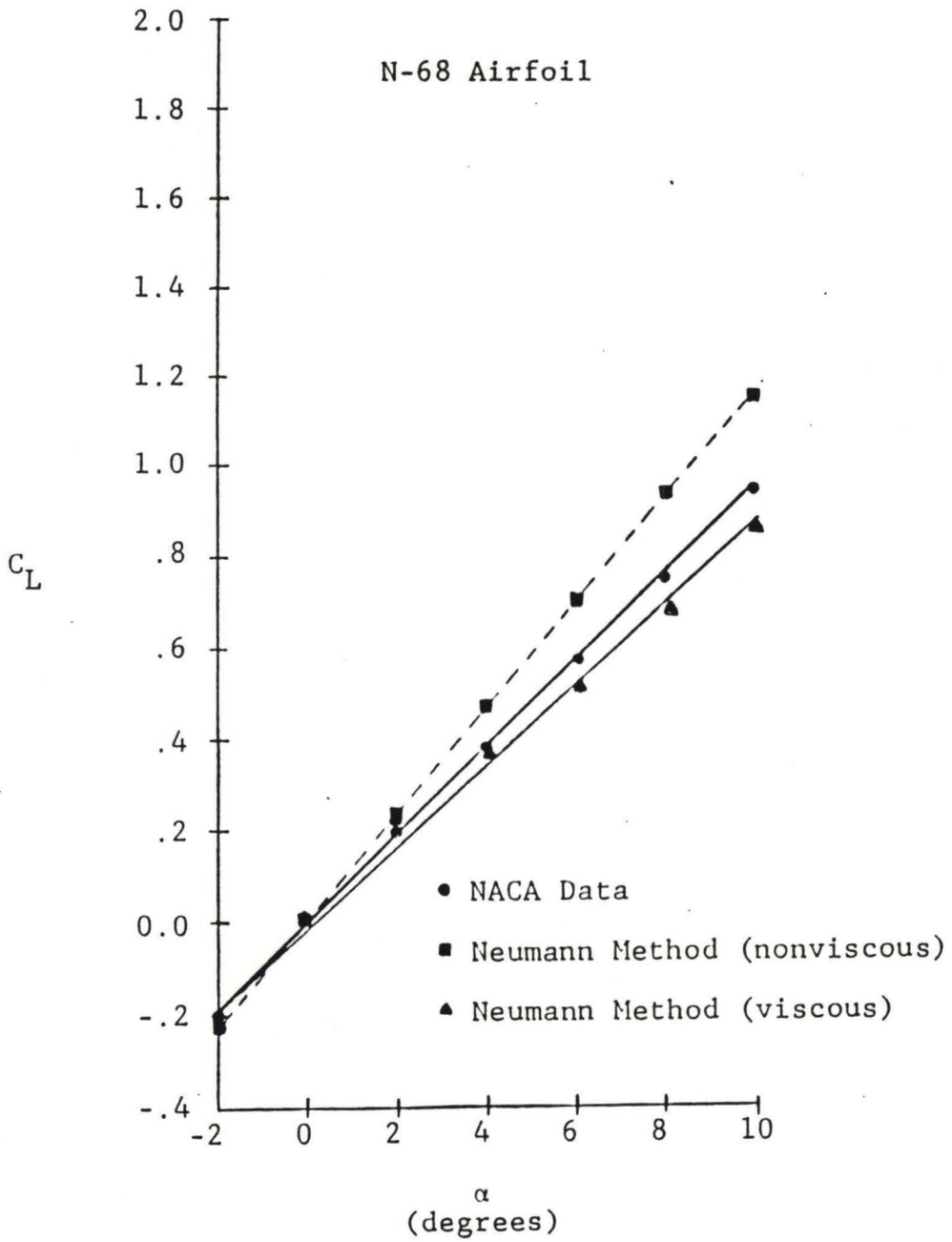


Figure 15 Graph Depicting C_L vs α for N-68 Airfoil

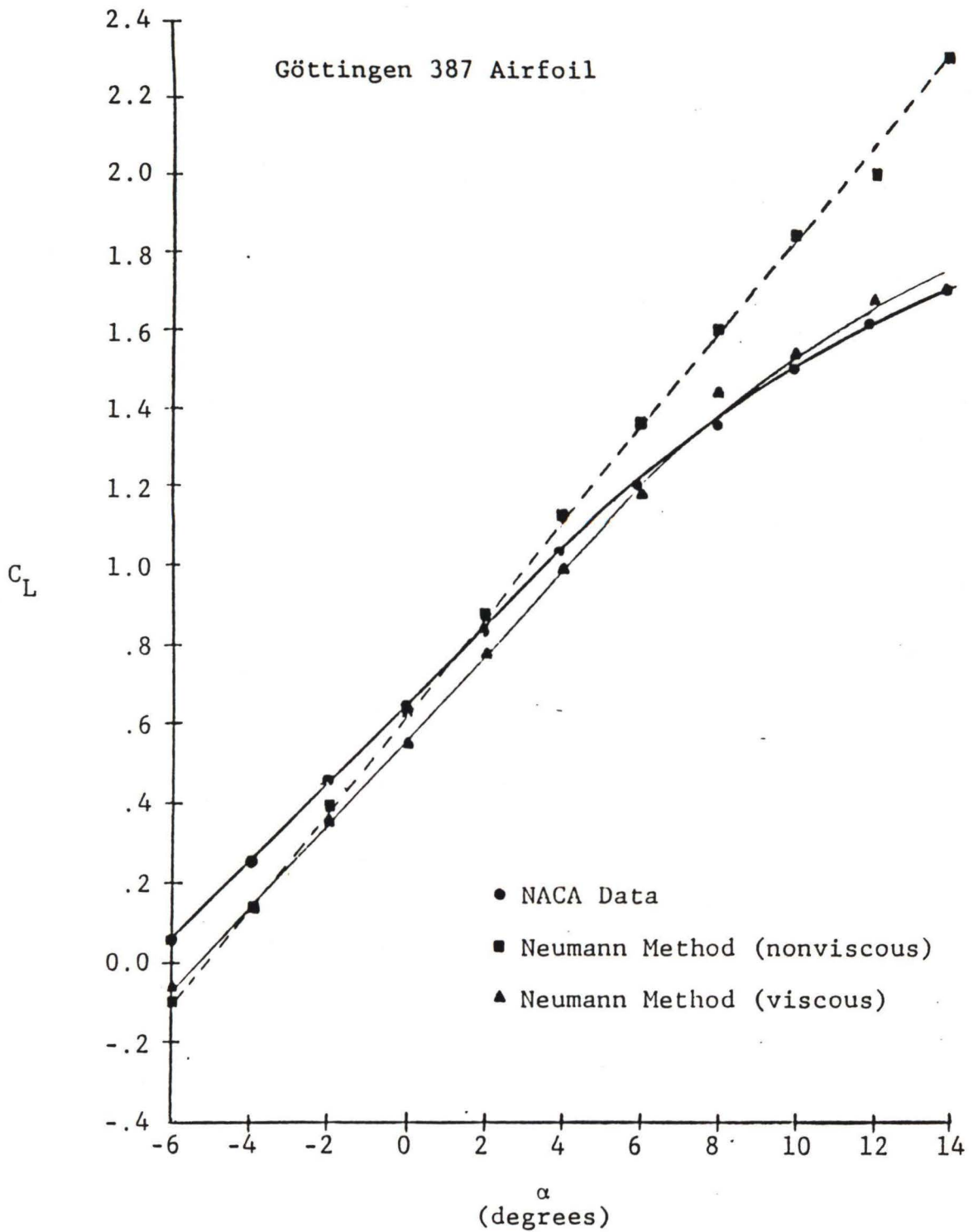


Figure 16 Graph Depicting C_L vs α for Göttingen 387 Airfoil

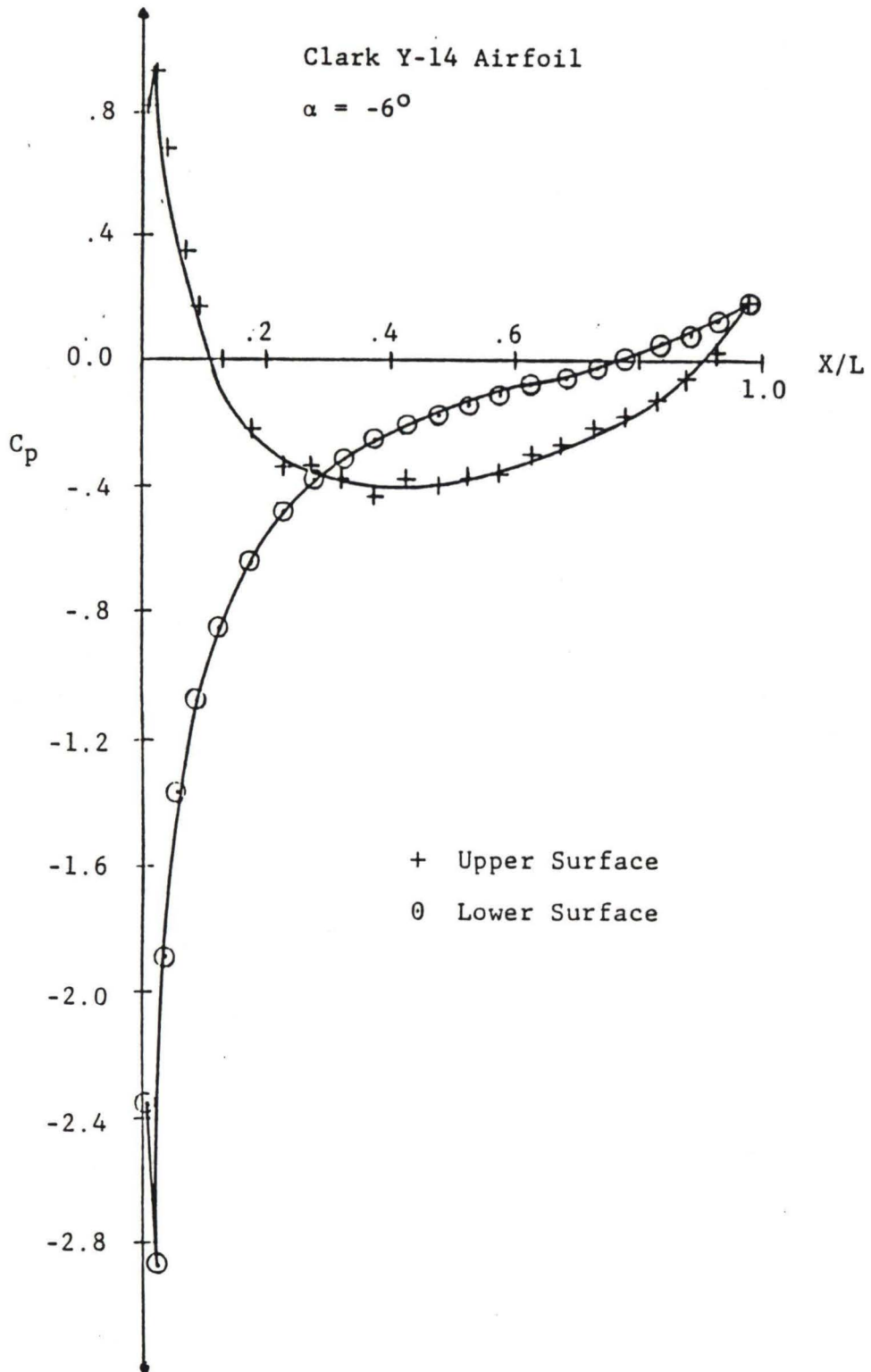


Figure 17 Graph Depicting C_p vs X/L for $\alpha = -6^\circ$ (CY-14 Airfoil)

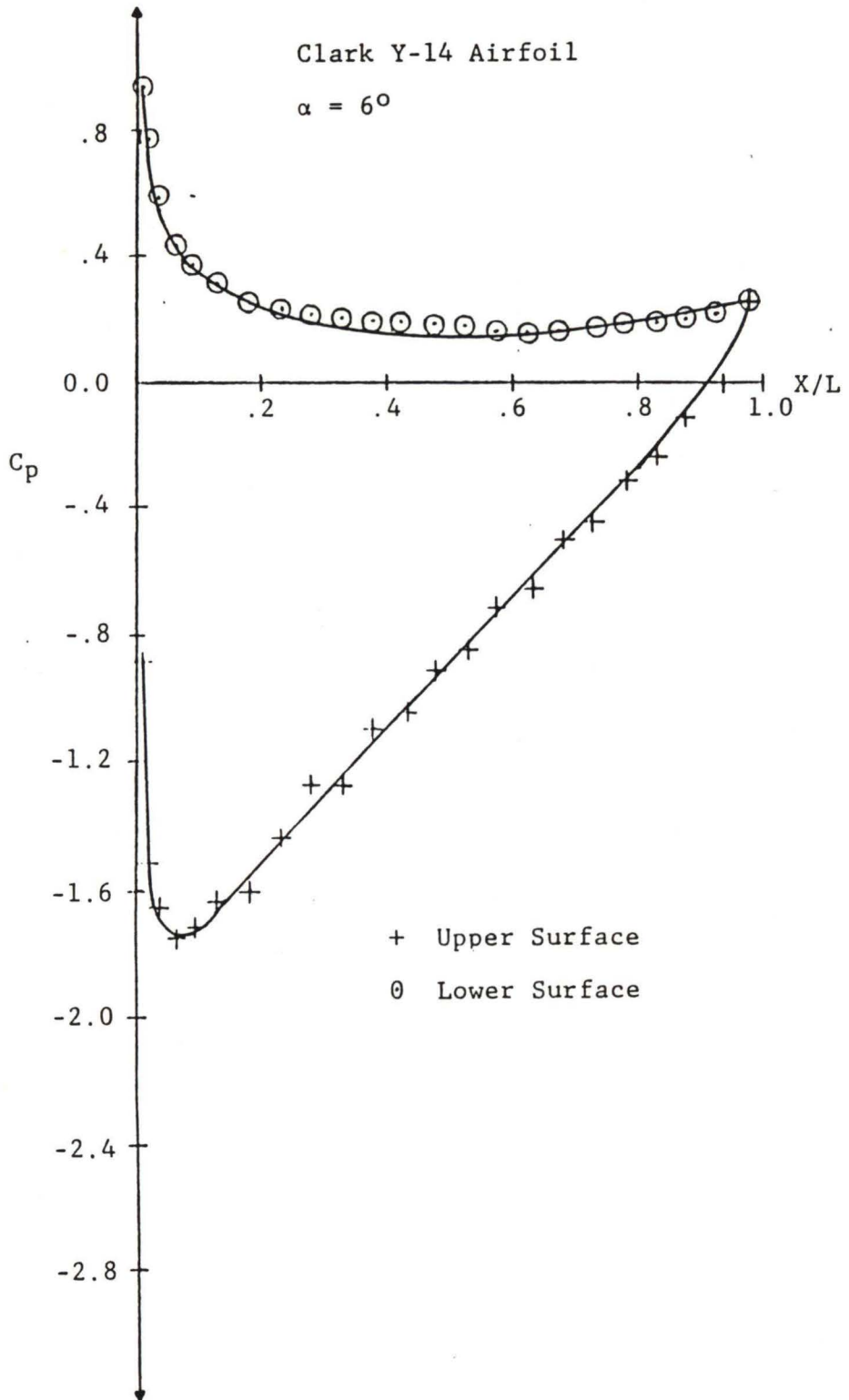


Figure 13 Graph Depicting C_p vs X/L for $\alpha = 6^\circ$ (CY-14 Airfoil)

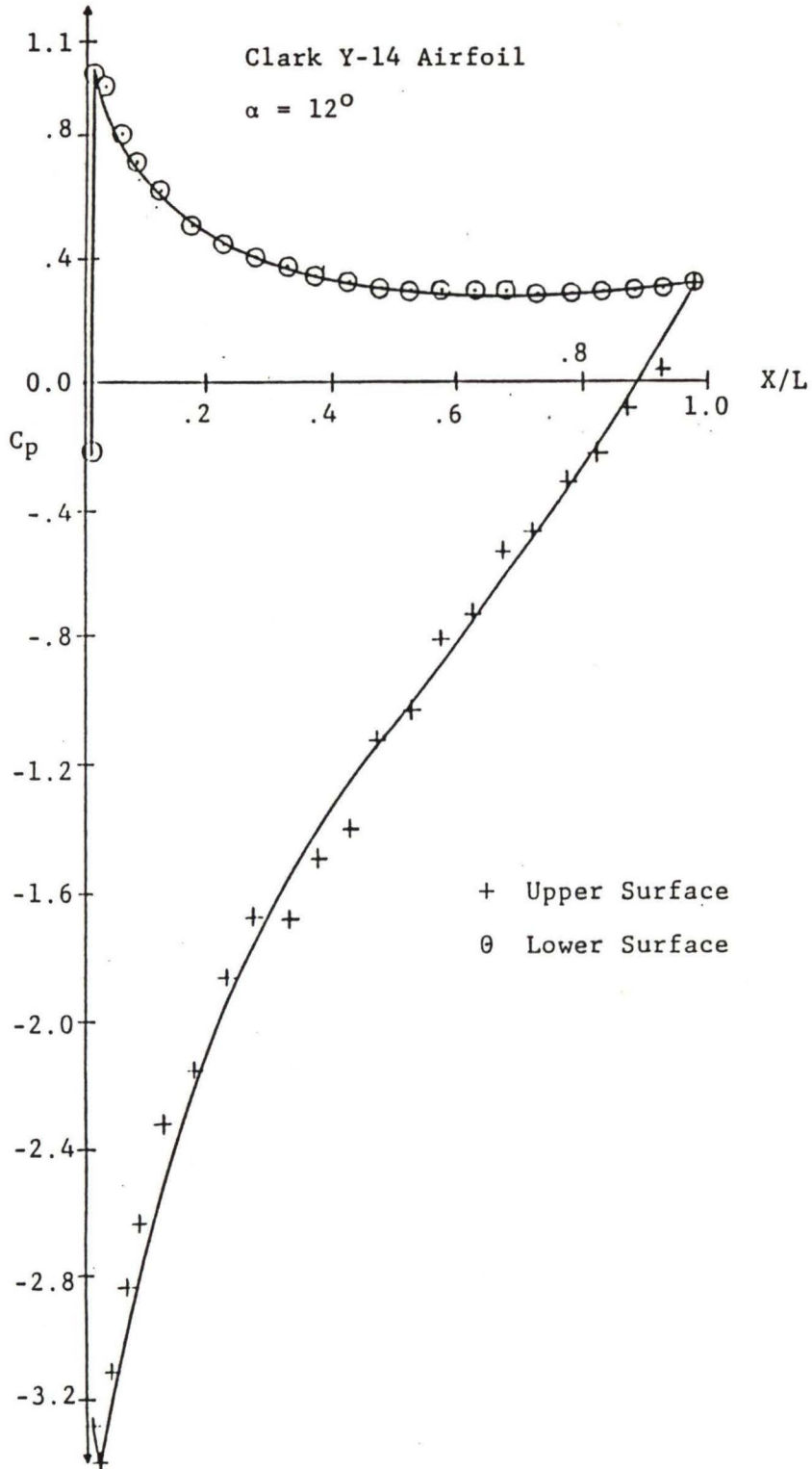


Figure 19 Graph Depicting C_p vs X/L for $\alpha = 12^\circ$ (CY-14 Airfoil)

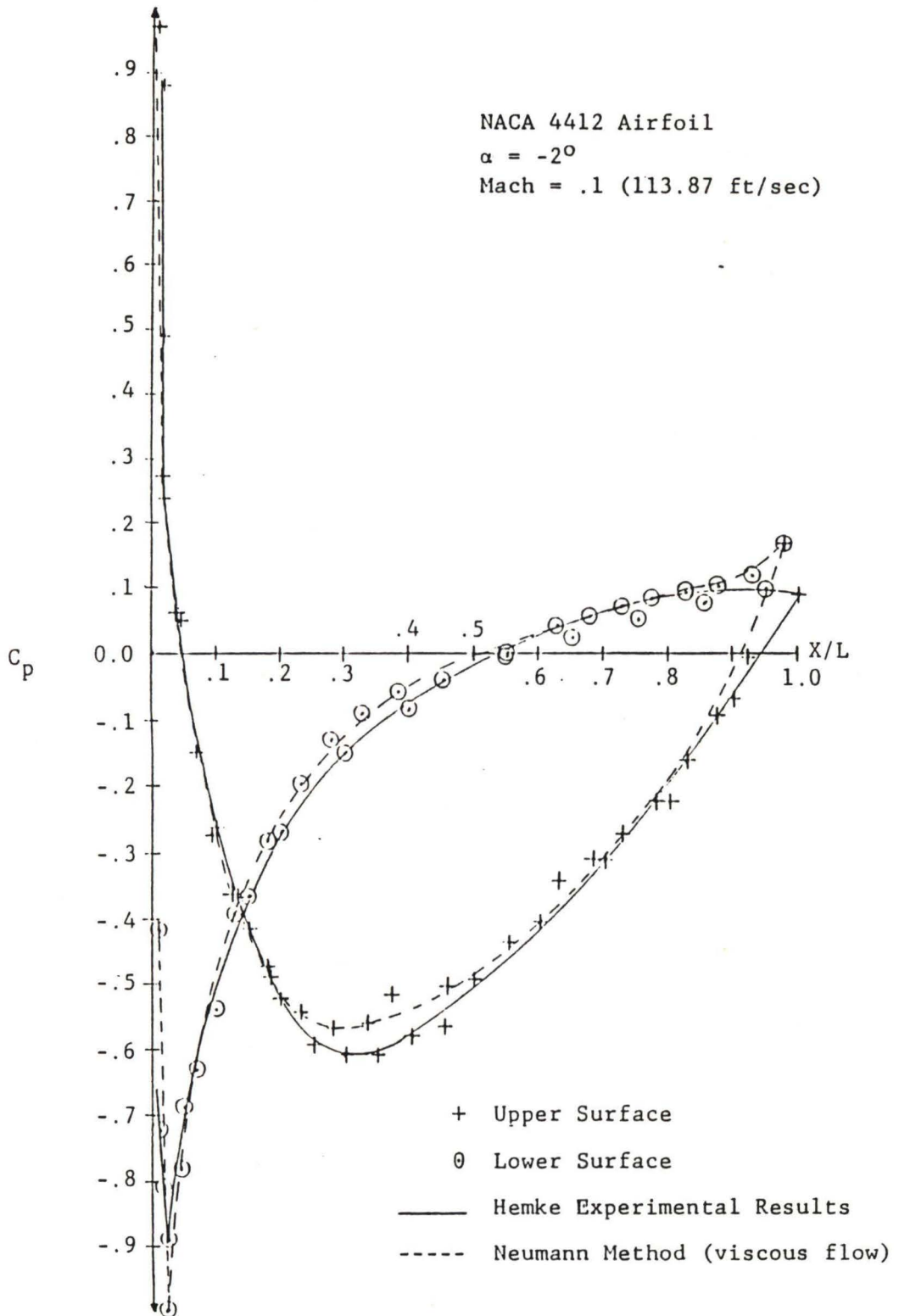


Figure 20 Graph Depicting C_p vs X/L for $\alpha = 2^\circ$ (NACA 4412 Airfoil)

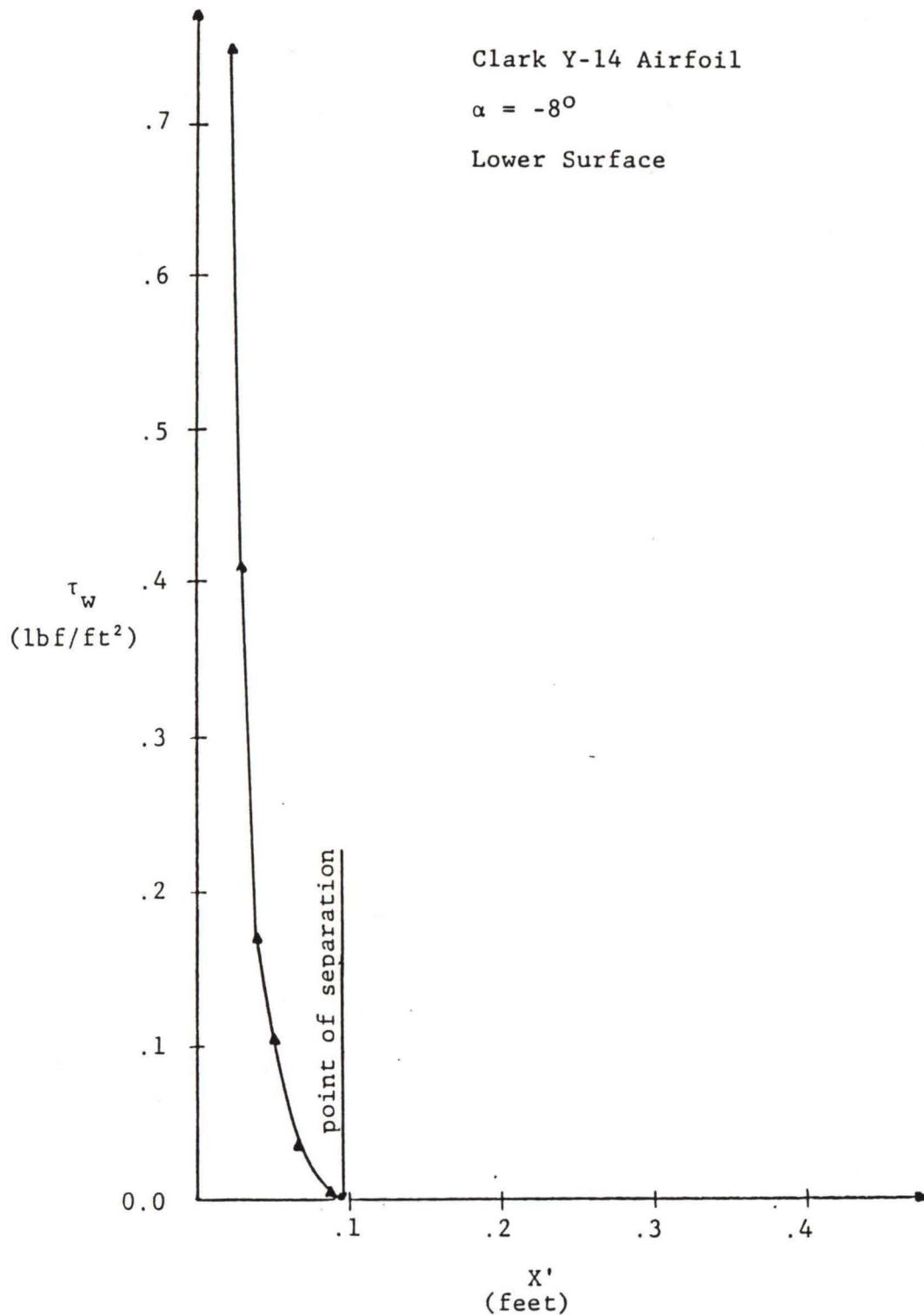


Figure 21 Graph Depicting τ_w vs X' for $\alpha = -8^\circ$, Lower Surface, CY-14 Airfoil

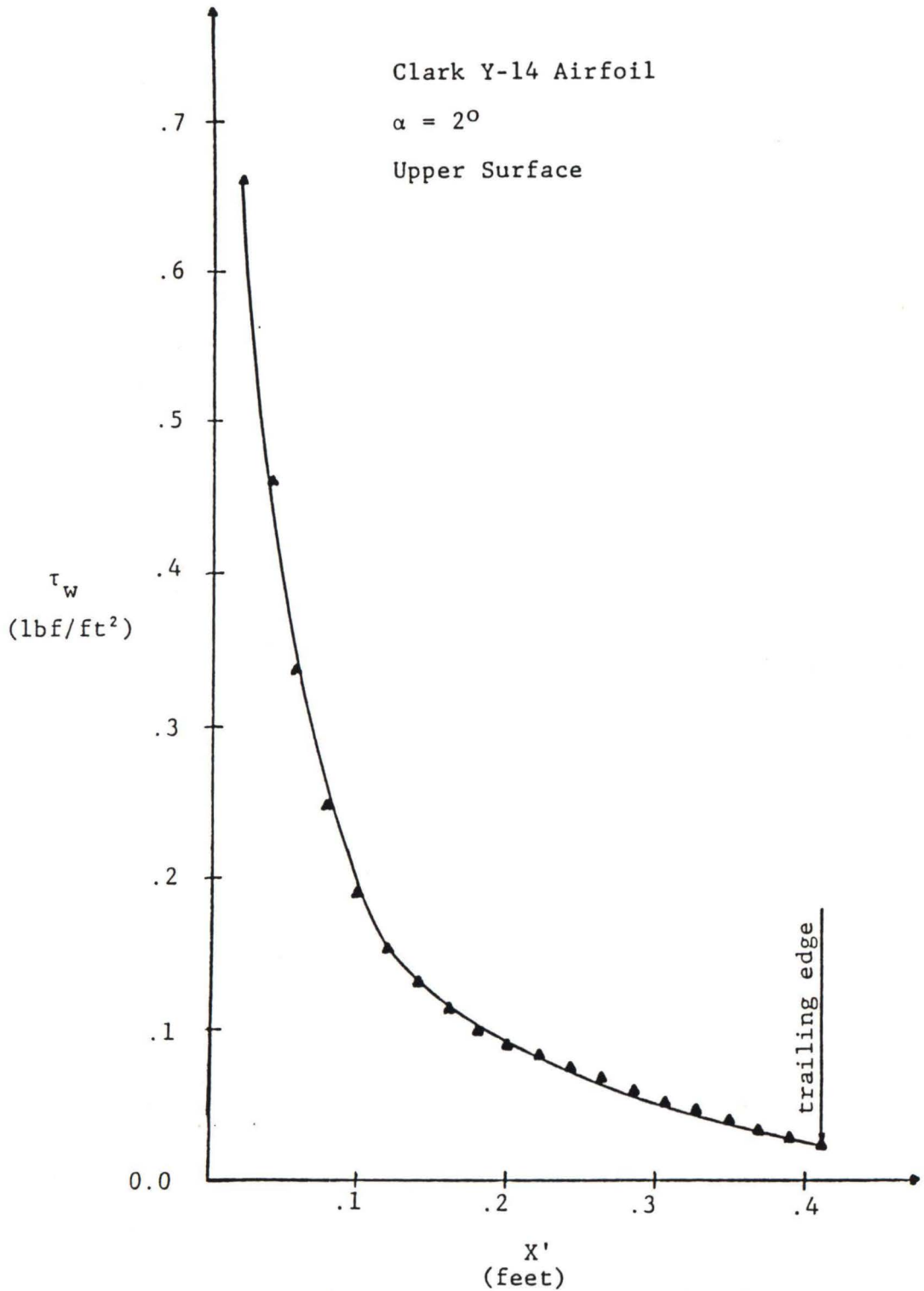


Figure 22 Graph Depicting τ_w vs X' for $\alpha = 2^\circ$,
 Upper Surface, CY-14 Airfoil

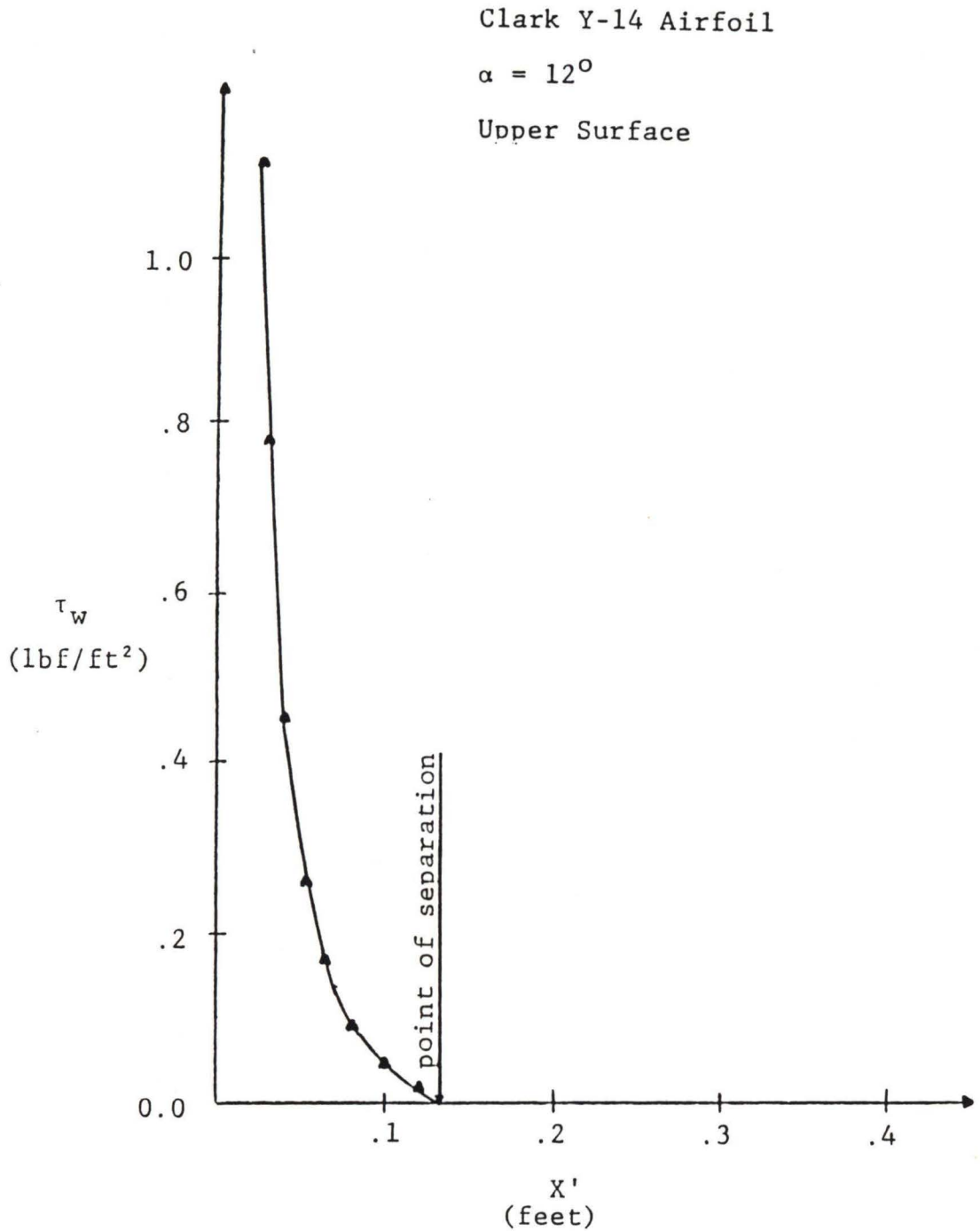


Figure 23 Graph Depicting τ_w vs X' for $\alpha = 12^\circ$,
Upper Surface, CY-14 Airfoil

Points of Flow Separation
Clark Y-14 Airfoil

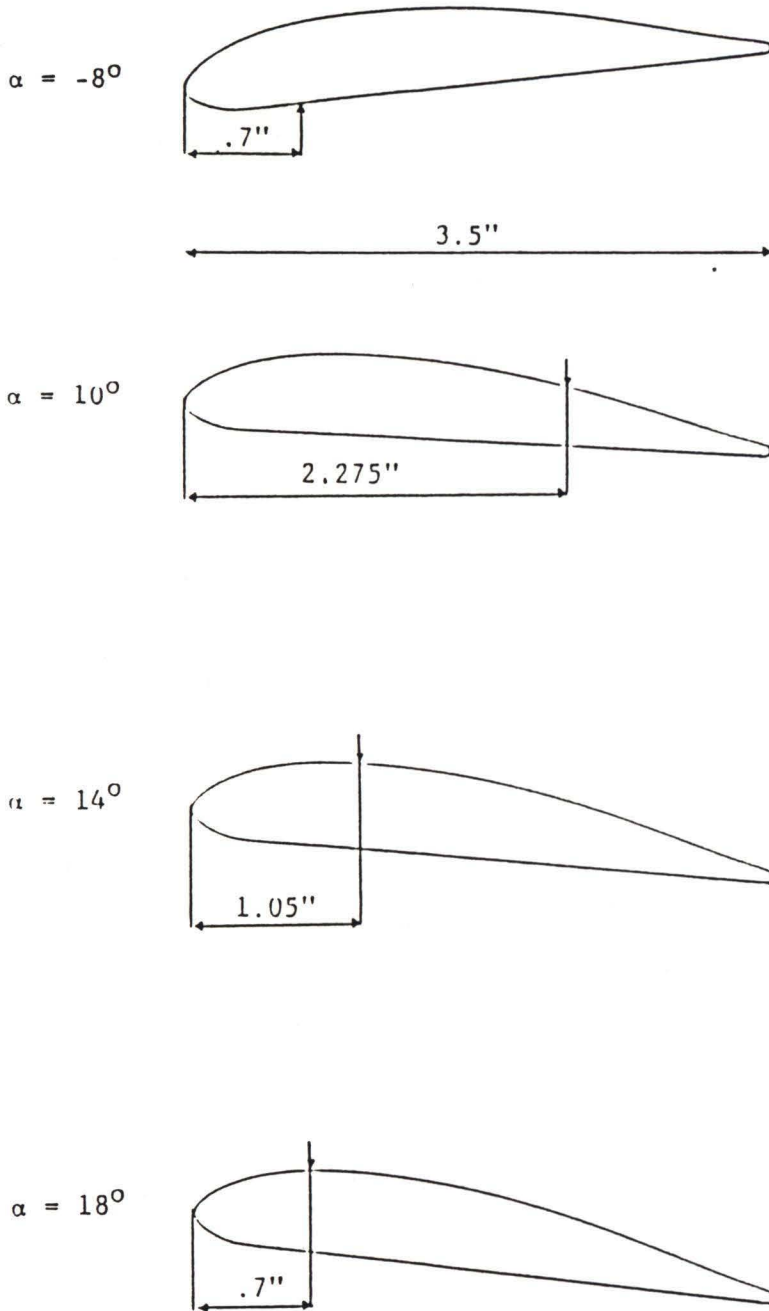


Figure 24 Points of Separation for the CY-14 Airfoil

APPENDIX C

```

C *****
C * THIS PROGRAM DETERMINES THE LOCAL PRESSURE DISTRIBUTION ALONG AN *
C * AIRFOIL USING THE SOURCE DISTRIBUTION METHOD. A DATA FILE MUST *
C * BE READ INTO THE PROGRAM (DEVICE NUMBER 007) PROVIDING: NUMBER *
C * OF DATA POINTS ALONG THE AIRFOIL, CHORD LENGTH (INCHES), A REFER- *
C * ENCE Y COORDINATE, FREE STREAM VELOCITY (FT/SEC), AND THE DATA *
C * POINTS ALONG THE SURFACE OF THE AIRFOIL PER PERCENT CHORD. THE *
C * PROGRAM WILL PROVIDE BOTH A NONVISCIOUS (DEVICE NUMBER 008) AND *
C * VISCIOUS (DEVICE NUMBER 009) FLOW SOLUTIONS FOR: LOCAL PRESSURE *
C * DIFFERENCES, COEFFICIENTS OF PRESSURE, AND TANGENTIAL VELOCITIES *
C * ALONG THE AIRFOIL; AND COEFFICIENT OF LIFT FOR ANGLES OF ATTACK *
C * OF -8 TO 18 DEGREES (EVERY 2 DEGREES). ALSO, SOLUTION OF THE *
C * BOUNDARY LAYER FLOW IS INCLUDED (DEVICE NUMBER 010). OUTPUT FROM *
C * THE BOUNDARY LAYER SOLUTION INCLUDES: TAUW VS LENGTH ALONG THE *
C * X-COORDINATE, BOUNDARY LAYER THICKNESS, AND SEPARATION POINT IF *
C * APPLICABLE.
C *****
C
C ARGUMENTS
C
C REAL NUMBERS
C
C A(N,M)..... COEFFICIENT MATRIX USED TO DETER-
C MINE UNKNOWN SIGMA'S.
C B(N)..... SOLUTION MATRIX USED TO DETERMINE
C UNKNOWN SIGMA'S.
C E1(N)..... UNIT VECTOR ON THE ELEMENT IN THE
C X DIRECTION.
C E2(N)..... UNIT VECTOR ON THE ELEMENT IN THE
C Y DIRECTION.
C SIGMA(N)..... SOURCE STRENGTHS.
C WKAREA(N)..... WORK SPACE NECESSARY FOR MATRIX SUB-
C ROUTINE LEGTIF.
C XBAR(N)..... CONTROL POINT (X COMPONENT).
C YBAR(N)..... CONTROL POINT (Y COMPONENT).
C XDAT(N)..... DATA POINT (X COMPONENT).
C YDAT(N)..... DATA POINT (Y COMPONENT).
C XDIF(N)..... DIFFERENCE BETWEEN CONTROL POINTS
C IN THE X DIRECTION.
C YDIF(N)..... DIFFERENCE BETWEEN CONTROL POINTS
C IN THE Y DIRECTION.
C GAMA(N)..... ANGLE OF OUTER NORMAL TO AN ELEMENT
C AT THE CONTROL POINTS.
C CP(N)..... COEFFICIENT OF PRESSURE PREDICTED
C AT THE CONTROL POINTS.
C VT(N)..... TANGENTIAL VELOCITY PREDICTED AT THE
C CONTROL POINTS.
C ALPHA..... ANGLE OF ATTACK OF AIRFOIL IN RADIANS.
C DEN..... FLUID DENSITY.
C P..... AMBIENT PRESSURE.
C T..... OUTPUT FROM SUBROUTINE THETA USED TO
C DETERMINE GAMA.
C CHORD..... AIRFOIL CHORD LENGTH.
C U..... FREE STREAM VELOCITY.
C YREF..... PARAMETER USED TO ROTATE AXIS OF
C NACA TECH REPORT DATA.
C X..... LOCAL X COORDINATE OF A POINT IN
C SPACE.

```

C	Y.....	LOCAL Y COORDINATE OF A POINT IN SPACE.
C	G.....	DUMMY VARIABLE USED TO DETERMINE GAMA.
C	UVT.....	TANGENTIAL VELOCITY CONTRIBUTION FROM THE FREE STREAM VELOCITY.
C	PI.....	3.1415927 RADIANS.
C	XGAM.....	PARAMETER USED TO ESTABLISH THE X DISTANCE IN DETERMINING GAMA.
C	YGAM.....	PARAMETER USED TO ESTABLISH THE Y DISTANCE IN DETERMINING GAMA.
C	EL.....	ELEMENT LENGTH.
C	SUM.....	SUMMATION USED TO DETERMINE THE TANGENTIAL VELOCITIES.
C	BSUM.....	SUMMATION USED TO DETERMINE VORS.
C	PSUM.....	SUMMATION USED TO DETERMINE THE VORTEX CONTRIBUTION TO TANGENTIAL VELOCITIES.
C	D.....	DUMMY ARRAY USED TO REORDER DATA FOR VARIABLE TWO DIMENSIONAL ARRAYS USED IN SUBROUTINES.
C	Z(M,N).....	DUMMY ARRAY USED FOR COEFFICIENT MATRIX TO REORDER DATA.
C	SIGV.....	VORTEX STRENGTH.
C	DD.....	ABSOLUTE VALUE OF THE TANGENTIAL VELOCITY AT CONTROL POINT A WITH NO VORTEX STRENGTH CONTRIBUTION.
C	EE.....	ABSOLUTE VALUE OF THE TANGENTIAL VELOCITY AT CONTROL POINT B WITH NO VORTEX STRENGTH CONTRIBUTION.
C	FF.....	UNITY VORTEX STRENGTH CONTRIBUTION TO THE TANGENTIAL VELOCITY AT CONTROL POINT A.
C	GG.....	UNITY VORTEX STRENGTH CONTRIBUTION TO THE TANGENTIAL VELOCITY AT CONTROL POINT B.
C	ABLE.....	ANGLE OF ATTACK OF AIRFOIL IN DEGREES.
C	GG.....	ABSOLUTE DIFFERENCE BETWEEN DD AND EE.
C	RR.....	DELTA SIGV.
C	ECHO.....	PARAMETER USED TO DETERMINE WHETHER TO ADD OR SUBTRACT RR.
C	EPS.....	CONVERGENCE TOLERANCE FOR KUTTA CONDITION.
C	XCOR(N).....	X COORDINATE FROM NACA DATA.
C	YCOR(N).....	Y COORDINATE FROM NACA DATA.
C	XD(N).....	DIFFERENCE IN X COORDINATE USED TO DETERMINE CONTROL POINTS A AND B.
C	YY.....	DUMMY VARIABLE FOR Y COORDINATE USED TO ROTATE AXIS.
C	SS.....	WEIGHTING FACTOR USED WITH DELTA SIGV.
C	VORS(N).....	VORTEX STRENGTH CONTRIBUTION.
C	VORVT(N).....	VORTEX STRENGTH CONTRIBUTION TO TANGENTIAL VELOCITIES.
C	A1(N,M).....	DUMMY ARRAY USED TO REORDER COEFFICIENT MATRIX.
C	PL(N).....	PRESSURE DIFFERENCE PREDICTED ALONG AIRFOIL.
C	VTT(N).....	DUMMY VARIABLE FOR TANGENTIAL VELOCITIES USED AS INPUT TO STAGNATION POINT DETERMINATION SUBROUTINE.
C	DELTA(N).....	ELEMENT LENGTHS USED AS INPUT TO STAQ-

C		NATION POINT DETERMINATION SUBROUTINE.
C	XBUP(N).....	X COORDINATE LOCATION ALONG FLAT PLATE
C		FOR UPPER SURFACE OF THE AIRFOIL.
C	VPUF(N).....	POTENTIAL VELOCITY FOR X COORDINATE A-
C		LONG THE FLAT PLATE COORESPONDING TO
C		THE UPPER SURFACE OF THE AIRFOIL.
C	XBLOW(N).....	X COORDINATE LOCATION ALONG FLAT PLATE
C		FOR LOWER SURFACE OF THE AIRFOIL.
C	VFLOW(N).....	POTENTIAL VELOCITY FOR X COORDINATE A-
C		LONG THE FLAT PLATE COORESPONDING TO
C		THE LOWER SURFACE OF THE AIRFOIL.
C	BPAR.....	INITIAL CONDITION VECTOR USED IN CUBIC
C		SPLINE SUBROUTINE ICSICU.
C	XOVL(N).....	X COORDINATE OF THE CONTROL POINTS
C		DIVIDED BY THE CHORD LENGTH.
C	PRINT.....	FLAG USED TO PRINT HEADER INFORMATION
C		ONLY ONCE.
C	E.....	DUMMY ARRAY USED TO REORDER VARIABLE
C		TWO DIMENSIONAL ARRAYS USED IN SUB-
C		ROUTINES.
C	XDAT1.....	ARRAY USED TO ORDER X COORDINATES
C		IN ASCENDING ORDER FOR USE IN CUBIC
C		SPLINE SUBROUTINE.
C	YDAT1.....	ARRAY USED IN CONJUNCTION WITH XDAT1.
C	XDAT2.....	SAME AS XDAT1.
C	YDAT2.....	SAME AS YDAT1.
C	XDAT3.....	SAME AS XDAT1.
C	YDAT3.....	SAME AS YDAT1.
C	XDAT4.....	SAME AS XDAT1.
C	YDAT4.....	SAME AS YDAT1.
C	XDAT5(N).....	USED TO STORE EXPANDED X COORDINATES
C		PER PERCENT CHORD.
C	YDAT5(N).....	USED TO STORE EXPANDED Y COORDINATES
C		PER PERCENT CHORD.
C	C.....	ARRAY FROM CUBIC SPLINE SUBROUTINE
C		(ICSICU) PROVIDING 1ST, 2ND, AND 3RD
C		ORDER DERIVATIVES.
C	CT.....	SAME AS C.
C	X1.....	DUMMY VARIABLE USED TO DETERMINE
C		WHETHER THE INTERVAL BETWEEN DATA
C		POINTS IN THE X DIRECTION IS GREATER
C		THAN 5 PERCENT CHORD.
C	BLA.....	DUMMY ARRAY USED IN SUBROUTINE BLIMP
C		PROVIDING SPACE FOR A COEFFICIENT
C		MATRIX.
C	BLB.....	DUMMY ARRAY USED IN SUBROUTINE BLIMP
C		PROVIDING SPACE FOR B COEFFICIENT
C		MATRIX.
C	BLC.....	DUMMY ARRAY USED IN SUBROUTINE BLIMP
C		PROVIDING SPACE FOR C COEFFICIENT
C		MATRIX.
C	CTT.....	SAME AS C.
C	DU.....	ARRAY DENOTING VELOCITY IN THE X DIREC-
C		TION USED IN CONJUNCTION WITH ICSICU TO
C		DETERMINE WALL SHEAR STRESS.
C	DDY.....	ARRAY DENOTING DISTANCE IN THE Y DIREC-
C		TION USED FOR THE SAME PURPOSE AS DU.
C	BLT2.....	DUMMY ARRAY USED TO TEMPORARILY STORE
C		BLT VALUES.
C	DX.....	DIFFERENCE BETWEEN CONTROL POINT OF

C		INTEREST AND CONTROL POINT IN FLOW
C		STREAM IN THE X DIRECTION.
C	DY.....	DIFFERENCE BETWEEN CONTROL POINT OF
C		INTEREST AND CONTROL POINT IN FLOW
C		STREAM IN THE Y DIRECTION.
C	DYB.....	ELEMENT SUBDIVISION USED IN DETERMINING
C		LIFT COEFFICIENT.
C	CIRVOR.....	ARRAY DEPICTING VORTEX STRENGTH CON-
C		TRIBUTION TO CIRCULATION.
C	BLOW.....	BOUNDARY LAYER THICKNESS ON LOWER SUR-
C		FACE.
C	BLUP.....	BOUNDARY LAYER THICKNESS ON UPPER SUR-
C		FACE.
C	STALOW.....	STATION POINT ON FLAT PLATE CORRES-
C		PONDING TO A CONTROL POINT ON THE LOWER
C		SURFACE OF THE AIRFOIL.
C	STAUP.....	STATION POINT ON FLAT PLATE CORRES-
C		PONDING TO A CONTROL POINT ON THE UPPER
C		SURFACE OF THE AIRFOIL.
C	SMXCI.....	LOCAL X COORDINATE USED IN DETERMINING
C		LIFT COEFFICIENT.
C	SMYCI.....	LOCAL Y COORDINATE USED IN DETERMINING
C		LIFT COEFFICIENT.
C	TERM3.....	SUMMATION TERM USED IN DETERMINING LIFT
C		COEFFICIENT.
C	TERM4.....	SUMMATION TERM USED IN DETERMINING LIFT
C		COEFFICIENT.
C	TAUUP.....	WALL SHEAR STRESS ON UPPER SURFACE OF
C		AIRFOIL.
C	TAULOW.....	WALL SHEAR STRESS ON LOWER SURFACE OF
C		AIRFOIL.
C	CIRVORT.....	FLOW CIRCULATION.
C	SMYB.....	SUB-ELEMENT LENGTH USED TO DETERMINE
C		LIFT COEFFICIENT (EL/100).
C	YDUM.....	DUMMY ARRAY USED IN BLIMP FOR Y DIREC-
C		TION STEP SIZE.
C	CAPUDX.....	DUMMY ARRAY USED IN BLIMP AS INPUT
C		PROVIDING POTENTIAL FLOW VELOCITIES
C		(TANGENTIAL VELOCITIES).
C	UDUM.....	DUMMY ARRAY USED IN BLIMP AS INPUT
C		PROVIDING SPACE FOR X DIRECTION
C		VELOCITIES.
C	VDUM.....	DUMMY ARRAY USED IN BLIMP AS INPUT
C		PROVIDING SPACE FOR Y DIRECTION
C		VELOCITIES.
C	DDX.....	DUMMY ARRAY USED IN BLIMP AS INPUT
C		PROVIDING SPACE FOR DIFFERENCES IN
C		STEP SIZE IN THE X DIRECTION (I. E.,
C		X HAS A VARIABLE STEP SIZE).
C	F.....	FLAG USED IN BLIMP TO INDICATE WHE-
C		DATA IS FROM THE UPPER OR LOWER SUR-
C		OF THE AIRFOIL.
C	ZXDUM.....	DUMMY VARIABLE USED TO DETERMINE XDIF.
C	ZYDUM.....	DUMMY VARIABLE USED TO DETERMINE YDIF.
C	BLD.....	DUMMY ARRAY USED IN BLIMP PROVIDING
C		SPACE FOR D COEFFICIENT MATRIX.
C	BLE.....	DUMMY ARRAY USED IN BLIMP PROVIDING
C		SPACE FOR E COEFFICIENT MATRIX.
C	BLT(N).....	BOUNDARY LAYER THICKNESS CORRESPONDING
C		TO CONTROL POINTS.

C GAM(N)..... DUMMY ARRAY USED TO OUTPUT GAMA IN
 C TERMS OF DEGREES.
 C TAUW(N)..... WALL SHEAR STRESS PER CONTROL POINTS.
 C YDVER..... VECTOR CONTAINING F', F'', AND F'''
 C USED IN RUNGE KUTTA SUBROUTINE (DVERK)
 C (STAGNATION POINT FLOW) IN BLIMP.
 C CDVER..... PARAMETER USED IN DVERK.
 C WDVER..... WORK SPACE USED IN DVERK.
 C DUM..... ARRAY USED IN BLIMP TO PROVIDE SPACE
 C TO DENOTE THE TANGENTIAL VELOCITIES.
 C ZDVDX..... DVDX TERM USED IN DETERMINING LIFT
 C COEFFICIENT.
 C ZDVDY..... DVDY TERM USED IN DETERMINING LIFT
 C COEFFICIENT.

INTERGERS

C N..... NUMBER OF DATA POINTS.
 C KSTARL..... START POINT ON LOWER SURFACE FOR EX-
 C PANDING DATA POINTS.
 C KSTARU..... START POINT ON UPPER SURFACE FOR EX-
 C PANDING DATA POINTS.
 C KENDL..... END POINT ON LOWER SURFACE FOR EX-
 C PANDING DATA POINTS.
 C KENDU..... END POINT ON UPPER SURFACE FOR EX-
 C PANDING DATA POINTS.
 C NVF..... FLAG FOR NONVISCIOUS FLOW SOLUTION.
 C MA..... CONTROL POINT A.
 C MB..... CONTROL POINT B.
 C NREF..... REFERENCE POINT DENOTING LOCATION OF
 C STAGNATION POINT.

SUBROUTINES AND SUBPROGRAMS (INTERNAL)

C THETA..... USED TO DETERMINE GAMA.
 C DUDX..... ANALYTICAL DERIVATION OF DU/DX.
 C DUDY..... ANALYTICAL DERIVATION OF DU/DY.
 C DVDX..... ANALYTICAL DERIVATION OF DV/DX.
 C DVDY..... ANALYTICAL DERIVATION OF DV/DY.
 C STORE..... USED TO REORDER DATA STORED IN
 C A TWO-DIMENSIONAL ARRAY (E. G.,
 C A)
 C STORE1..... SAME AS STORE EXCEPT USED FOR
 C C, CT, CTT, ETC.
 C STAG..... USED TO DETERMINE STAGNATION POINT.
 C BLIMP..... USED TO DETERMINE BOUNDARY LAYER
 C FLOW.
 C FCN..... EXTERNAL SUBPROGRAM USED IN DVERK
 C DEFINING FUNCTION.

SUBROUTINES (EXTERNAL)

C DVERK..... RUNGE KUTTA.
 C ICSICU..... CUBIC SPLINE.


```

C      ***** AXIS ROTATION *****
C
DO 1 IM=2, N
  LK=LK+1
  XD(IM-1)=XCOR(IM)-XCOR(IM-1)
  IF(XD(IM-1) .LT. 0.0 .AND. LK .EG. IM)THEN
    MA=IM-2
    MB=IM-1
    LK=LK-1
  ENDIF
1  CONTINUE
  XDAT(1)=(CHORD*XCOR(1))/12. /100.
  YDAT(1)=(CHORD*YCOR(1)-CHORD*YREF)/12. /100.
  DO 2 IJ=2, MB
    YY=YY*(100. -XCOR(IJ))/(100. -XCOR(IJ-1))
    XDAT(IJ)=(CHORD*XCOR(IJ))/12. /100.
    YDAT(IJ)=(CHORD*YCOR(IJ)-CHORD*YY)/12. /100.
2  CONTINUE
  YY=YREF*(100. -XCOR(N))/(100. -XCOR(1))
  XDAT(N)=(CHORD*XCOR(N))/12. /100.
  YDAT(N)=(CHORD*YCOR(N)-CHORD*YY)/12. /100.
  DO 3 IN=N-1, MB+1, -1
    YY=YY*(100. -XCOR(IN))/(100. -XCOR(IN+1))
    XDAT(IN)=(CHORD*XCOR(IN))/12. /100.
    YDAT(IN)=(CHORD*YCOR(IN)-CHORD*YY)/12. /100.
3  CONTINUE
C
C      ***** EXPANSION OF DATA POINTS *****
C
LK=1
DO 4 I=2, MB
  X1=ABS(XCOR(I)-XCOR(I-1))
  IF(X1 .GT. 5. .AND. KSTARL .EG. 0)THEN
    KSTARL=I-1
  ENDIF
  IF(X1 .LE. 5. .AND. KSTARL .GT. 0 .AND. LET .EG. 0)THEN
    KENDL=I-1
    LET=LET+1
  ENDIF
4  CONTINUE
  LET=0
  DO 5 I=N, MB+1, -1
    X1=ABS(XCOR(I)-XCOR(I-1))
    IF(X1 .GT. 5. .AND. KSTARU .EG. 0)THEN
      KSTARU=I
    ENDIF
    IF(X1 .LE. 5. .AND. KSTARU .GT. 0 .AND. LET .EG. 0)THEN
      KENDU=I
      LET=LET+1
    ENDIF
5  CONTINUE
  DO 6 I=1, 4
    BPAR(I)=0.0
6  CONTINUE
  ILOW=KENDL-KSTARL
  NLOW=ILOW+1
  IUP=KSTARU-KENDU
  NUP=IUP+1
  KB=KSTARL+ILOW*2
  KC=KENDU+IUP*2

```

```

KD=IUP*2+1
IF(NLOW .LT. 2)GO TO 20
DO 7 I=KSTARL,KENDL
  XDAT1(KA)=XDAT(I)
  YDAT1(KA)=YDAT(I)
  KA=KA+1
7 CONTINUE
KA=1
CALL ICSICU(XDAT1,YDAT1,NLOW,BPAR,C,ILOW,IER)
CALL STORE1(C,E,KT,ILOW,CT)
DO 8 I=1,ILOW
  XDAT2(I)=.5*(XDAT1(I+1)-XDAT1(I))+XDAT1(I)
  YDAT2(I)=YDAT1(I)+CT(I,3)*((XDAT2(I)-XDAT1(I))**3)+
+ CT(I,2)*((XDAT2(I)-XDAT1(I))**2)+CT(I,1)*
+ (XDAT2(I)-XDAT1(I))
8 CONTINUE
20 IF(NUP .LT. 2)GO TO 22
DO 9 I=KSTARU,KENDU,-1
  XDAT3(KA)=XDAT(I)
  YDAT3(KA)=YDAT(I)
  KA=KA+1
9 CONTINUE
KA=1
CALL ICSICU(XDAT3,YDAT3,NUP,BPAR,C,IUP,IER)
CALL STORE1(C,E,KT,IUP,CT)
DO 10 I=1,IUP
  XDAT4(I)=.5*(XDAT3(I+1)-XDAT3(I))+XDAT3(I)
  YDAT4(I)=YDAT3(I)+CT(I,3)*((XDAT4(I)-XDAT3(I))**3)+
+ CT(I,2)*((XDAT4(I)-XDAT3(I))**2)+CT(I,1)*
+ (XDAT4(I)-XDAT3(I))
10 CONTINUE
IF(NLOW .LT. 2)GO TO 21
DO 11 I=1,KSTARL-1
  XDAT5(KA)=XDAT(I)
  YDAT5(KA)=YDAT(I)
  KA=KA+1
11 CONTINUE
DO 12 I=KSTARL,KB
  JK=MOD(JK+1,2)
  IF(JK .EQ. 0)THEN
    XDAT5(KA)=XDAT1(KTT-IT)
    YDAT5(KA)=YDAT1(KTT-IT)
    KA=KA+1
    KTT=KTT+1
    IT=IT+1
  ELSE IF(JK .EQ. 1)THEN
    XDAT5(KA)=XDAT2(KTT-IT)
    YDAT5(KA)=YDAT2(KTT-IT)
    KA=KA+1
    KTT=KTT+1
  ENDIF
12 CONTINUE
21 IF(NLOW .LT. 2)THEN
  DO 13 I=1,KENDU-1
    XDAT5(KA)=XDAT(I)
    YDAT5(KA)=YDAT(I)
    KA=KA+1
13 CONTINUE
ENDIF
DO 14 I=KENDL+1,KENDU-1

```

```

      XDATS(KA)=XDAT(I)
      YDATS(KA)=YDAT(I)
      KA=KA+1
14  CONTINUE
      DO 15 I=1, KD
          JKK=MOD(JKK+1, 2)
          IF(JKK .EQ. 0) THEN
              XDATS(KA)=XDAT3(NUP-ITT)
              YDATS(KA)=YDAT3(NUP-ITT)
              KA=KA+1
          ELSE IF(JKK .EQ. 1) THEN
              XDATS(KA)=XDAT4(IUP-ITT)
              YDATS(KA)=YDAT4(IUP-ITT)
              KA=KA+1
              ITT=ITT+1
          ENDIF
15  CONTINUE
      DO 16 I=KSTARU+1, N
          XDATS(KA)=XDAT(I)
          YDATS(KA)=YDAT(I)
          KA=KA+1
16  CONTINUE
      N=KA-1
      NI=N
      IA=N
      DO 17 I=1, N
          XDAT(I)=XDATS(I)
          YDAT(I)=YDATS(I)
17  CONTINUE
      DO 18 I=1, N
          XDATS(I)=XDAT(I)*12. *100. /CHORD
          YDATS(I)=YDAT(I)*12. *100. /CHORD
18  CONTINUE
      DO 19 IM=2, N
          LK=LK+1
          XD(IM-1)=XDAT(IM)-XDAT(IM-1)
          IF(XD(IM-1) .LT. 0. .AND. LK .EQ. IM) THEN
              MA=IM-2
              MB=IM-1
              LK=LK-1
          ENDIF
19  CONTINUE
C
C ***** DETERMINATION OF GAMA *****
C
22  DO 23 IG=2, N
      XGAM=XDAT(IG)-XDAT(IG-1)
      YGAM=YDAT(IG)-YDAT(IG-1)
      CALL THETA(XGAM, YGAM, T)
      G=T-PI/2.
      IF(G .GE. 0. 0) THEN
          GAMA(IG-1)=G
      ELSE IF(G .LT. 0. 0) THEN
          GAMA(IG-1)=G+2. *PI
      ENDIF
23  CONTINUE
      XGAM=XDAT(1)-XDAT(N)
      YGAM=YDAT(1)-YDAT(N)
      CALL THETA(XGAM, YGAM, T)
      G=T-PI/2.

```



```

IF(G .GE. 0.0)THEN
  GAMA(N)=0
ELSE IF(G .LT. 0.0)THEN
  GAMA(N)=G+2. *PI
ENDIF
GAMA(N)=0
DO 24 I=1,N
  E1(I)=-SIN(GAMA(I))
  E2(I)=COS(GAMA(I))
  GAM(I)=GAMA(I)*360./2./PI
24 CONTINUE
DO 25 IH=2,N
  XBAR(IH-1)=(XDAT(IH)-XDAT(IH-1))/2. +XDAT(IH-1)
  YBAR(IH-1)=(YDAT(IH)-YDAT(IH-1))/2. +YDAT(IH-1)
  XOVL(IH-1)=XBAR(IH-1)*12./CHORD
25 CONTINUE
XBAR(N)=(XDAT(1)-XDAT(N))/2. +XDAT(N)
YBAR(N)=(YDAT(1)-YDAT(N))/2. +YDAT(N)
XOVL(N)=XBAR(N)*12./CHORD
C
C *****
C *
C *          POTENTIAL FLOW COMPUTATION
C *
C *****
C
DO 59 ABLE=-8.0,18.0,2.0
ALPHA=ABLE*PI/180.
IFLAG=1
NVF=1
DO 26 I=1,N
  BLT(I)=0.0
  BLUP(I)=0.0
  BLLOW(I)=0.0
  TAULOW(I)=0.0
  TAUUP(I)=0.0
  STAUP(I)=0.0
  STALOW(I)=0.0
26 CONTINUE
58 KK=0
MK=0
NK=0
NN1=1
NN2=N
SS=1.0
ZXDUM=0.0
ZYDUM=0.0
XDIF(1)=2.0*XBAR(1)
YDIF(1)=2.0*YBAR(1)
DO 27 I=2,N
  ZXDUM=ZXDUM+XDIF(I-1)
  ZYDUM=ZYDUM+YDIF(I-1)
  XDIF(I)=2.0*(XBAR(I)-ZXDUM)
  YDIF(I)=2.0*(YBAR(I)-ZYDUM)
27 CONTINUE
C
C ***** DETERMINATION OF VORTEX STRENGTH *****
C
DO 29 I=1,N
  BSUM=0.0

```

```

PSUM=0.0
DO 28 J=1,N
  EL=SQRT(XDIF(J)**2+YDIF(J)**2)
  DX=XBAR(I)+BLT(I)*E2(I)-XBAR(J)
  DY=YBAR(I)+BLT(I)*(-E1(I))-YBAR(J)
  X=E2(J)*DX-E1(J)*DY
  Y=E1(J)*DX+E2(J)*DY
  IF(I .NE. J)THEN
    BSUM=BSUM+E2(I)*E2(J)*DVDX(EL, X, Y)+E2(I)*E1(J)*
+     DVDY(EL, X, Y)+E1(I)*E1(J)*DVDX(EL, X, Y)-E1(I)*
+     E2(J)*DVDY(EL, X, Y)
    PSUM=PSUM+E1(I)*E2(J)*DVDX(EL, X, Y)+E1(I)*E1(J)*
+     DVDY(EL, X, Y)-E2(I)*E1(J)*DVDX(EL, X, Y)+E2(I)*
+     E2(J)*DVDY(EL, X, Y)
    ELSE IF(I .EQ. J)THEN
      PSUM=PSUM+PI
  ENDIF
28  CONTINUE
  VORS(I)=BSUM
  VORVT(I)=PSUM
29  CONTINUE
35  IF(KK .EQ. 0)THEN
  SIGV=0.
  ELSE IF(KK .EQ. 1)THEN
    DD=ABS(VT(MA))
    EE=ABS(VT(MB))
    FF=VORVT(MA)
    GG=VORVT(MB)
    SIGV=ABS(DD-EE)/(FF+GG)
    RR=SIGV*.5
  ELSE IF(KK .GE. 2)THEN
    EPS=ABS(ABS(VT(MA))-ABS(VT(MB)))*1.0E-5
    GO TO 37
  ENDIF
36  IF(KK .GE. 2)THEN
  NK=MOD(NK+1,2)
  IF(NK .EQ. 0)PP=SIGV
  ENDIF
C
C ***** DETERMINATION OF SIGMA *****
C
DO 31 I=1,N
DO 30 J=1,N
  EL=SQRT(XDIF(J)**2+YDIF(J)**2)
  DX=XBAR(I)+BLT(I)*E2(I)-XBAR(J)
  DY=YBAR(I)+BLT(I)*(-E1(I))-YBAR(J)
  X=E2(J)*DX-E1(J)*DY
  Y=E1(J)*DX+E2(J)*DY
  IF(I .NE. J)THEN
    Z(I, J)=E2(I)*E2(J)*DUDX(EL, X, Y)+E2(I)*E1(J)*
+     DUDY(EL, X, Y)+E1(I)*E1(J)*DUDX(EL, X, Y)-
+     E1(I)*E2(J)*DUDY(EL, X, Y)
    ELSE IF(I .EQ. J)THEN
      Z(I, J)=PI
  ENDIF
30  CONTINUE
  B(I, M)=U*(SIN(ALPHA)*E1(I)-COS(ALPHA)*E2(I))-SIGV*VORS(I)
31  CONTINUE
  CALL STORE(Z, D, NA, N, A)
  CALL LEGT1F(A, M, N1, IA, B, IDGT, WKAREA, IER)

```

```

DO 32 L=1,N
  SIGMA(L)=B(L,M)
32 CONTINUE
DO 34 IB=1,N
  SUM=0.0
  DO 33 IF=1,N
    EL=SQRT(XDIF(IF)**2+YDIF(IF)**2)
    DX=XBAR(IB)+BLT(IF)*E2(IF)-XBAR(IF)
    DY=YBAR(IB)+BLT(IF)*(-E1(IF))-YBAR(IF)
    X=(DX*E2(IF)+(DY*(-E1(IF))))
    Y=(-DX*(-E1(IF))+(DY*E2(IF)))
    IF(IB .NE. IF)THEN
      SUM=SUM+SIGMA(IF)*(E1(IF)*(E2(IF)*DUDX(EL,X,Y)+E1(IF)*
+      DUDY(EL,X,Y))+(E2(IF)*(-E1(IF)*DUDX(EL,X,Y)+E2(IF)*
+      DUDY(EL,X,Y)))
    ELSE IF(IB .EQ. IF)THEN
      SUM=SUM+0.0
    ENDIF
33 CONTINUE
    UVT=U*(COS(ALPHA)*E1(IF)+SIN(ALPHA)*E2(IF))
    VT(IF)=SUM+SIGV*VORVT(IF)+UVT
34 CONTINUE
C
C ***** BEGINNING OF ITERATIVE SCHEME *****
C
37 IF(KK .GE. 2)THEN
  GG=ABS(ABS(VT(MA))-ABS(VT(MB)))
  ECHO=VT(MA)-ABS(VT(MB))
  IF(GG .LE. EPS)THEN
    GO TO 38
  ELSE IF(GG .GT. EPS)THEN
    MK=MK+1
    IF(MK .EQ. 50)GO TO 38
    IF(RR .LT. 1.0E-10)GO TO 38
    IF(ECHO .LT. 0.0)THEN
      SIGV=SIGV+RR
      IF(ABS(SIGV-PP) .LE. 1.0E-5)THEN
        RR=RR*SS*.75
        SS=SS*.8
      ENDIF
    ELSE IF(ECHO .GE. 0.0)THEN
      SIGV=SIGV-RR
      IF(ABS(SIGV-PP) .LE. 1.0E-5)THEN
        RR=RR*SS*.75
        SS=SS*.8
      ENDIF
    ENDIF
    GO TO 36
  ENDIF
  ENDIF
  KK=KK+1
  GO TO 35
C
C *****
C *
C *          BOUNDARY LAYER COMPUTATION          *
C *
C *****
38 IF(IFLAG .GE. 2. OR. NVF .EQ. 1)GO TO 57

```

```

C
C ***** STAGNATION POINT DETERMINATION *****
C
DO 39 I=1, N
  VTT(I)=VT(I)
39 CONTINUE
  DELTA(1)=SQRT(XBAR(1)**2+YBAR(1)**2)
  DO 40 I=2, MA
    DELTA(I)=SQRT((XBAR(I)-XBAR(I-1))**2+(YBAR(I)-
+      YBAR(I-1))**2)
40 CONTINUE
  DO 41 I=MB, N-1
    DELTA(I)=SQRT((XBAR(I)-XBAR(I+1))**2+(YBAR(I)-
+      YBAR(I+1))**2)
41 CONTINUE
  DELTA(N)=SQRT(XBAR(N)**2+YBAR(N)**2)
  CALL STAG(VTT, DELTA, MA, MB, N, XBUP, VPUP, XBLow, VPLOW, LL, LU, NREFF)
  F=-1.0
  IF(ABLE. LT. 0.0) THEN
    NREF=NREFF+1
    IF(NREF. GT. N) NREF=1
  ELSE IF(ABLE. GE. 0.0) THEN
    NREF=NREFF
  ENDIF

C
C ***** BOUNDARY LAYER DETERMINATION *****
C
IF(ABLE. EQ. -8.0) THEN
  DDDY=.001625/80.
  ELSE IF(ABLE. EQ. -6.0) THEN
  DDDY=.001125/80.
  ELSE IF(ABLE. EQ. -4.0) THEN
  DDDY=.001625/80.
  ELSE IF(ABLE. EQ. -2.0) THEN
  DDDY=.000625/80.
  ELSE IF(ABLE. EQ. 0.0) THEN
  DDDY=.000625/80.
  ELSE IF(ABLE. EQ. 2.0) THEN
  DDDY=.001125/80.
  ELSE IF(ABLE. EQ. 4.0) THEN
  DDDY=.001125/80.
  ELSE IF(ABLE. EQ. 6.0) THEN
  DDDY=.001125/80.
  ELSE IF(ABLE. EQ. 8.0) THEN
  DDDY=.001625/80.
  ELSE IF(ABLE. GT. 8.0. AND. ABLE. LT. 18.0) THEN
  DDDY=.001625/80.
  ELSE IF(ABLE. EQ. 18.0) THEN
  DDDY=.001/80.
  ENDIF
  CALL BLIMP(ABLE, DDDY, YDVER, CDVER, WDVER, BLA, BLB, BLC, BLD, BLE,
+    F, BPAR, CTT, C, CT, E, DU, DDY, XBLow, YDUM, VPLOW, CAPUDX, UDUM,
+    VDUM, DDX, N, MA, NREF, LL, DUM, TAUW, BLT2)
  BLOW(1)=0.0
  STALOW(1)=0
  TAULOW(1)=0.0
  IF(ABLE. LT. 0.0) THEN
    NREF=NREFF+1
    IF(NREF. GT. N) NREF=1
  ELSE IF(ABLE. GE. 0.0) THEN

```

```

      NREF=NREFF
ENDIF
IF(NREF. LT. MA) THEN
  DO 42 I=2, LL
    BLOW(I)=BLT2(NREF)
    STALOW(I)=NREF
    TAULOW(I)=TAUW(I)
    NREF=NREF+1
42  CONTINUE
  ELSE IF(NREF. GT. MA) THEN
    DO 43 I=2, LL
      IF(NREF. LE. N) THEN
        BLOW(I)=BLT2(NREF)
        STALOW(I)=NREF
        TAULOW(I)=TAUW(I)
        NREF=NREF+1
      ELSE IF(NREF. GT. N) THEN
        BLOW(I)=BLT2(NN1)
        STALOW(I)=NN1
        TAULOW(I)=TAUW(I)
        NN1=NN1+1
      ENDIF
43  CONTINUE
ENDIF
DO 44 I=1, N
  BLT(I)=BLT2(I)
44  CONTINUE
F=1. 0
IF(ABLE. LT. 0. 0) THEN
  NREF=NREFF
ELSE IF(ABLE. GE. 0. 0) THEN
  NREF=NREFF-1
  IF(NREF. LE. 0) NREF=N
ENDIF
IF(ABLE. EQ. -8. 0) THEN
  DDDY=. 001625/80.
ELSE IF(ABLE. EQ. -6. 0) THEN
  DDDY=. 001625/80.
ELSE IF(ABLE. EQ. -4. 0) THEN
  DDDY=. 001125/80.
ELSE IF(ABLE. EQ. -2. 0) THEN
  DDDY=. 001125/80.
ELSE IF(ABLE. EQ. 0. 0) THEN
  DDDY=. 001125/80.
ELSE IF(ABLE. EQ. 2. 0) THEN
  DDDY=. 001125/80.
ELSE IF(ABLE. EQ. 4. 0) THEN
  DDDY=. 001625/80.
ELSE IF(ABLE. EQ. 6. 0) THEN
  DDDY=. 001625/80.
ELSE IF(ABLE. EQ. 8. 0) THEN
  DDDY=. 000625/80.
ELSE IF(ABLE. GT. 8. 0. AND. ABLE. LT. 18. 0) THEN
  DDDY=. 001625/80.
ELSE IF(ABLE. EQ. 18. 0) THEN
  DDDY=. 001/80.
ENDIF
CALL BLIMP(ABLE, DDDY, YDVER, CDVER, WDVER, BLA, BLB, BLC, BLD,
+         BLE, F, BPAR, CTT, C, CT, E, DU, DDY, XBUP, YDUM, VPUP, CAPUDX,
+         UDUM, VDUM, DDX, N, MA, NREF, LU, DUM, TAUW, BLT2)

```



```

BLUP(1)=0.0
STAUP(1)=0
TAUUP(1)=0.0
IF(ABLE.LT.0.0)THEN
  NREF=NREFF
ELSE IF(ABLE.GE.0.0)THEN
  NREF=NREFF-1
  IF(NREF.LE.0)NREF=N
ENDIF
IF(NREF.LT.MA)THEN
  DO 45 I=2,LU
    IF(NREF.GT.0)THEN
      BLUP(I)=BLT2(NREF)
      STAUP(I)=NREF
      TAUUP(I)=TAUW(I)
      NREF=NREF-1
    ELSE IF(NREF.LE.0)THEN
      BLUP(I)=BLT2(NN2)
      STAUP(I)=NN2
      TAUUP(I)=TAUW(I)
      NN2=NN2-1
    ENDIF
45  CONTINUE
  ELSE IF(NREF.GT.MA)THEN
    DO 46 I=2,LU
      BLUP(I)=BLT2(NREF)
      STAUP(I)=NREF
      TAUUP(I)=TAUW(I)
      NREF=NREF-1
46  CONTINUE
  ENDIF
  DO 47 I=1,N
    IF(BLT2(I).NE.0.)THEN
      BLT(I)=BLT2(I)
    ENDIF
47  CONTINUE
  IFLAG=IFLAG+1
  IF(IFLAG.LE.2)GO TO 58
57  DO 48 I=1,N
    CP(I)=1.-((VT(I)/U)**2)
    PL(I)=((CP(I)*DEN*(U**2))/(2.*GC))
48  CONTINUE
C
C *****
C *
C *          CALCULATION OF LIFT COEFFICIENT
C *
C *****
C
NYI=100
NYIP1=101
NYIM1=99
CIRVORT=0.0
CIRVT=0.0
DO 56 I=1,N
  DYB=SQRT(XDIF(I)**2+YDIF(I)**2)/NYI
  DO 54 J=1,N
    IF(J.EG.1)GO TO 52
    DO 50 K=1,NYIP1
      SMYB=-SQRT(XDIF(I)**2+YDIF(I)**2)/2.0+(K-1)*DYB

```



```

      SMXCI(K)=(XBAR(I)-XBAR(J)+E1(I)*SMYB)*E2(J)-
+      (YBAR(I)-YBAR(J)+E2(I)*SMYB)*E1(J)
      SMYCI(K)=(XBAR(I)-XBAR(J)+E1(I)*SMYB)*E1(J)+
+      (YBAR(I)-YBAR(J)+E2(I)*SMYB)*E2(J)
50      CONTINUE
      ZDVDX=0.0
      ZVDY=0.0
      DO 51 K=2, NYI
          EL=SQRT(XDIF(J)**2+YDIF(J)**2)
          ZDVDX=ZDVDX+DVDX(EL, SMXCI(K), SMYCI(K))*DYB
          ZVDY=ZVDY+VDY(EL, SMXCI(K), SMYCI(K))*DYB
51      CONTINUE
      GO TO 53
52      ZDVDX=0.0
      ZVDY=PI*SQRT(XDIF(I)**2+YDIF(I)**2)
53      TERM3(J)=(E1(I)*E2(J)-E2(I)*E1(J))*ZDVDX
      TERM4(J)=(E1(I)*E1(J)+E2(I)*E2(J))*ZVDY
54      CONTINUE
      CIRVOR(I)=0.0
      DO 55 J=1, N
          CIRVOR(I)=CIRVOR(I)+SIGV*(TERM3(J)+TERM4(J))
55      CONTINUE
      CIRVORT=CIRVORT+CIRVOR(I)
56      CONTINUE
      CL=-2.0*CIRVORT*12./U/CHORD
      *****
C      *
C      *
C      *
C      *
      *****
      IF(PRINT .LE. 1.0 .AND. NVF .LE. 1)THEN
          WRITE (8,70)
          WRITE (8,72)(XDAT5(IE), YDAT5(IE), GAM(IE), XBAR(IE), YBAR(IE),
+          E1(IE), E2(IE), IE=1, N)
      ELSE IF(PRINT .LE. 1.0 .AND. NVF .GT. 1)THEN
          WRITE (9,71)
          WRITE (9,72)(XDAT5(I), YDAT5(I), GAM(I), XBAR(I), YBAR(I), E1(I),
+          E2(I), I=1, N)
      PRINT=PRINT+1.0
      ENDIF
      IF(NVF .LE. 1)THEN
          WRITE (8,73)(CL)
          WRITE (8,74)(ABLE, U, CHORD, P, DEN, SIGV)
          WRITE (8,75)(IK, XOVL(IK), VT(IK), CP(IK), PL(IK), IK=1, N)
          NVF=NVF+1
          GO TO 38
      ELSE IF(NVF .GT. 1)THEN
          WRITE (9,73)(CL)
          WRITE (9,74)(ABLE, U, CHORD, P, DEN, SIGV)
          WRITE (9,75)(IK, XOVL(IK), VT(IK), CP(IK), PL(IK), IK=1, N)
          WRITE (10,76)(ABLE)
          WRITE (10,77)(STALOW(I), XBLOW(I), TAULOW(I), BLOW(I),
+          I=1, LL)
      WRITE (10,76)(ABLE)
      WRITE (10,78)(STAUP(I), XBUP(I), TAUUP(I), BLUP(I),
+          I=1, LU)
      ENDIF
59      CONTINUE
60      FORMAT (I2/, F5.2/, F6.2/, F6.2/, 50(F6.2, 3X, F6.2/))
70      FORMAT ('1', //, 40X,

```

```

+ 'FLOW AROUND AN AIRFOIL BY SOURCE DISTRIBUTION METHOD',/,
+ 54X, '(NONVISCIOUS FLOW SOLUTION)',/)
71 FORMAT ('1', //, 40X,
+ 'FLOW AROUND AN AIRFOIL BY SOURCE DISTRIBUTION METHOD',/,
+ 53X, '(VISCIOUS FLOW SOLUTION)',/)
72 FORMAT (/, 31X, 'X-COORD.', 4X, 'YCOORD.', 5X, 'GAMA', 8X, 'X BAR',
+ 6X, 'Y BAR', 7X, 'E1', 8X, 'E2', //, 30X, '(% CHORD)', 3X,
+ '(% CHORD)', 2X, '(DEGREES)', 5X, '(FT)', 7X, '(FT)', //,
+ 75(30X, F8. 4, 4X, F8. 4, 5X, F5. 1, 5X, F8. 5, 3X, F8. 5, 3X, F7. 4,
+ 3X, F7. 4, //)
73 FORMAT ('1', //, 53X, 'LIFT COEFFICIENT -', 1X, F6. 3, //)
74 FORMAT (13X, 'ANGLE OF ATTACK', 3X, 'FREE STREAM VELOCITY', 3X
+ 'CHORD LENGTH', 3X, 'AMBIENT PRESSURE', 3X, 'DENSITY',
+ 5X, 'VORTEX STRENGTH', //, 15X, '(DEGREES)', 12X, '(FT/SEC)',
+ 12X, '(INCHES)', 8X, '(LBF/SGFT)', 5X, '(LBM/CUFT)', //,
+ 16X, F6. 2, 16X, F5. 2, 15X, F3. 1, 13X, F6. 1, 9X, F6. 4, 7X, E12. 5, //)
75 FORMAT (/, 22X, 'STATION', 6X, 'X/L', 6X, 'TANGENTIAL VELOCITY',
+ 5X, 'COMPUTED VALUE OF CP', 8X, 'LOCAL PRES. DIF', //, 75(25X,
+ I2, 6X, F6. 5, 10X, E12. 5, 13X, E12. 5, 12X, E12. 5//)
76 FORMAT ('1', 17X, 'BOUNDARY LAYER SOLUTION', //, 12X,
+ 'ANGLE OF ATTACK (DEGREES) - ', F4. 1)
77 FORMAT (//, 23X, 'LOWER SURFACE', //, 1X, 'STATION', 2X,
+ 'X-COORDINATE', 7X, 'TAUW', 6X, 'BOUND. LAYER THICK.', //,
+ 14X, '(FT)', 7X, '(LBF/SQ FT)', 10X, '(FT)', //, 50(2X, F3. 0,
+ 8X, F6. 5, 7X, E10. 3, 9X, F8. 7//)
78 FORMAT (//, 23X, 'UPPER SURFACE', //, 1X, 'STATION', 2X,
+ 'X-COORDINATE', 7X, 'TAUW', 6X, 'BOUND. LAYER THICK.', //,
+ 14X, '(FT)', 7X, '(LBF/SQ FT)', 10X, '(FT)', //, 50(2X, F3. 0,
+ 8X, F6. 5, 7X, E10. 3, 9X, F8. 7//)
STOP
END

```

```

SUBROUTINE THETA(X, Y, Z)
REAL X, Y, Z
COMMON PI
IF(X .EQ. 0.0 .AND. Y .GT. 0.0)THEN
  Z=PI/2.
  ELSE IF(X .EQ. 0.0 .AND. Y .LT. 0.0)THEN
    Z=3.*PI/2.
  ELSE IF(X .GT. 0.0 .AND. Y .EQ. 0.0)THEN
    Z=0.0
  ELSE IF(X .LT. 0.0 .AND. Y .EQ. 0.0)THEN
    Z=PI
  ELSE IF(X .GT. 0.0 .AND. Y .GT. 0.0)THEN
    Z=ATAN(Y/X)
  ELSE IF(X .LT. 0.0 .AND. Y .GT. 0.0)THEN
    Z=ATAN(Y/X)+PI
  ELSE IF(X .GT. 0.0 .AND. Y .LT. 0.0)THEN
    Z=ATAN(Y/X)+2.*PI
  ELSE IF(X .LT. 0.0 .AND. Y .LT. 0.0)THEN
    Z=ATAN(Y/X)+PI
ENDIF
RETURN
END

```

```

FUNCTION DUDX(EL, X, Y)
REAL A, B, X, Y, EL
COMMON PI
A=Y+EL/2.
B=Y-EL/2.

```

```

IF (X. EQ. 0.) THEN
  DUDX=PI
ELSE IF (X. NE. 0.) THEN
  DUDX=ATAN(A/X)-ATAN(B/X)
ENDIF
RETURN
END

```

```

FUNCTION DUDY(EL, X, Y)
REAL A, B, X, Y, EL
COMMON PI
A=(X**2)+((Y+EL/2.)**2)
B=(X**2)+((Y-EL/2.)**2)
DUDY=. 5*LOG(A/B)
RETURN
END

```

```

FUNCTION DVDX(EL, X, Y)
REAL A, B, X, Y, EL
COMMON PI
A=(X**2)+((Y-EL/2.)**2)
B=(X**2)+((Y+EL/2.)**2)
DVDX=. 5*LOG(A/B)
RETURN
END

```

```

FUNCTION DVDY(EL, X, Y)
REAL A, B, X, Y, EL
COMMON PI
A=Y+EL/2.
B=Y-EL/2.
IF (X. EQ. 0.) THEN
  DVDY=PI
ELSE IF (X. NE. 0.) THEN
  DVDY=ATAN(A/X)-ATAN(B/X)
ENDIF
RETURN
END

```

```

SUBROUTINE STORE(Z, D, NA, N, A)
REAL A(NA, NA), Z(NA, NA), D(5000)
INTEGER I, J, K, L, M
K=0
DO 101 J=1, N
  DO 100 I=1, N
    K=K+1
    D(K)=Z(I, J)
100 CONTINUE
101 CONTINUE
K=0
DO 103 M=1, NA
  DO 102 L=1, NA
    K=K+1
    A(L, M)=D(K)
102 CONTINUE
103 CONTINUE
RETURN
END

```

```

SUBROUTINE STORE1(Z, D, NA, N, A)

```

```

REAL A(NA,3),Z(NA,3),D(400)
INTEGER I,J,K,L,M
K=0
DO 201 J=1,3
  DO 200 I=1,N
    K=K+1
    D(K)=Z(I,J)
200 CONTINUE
201 CONTINUE
K=0
DO 203 M=1,3
  DO 202 L=1,NA
    K=K+1
    A(L,M)=D(K)
202 CONTINUE
203 CONTINUE
RETURN
END

C
C *****
C *
C *          STAGNATION POINT DETERMINATION          *
C *
C *****
C

SUBROUTINE STAG(V,DELTA,MA,MB,N,XBUP,VPUP,XBLOW,VPLOW,LL,LU,NREF)
REAL V(N),DELTA(N),XBUP(N),VPUP(N),XBLOW(N),VPLOW(N),X1,X2,
+  X3,SUML,SUMU
INTEGER I,J,L,LL,LU,NREF
XBLOW(1)=0.0
VPLOW(1)=0.0
XBUP(1)=0.0
VPUP(1)=0.0
SUML=0.0
SUMU=0.0
L=3
DO 300 I=MB,N
  V(I)=-V(I)
300 CONTINUE
DO 309 I=2,N
  IF(V(I-1).LT.0.0.AND.V(I).GE.0.0)THEN
    NREF=I
    X1=DELTA(I)*ABS(V(I))/ABS(V(I)-V(I-1))
    SUML=SUML+X1
    XBLOW(2)=SUML
    VPLOW(2)=ABS(V(I))
    DO 301 J=I+1,MA
      SUML=SUML+DELTA(J)
      XBLOW(L)=SUML
      VPLOW(L)=ABS(V(J))
      L=L+1
301 CONTINUE
    LL=L-1
    L=3
    SUMU=SUMU+DELTA(I)-X1
    XBUP(2)=SUMU
    VPUP(2)=ABS(V(I-1))
    IF((I-2).LE.0)THEN
      SUMU=SUMU+DELTA(1)+DELTA(N)
      XBUP(L)=SUMU

```

```

VPUPI(L)=ABS(V(N))
L=L+1
DO 302 J=N-1, MB, -1
  SUMU=SUMU+DELTA(J)
  XBUP(L)=SUMU
  VPUPI(L)=ABS(V(J))
  L=L+1
302 CONTINUE
LU=L-1
ELSE IF((I-2) .GE. 1) THEN
  DO 303 J=I-2, 1, -1
    SUMU=SUMU+DELTA(J)
    XBUP(L)=SUMU
    VPUPI(L)=ABS(V(J))
    L=L+1
303 CONTINUE
SUMU=SUMU+DELTA(1)+DELTA(N)
XBUP(L)=SUMU
VPUPI(L)=ABS(V(N))
L=L+1
DO 304 J=N-1, MB, -1
  SUMU=SUMU+DELTA(J)
  XBUP(L)=SUMU
  VPUPI(L)=ABS(V(J))
  L=L+1
304 CONTINUE
LU=L-1
ENDIF
RETURN
ELSE IF(V(I) .LT. 0.0 .AND. V(I-1) .GE. 0.0) THEN
  NREF=I-1
  X2=DELTA(I-1)*ABS(V(I-1))/ABS(V(I-1)-V(I))
  SUMU=SUMU+X2
  XBUP(2)=SUMU
  VPUPI(2)=ABS(V(I-1))
  DO 305 J=I-2, MB, -1
    SUMU=SUMU+DELTA(J)
    XBUP(L)=SUMU
    VPUPI(L)=ABS(V(J))
    L=L+1
305 CONTINUE
LU=L-1
L=3
SUML=SUML+DELTA(I-1)-X2
XBLOW(2)=SUML
VPLOW(2)=ABS(V(I))
IF((I+1) .GT. N) THEN
  SUML=SUML+DELTA(N)+DELTA(1)
  XBLOW(L)=SUML
  VPLOW(L)=ABS(V(1))
  L=L+1
  DO 306 J=2, MA
    SUML=SUML+DELTA(J)
    XBLOW(L)=SUML
    VPLOW(L)=ABS(V(J))
    L=L+1
306 CONTINUE
LL=L-1
ELSE IF((I+1) .LE. N) THEN
  DO 307 J=I+1, N

```



```

        SUML=SUML+DELTA(J)
        XBLOW(L)=SUML
        VPLOW(L)=ABS(V(J))
        L=L+1
307    CONTINUE
        SUML=SUML+DELTA(N)+DELTA(1)
        XBLOW(L)=SUML
        VPLOW(L)=ABS(V(1))
        L=L+1
        DO 308 J=2, MA
            SUML=SUML+DELTA(J)
            XBLOW(L)=SUML
            VPLOW(L)=ABS(V(J))
            L=L+1
308    CONTINUE
        LL=L-1
        ENDIF
        RETURN
    ENDIF
309    CONTINUE
    NREF=1
    DO 310 I=MB, N
        V(I)=-V(I)
310    CONTINUE
        X3=ABS(V(1))*(DELTA(N)+DELTA(1))/ABS(V(1)-V(N))
        SUML=SUML+X3
        XBLOW(2)=SUML
        VPLOW(2)=ABS(V(1))
        DO 311 I=2, MA
            SUML=SUML+DELTA(I)
            XBLOW(L)=SUML
            VPLOW(L)=ABS(V(I))
            L=L+1
311    CONTINUE
        LL=L-1
        L=3
        SUMU=SUMU+DELTA(N)+DELTA(1)-X3
        XBUP(2)=SUMU
        VPUP(2)=ABS(V(N))
        DO 312 I=N-1, MB, -1
            SUMU=SUMU+DELTA(I)
            XBUP(L)=SUMU
            VPUP(L)=ABS(V(I))
            L=L+1
312    CONTINUE
        LU=L-1
        RETURN
    END
C
C *****
C *
C *          BOUNDARY LAYER DETERMINATION          *
C *
C *****
C
SUBROUTINE BLIMP (ABLE, DY, YDVER, CDVER, WDVER, A, B, C, D, E, F, BPAR,
+             CTT, CC, CT, EE, DU, DDY, X, Y, CAPU, CAPUDX, U, V, DX, N1,
+             MA, NREF, L, VT, TAUW, BLT2)
REAL X(L), Y(B1), DX(L), CAPU(L), CAPUDX(L), U(L, B1), V(L, B1),
+     A(B1), B(B1), C(B1), D(B1), E(B1), DEN, PNU, DY, CTT(3, 3), TAUW(41),

```



```

+      BPAR(4), DU(4), DDY(4), F, CT(40, 3), EE(1600), CC(40, 3), REC, REG,
+      YDVER(3), ABLE, CDVER(24), WDVER(3, 9), ETA, ETAEND, BVER, TOL, YY,
+      XDUM, VT(81), BLT2(75)
+      INTEGER I, J, K, L, M, N, IE, IF, IG, IH, IJ, IK, IL, IM, IN, IC, IER, NX, N1, N2, N3,
+      MA, NDUM, ICC, KT, NN, NW, IND, IT, IFLAG
EXTERNAL ICSICU, STORE1, DVERK, FCN
A(1)=0.0
B(1)=0.0
C(1)=0.0
D(1)=0.0
E(1)=0.0
Y(1)=0.0
A(81)=0.0
B(81)=0.0
E(81)=0.0
XDUM=1.0E-7
DEN=.0735/32.174
PNU=.0001688
REC=0.9
U(1,1)=0.0
V(1,1)=0.0
BVER=CAPU(2)/X(2)
YDVER(1)=1.232588
YDVER(2)=0.0
YDVER(3)=0.0
IT=1
KT=40
NW=3
NN=3
TOL=.01
IND=1
ETA=0.0
DO 401 I=2, 81
  Y(I)=Y(I-1)+DY
401  CONTINUE
C
C ***** STAGNATION POINT FLOW *****
C
DO 414 I=2, 81
  ETAEND=Y(I)*SQRT(BVER/PNU)
  CALL DVERK(NN, FCN, ETA, YDVER, ETAEND, TOL, IND, CDVER,
+          NW, WDVER, IER)
  V(1, I)=-SQRT(BVER*PNU)*YDVER(3)
  U(1, I)=BVER*XDUM*YDVER(2)
414  CONTINUE
  NX=4
  IC=3
  ICC=L-1
  N2=1
  N3=N1
  NDUM=0
  TAU=0.0
  DO 402 I=1, L-1
    DX(I)=X(I+1)-X(I)
402  CONTINUE
  CALL ICSICU(X, CAPU, L, BPAR, CC, ICC, IER)
  CALL STORE1(CC, EE, KT, ICC, CT)
  DO 403 I=1, ICC
    CAPUDX(I)=CT(I, 1)
403  CONTINUE

```

```

DO 412 N=1,L-1
DO 405 IN=2,80
  REG=ABS(V(N, IN))*DY/PNU
  IF(V(N, IN) .EQ. 0.0)THEN
    C(IN)=(U(N, IN)**2/DX(N)+CAPU(N)*CAPUDX(N))/
+     (U(N, IN)/DX(N)+2.*PNU/DY**2)
+     A(IN)=(PNU/DY**2-V(N, IN)/2./DY)/(U(N, IN)/
+     DX(N)+2.*PNU/DY**2)
+     B(IN)=(PNU/DY**2+V(N, IN)/2./DY)/(U(N, IN)/
+     DX(N)+2.*PNU/DY**2)
  ELSE IF(V(N, IN) .LT. 0.0)THEN
+     A(IN)=(PNU/DY**2-REC/REG*V(N, IN)/2./DY-
+     (1.-REC/REG)*V(N, IN)/DY)/(U(N, IN)/
+     DX(N)+2.*PNU/DY**2-(1.0-REC/REG)*
+     V(N, IN)/DY)
+     B(IN)=(PNU/DY**2+REC/REG*V(N, IN)/2./DY)/
+     (U(N, IN)/DX(N)+2.*PNU/DY**2-(1.0-
+     REC/REG)*V(N, IN)/DY)
+     C(IN)=(U(N, IN)**2/DX(N)+CAPU(N)*CAPUDX(N))/
+     (U(N, IN)/DX(N)+2.*PNU/DY**2-(1.0-REC/
+     REG)*V(N, IN)/DY)
  ELSE IF(V(N, IN) .GT. 0.0)THEN
+     A(IN)=(PNU/DY**2-REC/REG*V(N, IN)/2./DY)/
+     (U(N, IN)/DX(N)+2.*PNU/DY**2+(1.0-REC/
+     REG)*V(N, IN)/DY)
+     B(IN)=(PNU/DY**2+REC/REG*V(N, IN)/2./DY+
+     (1.-REC/REG)*V(N, IN)/DY)/(U(N, IN)/
+     DX(N)+2.*PNU/DY**2+(1.0-REC/REG)*
+     V(N, IN)/DY)
+     C(IN)=(U(N, IN)**2/DX(N)+CAPU(N)*CAPUDX(N))/
+     (U(N, IN)/DX(N)+2.*PNU/DY**2+(1.0-REC/
+     REG)*V(N, IN)/DY)
  ENDIF
405 CONTINUE
DO 406 J=2,80
  D(J)=(C(J)+B(J)*D(J-1))/(1.-B(J)*E(J-1))
  E(J)=A(J)/(1.-B(J)*E(J-1))
406 CONTINUE
C(81)=CAPU(N)
D(81)=(C(81)+B(81)*D(80))/(1.-B(81)*E(80))
U(N+1,81)=D(81)
DO 407 K=80,1,-1
  U(N+1,K)=D(K)+E(K)*U(N+1,K+1)
407 CONTINUE
DO 408 M=2,81
+ V(N+1,M)=V(N+1,M-1)-(DY*(U(N+1,M)-U(N,M)+U(N+1,M-1)-
+ U(N,M-1)))/2./DX(N)
408 CONTINUE
C
C ***** BOUNDARY LAYER THICKNESS *****
C
VT(1)=0.0
DO 409 I=2,81
  VT(I)=ABS(U(N, I))
409 CONTINUE
IF(X(N) .GT. 0.0)THEN
  IF(N.EQ.2)THEN
    YY=0.0
    GO TO 417
  ENDIF

```

```

      IFLAG=1
      DO 413 I=2,81
        IF(VT(I-1).LT..95*CAPU(N).AND.VT(I).GE.
+       .95*CAPU(N).AND.IFLAG.EQ.1)THEN
+       YY=Y(I-1)+(CAPU(N)-VT(I-1))/(VT(I)-VT(I-1))*
+       (Y(I)-Y(I-1))
          IFLAG=IFLAG+1
          GO TO 417
        ENDIF
413    CONTINUE
      IF(VT(81).LT..95*CAPU(N).AND.VT(81).GT.25.)THEN
        YY=Y(81)
      ENDIF
417    IF(NREF.LE.N1.AND.F.LT.0.)THEN
      BLT2(NREF)=YY
      NREF=NREF+1
      ELSE IF(NREF.GT.N1.AND.F.LT.0.)THEN
        BLT2(N2)=YY
        N2=N2+1
      ELSE IF(NREF.GT.0.AND.F.GT.0.)THEN
        BLT2(NREF)=YY
        NREF=NREF-1
      ELSE IF(NREF.LE.0.AND.F.GT.0.)THEN
        BLT2(N3)=YY
        N3=N3-1
      ENDIF
    ENDIF
C
C   ***** WALL SHEAR STRESS *****
C
      DO 410 IK=1,4
        DU(IK)=U(N+1,IK)
        DDY(IK)=Y(IK)
410    CONTINUE
      DO 411 IL=1,4
        BPAR(IL)=0.0
411    CONTINUE
      CALL ICSICU(DDY,DU,NX,BPAR,CTT,IC,IER)
      TAUW(N+1)=DEN*PNU*CTT(1,1)
412  CONTINUE
C
C   ***** BOUNDARY LAYER THICKNESS (AT LAST STATION PT.) *****
C
      VT(1)=0.0
      DO 415 I=2,81
        VT(I)=ABS(U(L,I))
415    CONTINUE
      IFLAG=1
      DO 416 I=2,81
        IF(VT(I-1).LT..95*CAPU(L).AND.VT(I).GE.
+       .95*CAPU(L).AND.IFLAG.EQ.1)THEN
+       YY=Y(I-1)+(CAPU(L)-VT(I-1))/(VT(I)-VT(I-1))*
+       (Y(I)-Y(I-1))
          IFLAG=IFLAG+1
          GO TO 419
        ENDIF
416    CONTINUE
      IF(VT(81).LT..95*CAPU(L).AND.VT(81).GT.25.)THEN
        YY=Y(81)
      ENDIF

```

```
419  IF(NREF. LE. N1. AND. F. LT. O. )THEN
      BLT2(NREF)=YY
      ELSE IF(NREF. GT. N1. AND. F. LT. O. )THEN
          BLT2(N2)=YY
          ELSE IF(NREF. GT. O. AND. F. GT. O. )THEN
              BLT2(NREF)=YY
              ELSE IF(NREF. LE. O. AND. F. GT. O. )THEN
                  BLT2(N3)=YY
          ENDIF
      RETURN
  END
```

```
SUBROUTINE FCN(N, X, Y, YPRIME)
REAL Y(N), YPRIME(N), X
INTEGER N
YPRIME(1)=(Y(2)*Y(2)-1. )-Y(1)*Y(3)
YPRIME(2)=Y(1)
YPRIME(3)=Y(2)
RETURN
END
```

APPENDIX D

PROPOSED EXPERIMENTAL PROCEDURE

The purpose of the proposed experiment was to compare local C_p values obtained experimentally with those obtained in the numerical scheme. The apparatus necessary to conduct such an experiment are:

1. Wind tunnel (Aerolab located in the Department of Ocean Engineering).
2. Airfoil with pressure taps (CY-14 airfoil).
3. Digital multimanometer (Aerolab).

The test section of the Aerolab wind tunnel is 28" x 40". By placing the airfoil vertically in the center of the test section (approximately 27.5" long -- spanning the entire height of the test section) with the pressure taps located near the centerline of the airfoil (see Figure 25), local pressures on the airfoil can be measured. The center location of the pressure taps minimizes wall and end effects.

The experiment had to be aborted due to the extraordinary effort required to remove another piece of test equipment from the wind tunnel test section (i.e., sting measuring device).

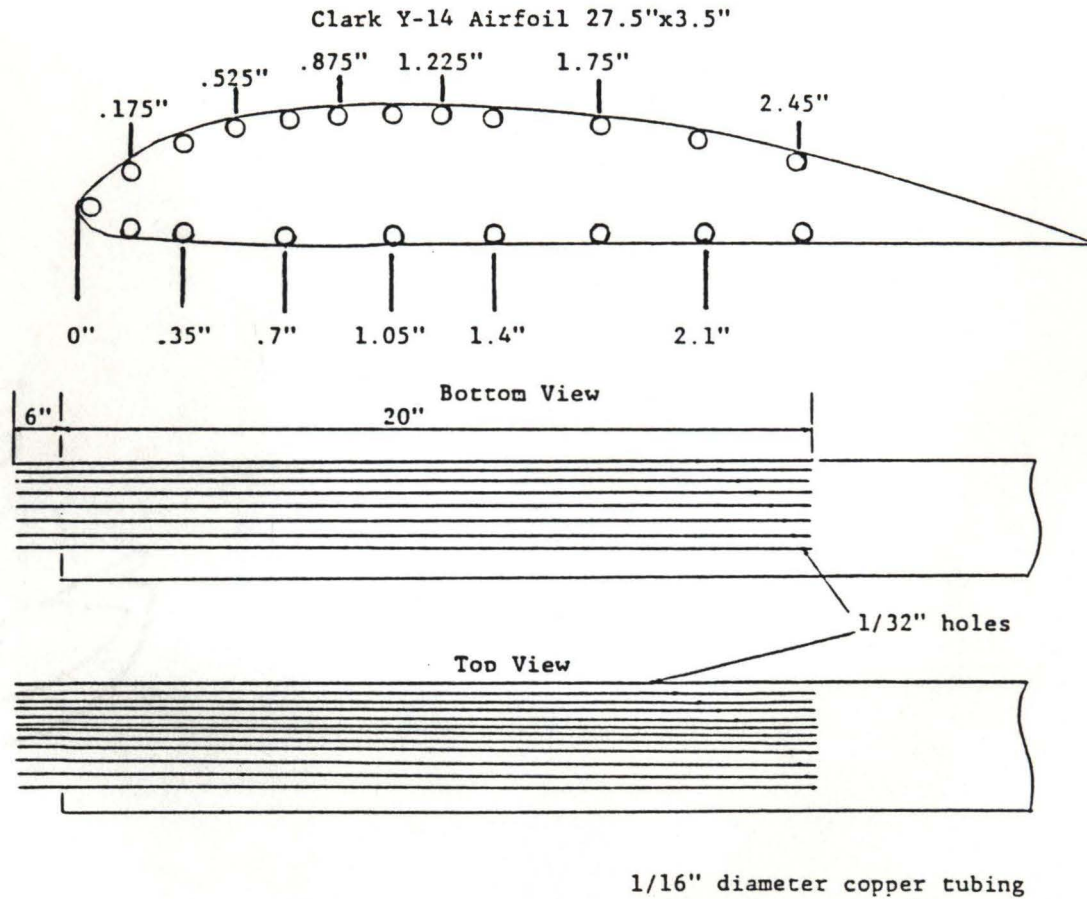


Figure 25 Diagram of CY-14 Airfoil for Use in Proposed Experiment

REFERENCES

1. A. B. Bauer, A. M. O. Smith and T. L. Hess; Potential Flow and Boundary Layer Theory as Design Tools in Aerodynamics, Canadian Aeronautics and Space Journal, Vol. 16, No. 2, Feb. 1970, pp. 53.
2. J. L. Hess and A. M. O. Smith, Calculation of Potential Flow About Arbitrary Bodies, Progress in Aeronautical Sciences, Vol. 8, Pergaman Press, New York, 1966.
3. A. M. O. Smith and D. W. Clutter, Solution of the Incompressible Laminar Boundary - Layer Equations, Douglas Aircraft Co. Rept. ES 40446, July 1961.
4. _____, Solution of the Incompressible Laminar Boundary - Layer Equations, AIAA Journal, Vol. 1, 1963, pp. 2062-2071.
5. D. W. Clutter and A. M. O. Smith, Solution of the General Boundary - Layer Equations for Compressible Laminar Flow, Including Transverse Curvature, Douglas Aircraft Co. Rept. LB 31088, February 1963, Revised, October 1964.
6. D. W. Clutter, A. M. O. Smith, and N. A. Jaffe; "General Method for Solving the Nonequilibrium Laminar Boundary Layer Equations of a Binary Gas," Douglas Aircraft Co. Rept. LB 31616, October 1964.
7. A. M. O. Smith and D. W. Clutter, Machine Calculation of Compressible Boundary - Layers, AIAA Journal, Vol. 3, 1965, pp. 639-647.
8. A. M. O. Smith and N.A. Jaffe, General Method for Solving the Nonequilibrium Boundary - Layer Equations of a Dissociating Gas, AIAA Journal, Vol.4, 1966, pp. 611-620.
9. A. M. O. Smith, N. A. Jaffe, and P. C. Lind, "Study of a General Method of Solution of the Incompressible Turbulent Boundary - Layer Equations," Douglas Aircraft Co. Rept. LB 52949, November 1965.
10. A. M. O. Smith and T. Cebeci, "Numerical Solution of the Turbulent Boundary - Layer Equations," Douglas Aircraft Co. Rept. DAC 33735, May 1967.
11. _____, "Solution of the Boundary - Layer Equations for Incompressible Turbulent Flow," Proc. of the 1968 Heat Transfer and Fluid Mechanics Institute.

12. T. Cebeci and A. M. O. Smith, "A Finite - Difference Solution of the Incompressible Turbulent Boundary - Layer Equations by an Eddy - Viscosity Concept," Douglas Paper 4958, Pres. to 1968 Symp. of Turbulent Boundary - Layers, Stanford University.
13. _____, "A Finite - Difference Solution of the Incompressible Turbulent Boundary - Layer Equations by an Eddy - Viscosity Concept," Douglas Aircraft Co. Rept. DAC 67130, October 1968.
14. T. Cebeci, A. M. O. Smith and L. C. Wang, "A Finite - Difference Solution of the Boundary - Layer Equations," Douglas Aircraft Co. Rept. DAC 67131, December 1968.
15. M. R. Head, "Entrainment in the Turbulent Boundary - Layer," Rand M 3152, British ARC 1960.
16. E. Truckenbrodt, "A Method of Quadratures for the Calculation of the Laminar and Turbulent Boundary - Layer in Case of Plane and Rotationally Symmetrical Flow", NACA TM 1379, 1955.
17. B. G. J. Thompson, "A Critical Review of Existing Methods of Calculating the Turbulent Boundary - Layer", FM 3492, British ARC 26109, 1964.
18. J. G. Callaghan and T. D. Beatty A Theoretical Method For the Analysis and Design of Multielement Airfoils, Journal of Aircraft, Vol. 9, No. 12, December 1972, pp. 844-848.
19. J. L. Hess, "Progress in the Calculation of Incompressible Three - Dimensional Lifting Flows Including Viscosity Effects," Douglas Rept. No. MDC 36516, April 1974, pp. 1-20.
20. _____, "Review of Integral - Equation Techniques for Solving Potential - Flow Problems With Emphasis on the Surface - Source Method," Computer Methods in Applied Mechanics and Engineering, Vol. 5, 1975, pp. 145-196.
21. J. L. Hess and A. M. O. Smith, "A General Method for Calculating Low Speed Flow About Inlets," AGAR Dograph 103, Aerodynamics of Power Plant Installation, 1965, pp. 345-372.
22. J. L. Hess, "Numerical Solution of the Integral Equation for the Neumann Problem With Application to Aircraft and Ships," Proceedings of SIAM Symposium on Numerical Solution of Integral Equations With Physical Applications, Engineering Paper 5987, Douglas Aircraft Co., Long Beach, California.

23. William Bober and Richard Kenyon. "Fluid Mechanics," John Wiley & Sons, New York, 1980, pp. 407-410.
24. _____, "Fluid Mechanics," John Wiley & Sons, New York, 1980, pp. 272.
25. Frank M. White, "Viscous Fluid Flow," McGraw Hill, New York, 1974, pg. 4.
26. William Bober and Richard Kenyon, "Fluid Mechanics," John Wiley & Sons, New York, 1980, pp. 408-409.
27. Frank M. White, "Viscous Fluid Flow," McGraw Hill, New York, 1974, pg. 3.
28. William Bober and Richard Kenyon. "Fluid Mechanics," John Wiley & Sons, New York, 1980, pp. 465-466.
29. _____, "Fluid Mechanics," John Wiley & Sons, New York, 1980, pp. 409-410.
30. _____, "Fluid Mechanics," John Wiley & Sons, New York, 1980, pg. 410.
31. _____, "Fluid Mechanics," John Wiley & Sons, New York, 1980, pg. 424.
32. _____, "Fluid Mechanics," John Wiley & Sons, New York, 1980, pg. 410.
33. William Bober class notes.
34. _____, class notes.
35. Robert M. Pinkerton and Harry Greenberg, "Dynamic Characteristics of a Large Number of Airfoils Tested in the Variable-Density Wind Tunnel," NACA Technical Report No. 628, October 1, 1937, pp. 297-345.
36. J. L. Hess, "Review of Integral - Equation Techniques for Solving Potential - Flow Problems With Emphasis on the Surface - Source Method," Computer Methods in Applied Mechanics and Engineering, Vol. 15, 19, July 1974, pg. 160.
37. William Bober, class notes.
38. _____, class notes.
39. Frank M. White, "Viscous Fluid Flow," McGraw Hill, New York, 1974, pg. 4.

40. S. Kakac and Y. Yener, "Heat Conduction," Hemisphere Publishing Co., New York, 1985, pg. 318.
41. A. M. O. Smith and D. W. Clutter, Solution of the Incompressible Laminar Boundary - Layer Equations, AIAA Journal, Vol. 1, No. 9, pg. 2064.
42. S. Kakac and Y. Yener, "Heat Conduction," Hemisphere Publishing Co., New York, 1985, pg. 324.
43. William Bober, class notes.
44. Dale A. Anderson, John C. Tannehill and Richard H. Fletcher, "Application of Finite - Difference Methods," McGraw Hill Book Co., New York, pg. 343.
45. Frank M. White, "Viscous Fluid Flow," McGraw Hill, New York, 1974, pg. 124.
46. Robert M. Pinkerton and Harry Greenberg, "Dynamic Characteristics of a Large Number of Airfoils Tested in the Variable-Density Wind Tunnel," NACA Technial Rept, No. 628, October 1, 1937, pp. 297-345.
47. J. P. Holman, "Experimental Methods for Engineers," 2nd Edition, McGraw Hill, New York, 1966, pg. 66.
48. J.L. Hess, "Review of Integral - Equation Techniques for Solving Potential - Flow Problems with Emphasis on the Surface - Source Method, Vol. 5, 1975, pg. 160.
49. P. E. Hemke, "Elementary Applied Aerodynamics," Prentice-Hall, Inc., New York, 1946, pg. 130-132.
50. A. B. Bauer, A. M. O. Smith, and J. L. Hess; Potential Flow and Boundary Layer Theory as Design Tools in Aerodynamics, Canadian Aeronautics and Space Journal, Vol. 16, No. 2, Feb. 1970, pg. 55.
51. Frank White, "Viscous Fluid Flow," McGraw Hill, New York, 1974, pg. 301.
52. R. E. Sheridan (1968): Pa. State Univ. Ordnance Res. Lab. Tech. Mem. 502.2421-19.
53. J. L. Hess, "Progress in the Calculation of Incompressible Three-Dimensional Lifting Flows Including Viscosity Effects," Douglas Rept. No. MDC 35416, April 1974, pg. 15.
54. _____, "Progress in the Calculation of Incompressible Three-Dimensional Lifting Flows Including Viscosity Effects," Douglas Rept. No. MDC 35416, April 1974, pg. 16.

BIBLIOGRAPHY

- Anderson, Dale A.; John C. Tannehill; and Richard H. Fletcher. "Application of Finite - Difference Methods." McGraw Hill Book Co., New York.
- Bauer, A. B.; A. M. O. Smith; and J. L. Hess. Potential Flow and Boundary Layer Theory as Design Tools in Aerodynamics. Canadian Aeronautics and Space Journal, Vol. 16, No. 2, Feb. 1970, pp. 53-69.
- Bober, William and Richard Kenyon. "Fluid Mechanics." John Wiley & Sons, New York, 1980.
- Callaghan, J. G. and T. O. Beatty. Theoretical Method for the Analysis of Multielement Airfoils. Journal of Aircraft, Vol. 9, No. 12, December 1972, pp. 844-848.
- Cebeci, T. and A. M. O. Smith. "A Finite - Difference Solution of the Incompressible Turbulent Boundary - Layer Equations by an Eddy - Viscosity Concept." Douglas Paper 4958, Pres. to 1968 Symp. of Turbulent Boundary - Layers, Stanford University.
- _____, "A Finite - Difference Solution of the Incompressible Turbulent Boundary - Layer Equations by an Eddy - Viscosity Concept." Douglas Aircraft Co. Rept. DAC 67130, October 1968.
- Cebeci, T.; A. M. O. Smith; and L. C. Wang. "A Finite - Difference Solution of the Boundary - Layer Equations." Douglas Aircraft Co. Rept. DAC 67131, December 1968.
- Clutter, D. W. and A. M. O. Smith. Solution of the General Boundary - Layer Equations For Compressible Laminar Flow, Including Transverse Curvature. Douglas Aircraft Co. Rept. LB 31098, February 1963, Revised, October 1964.
- Clutter, D. W.; A. M. O. Smith; and N. A. Jaffe. "General Method For Solving the Nonequilibrium Laminar Boundary Layer Equations of a Binary Gas." Douglas Aircraft Co. Rept. LB 31616, October 1964.
- Head, M. R. "Entrainment in the Turbulent Boundary - Layer." FM 3492, British ARC 26109, 1964.
- Hemke, P. E. "Elementary Applied Aerodynamics." Prentice-Hall, Inc., New York, 1946.
- Hess, J. L. "Numerical Solution of the Integral Equation for the Neumann Problem with Application to Aircraft and Ships." Proceedings of SIAM Symposium on Numerical Solution of Integral Equations with Physical Applications, Engineering Paper 5987, Douglas Aircraft Co., Long Beach, California.

Hess, J. L. and A. M. O. Smith. "A General Method for Calculating Low Speed Flow About Inlets." AGAR Dograph 103, Aerodynamics of Power Plant Installation, 1965, pp. 345-372.

_____, Calculation of Potential Flow About Arbitrary Bodies. Progress in Aeronautical Sciences, Vol. 8, Pergamon Press, New York, 1966.

Hess, J. L. "Progress in the Calculation of Incompressible Three - Dimensional Lifting Flows Including Viscosity Effects." Douglas Rept. No. MDC 36516, April 1974.

_____, "Review of Integral - Equation Techniques for Solving Potential - Flow Problems With Emphasis on the Surface - Source Method." Computer Methods in Applied Mechanics and Engineering, Vol. 5, 1975.

Holman, J. P. "Experimental Methods for Engineers." 2nd Edition. McGraw-Hill, New York, 1966.

Kakac, S. and Y. Yener. "Heat Condition." Hemisphere Publishing Co., New York, 1985.

Pinterton, Robert M. and Harry Greenberg. "Dynamic Characteristics of a Large Number of Airfoils Tested in a Variable - Density Wind Tunnel." NACA Technical Rept. No. 628, October 1, 1937, pp. 297-345.

Sheridan, R. E. Pa. State Univ. Ordnance Res. Lab. Tech. Mem. 502.2421-19, 1968.

Smith, A. M. O. and D. W. Clutter. Solution of the Incompressible Laminar Boundary Layer Equations. Douglas Aircraft Co. Rept. ES 40446, July 1961.

_____, Solution of the Incompressible Laminar Boundary Layer Equations. AIAA Journal, Vol. 1, 1963, pp. 2062-2071.

_____, Machine Calculation of Compressible Boundary - Layers. AIAA Journal, Vol. 3, 1965, pp. 639-647.

Smith, A. M. O.; N. A. Jaffe; and P. C. Lind. "Study of a General Method of Solution of the Incompressible Turbulent Boundary - Layers Equations." Douglas Aircraft Co., Rept. LB 52949, November 1965.

_____, General Method For Solving the Nonequilibrium Boundary Layer Equations of a Dissociating Gas. AIAA Journal, Vol. 4, 1966, pp. 611-620.

Smith, A. M. O. and T. Cebeci. "Numerical Solution of the Turbulent Boundary-Layer Equations." Douglas Aircraft Co. Rept. DAC 33735, May 1967.

_____, "Solution of the Boundary-Layer Equations for Incompressible Turbulent Flow." Proc. of the 1968 Heat Transfer and Fluid Mechanics Institute.

Thompson, B. G. J. "A Critical Review of Existing Methods of Calculating the Turbulent Boundary-Layer." FM 3492, British ARC 26109, 1964.

Truckenbrodt, E. "A Method of Quadratures for the Calculation of the Laminar and Turbulent Boundary-Layer in Case of Plane and Rotationally Symmetrical Flow." NACA TM 1379, 1955.

White, Frank M. "Viscous Fluid Flow." McGraw Hill, New York, 1974.

